NTNU
Norwegian University of
Science and Technology

TECHNICAL AND ECONOMICAL EVALUATION OF THE DELIQUIFICATION METHOD FOR GAS WELL(SS7) IN THE SONGO SONGO GAS FIELD

Thobias Isaya Magige

Petroleum Engineering
Submission date: August 2017
Supervisor: Milan Stanko, IGP

Norwegian University of Science and Technology
Department of Geoscience and Petroleum

ABSTRACT

This study was conducted to investigate the most suitable deliquification method for removing the accumulated liquid from the well SS7 to surface. This study began by determining different sources of liquid into the well SS7 and then predicting liquid loading problem. The identification of liquid sources in the well SS7 was performed using correlations and identified the contribution of both liquid from condensation and coning water to the produced liquid from the well SS7.

Liquid loading prediction was performed using Turner droplet model and the system performance curve developed in Prosper software. Both of the two alternatives predicted the existence of liquid loading at the current producing period (2016) in the well SS7. The predicted liquid loading in the well SS7 gave the challenge which leads to the new study of finding the best alternative of removing the accumulated liquid to surface and increases gas flow.

Several liquid unloading method were evaluated both technically and economically to find the best alternative which can be proposed for SS7. Technical factor selected Gas lift, Plunger lift, Velocity string and ESP as the most effective method in accordance with the SS7 conditions.

The selected methods by technical criteria were further evaluated considering the economics factors to find out which among the four selected method gave positive NPV. The results from economical evaluation selected Plunger lift, Gas lift and ESP as the most suitable method for SS7 because they generated the positive NPV. Final decision was performed based on the magnitude of the generated positive NPV which leads to the selection of Plunger Lift to be the optimum method for removing liquid from the bottom of the well SS7.

An engineering design of the Plunger lift operating parameters for lifting an average liquid of 122STB produced from well SS7 was performed. The estimated parameters were, maximum and minimum casing build up pressure 1442 psia and 1199 psia respectively. The other parameter calculated were the minimum gas rate per cycle of 15Mscf/day required to lift the Plunger and the liquid above it to surface and the maximum number of cycle required per day were 149 cycle/day.

ACKNOWLEDGEMENT

Foremost, I would like to express my sincere gratitude to my Supervisor Prof. Milan W. Stanko for his patience, motivation, enthusiasm, and immense knowledge towards Master Thesis study.

His guidance helped me in all the time of data gathering, analysis and writing of this thesis. I could not have imagined having a gracious Supervisor and Mentor for my Master Degree study. His treatment and guidance

Besides my Supervisor, I would like to thank Prof. Richard Rwechungura from Statoil, Dr. Ambrose Itika from University of Dar es Salaam, for their contribution, encouragement, insightful comments towards the completion of my Master Thesis.

My sincere thanks also goes to Engineer Sunday Kasheshe and Engineer Peter Sololo both from PAET, and Engineer Felix Nanguka from TPDC for offering a place for my Master Thesis study and the guidance and contribution they provided is appreciated.

I would like to thank Statoil Tanzania through AnThei program and the program coordinator Dr. Ambrose Itika for supporting me financially during my stay in Trondheim, Norway and in Tanzania.

I thank my fellow students without forgetting Zuhura Nuru, for the stimulating discussions, for the sleepless nights we were working together before deadlines, and for all the fun we have had in the last two years together.

Last but not the least; I would like to thank my family and my girlfriend, Magreth Wambura as they were always there cheering me up and stood by me through the good and bad times.

CONTENTS

LIST OF FIGURES

LIST OF TABLES

NOMENCLATURE

Symbol	Meaning
ALRDC	Artificial Lift Research and Development Council
bbls	Barrels
CAPEX	Capital Expenditure
^{o}C	Degree Celsius
^{O}F	Degree Fahrenheit
^{o}R	Degree Rankine
re	Drainage radius, ft
ESP	Electrical Submersible Pump
ft	Feet
Z	Gas deviation factor
B_g	Gas formation factor
GLR	Gas Liquid Ratio
μ_g	Gas viscosity, cp
IPR	Inflow Performance Relationship
ID	Internal diameter
Pc max	Maximum Casing build up pressure
Nc max	Maximum Plunger Cycles
MMscf/D	Millions standard cubic feet per day
Pc min	Minimum Casing build up pressure
NPV	Net Present Value
OPEX	Operational Expenditure
PAET	Pan African Energy Tanzania
Wp	Plunger weight
Pp	Plunger weight pressure, Psia
lbm	Pound Mass
lbs	Pounds
Psia	Pounds per square inch absolute
PV	Present value

PCP	Progressive Cavity Pump
Ppr	Pseudo reduced Pressure
Tpr	Pseudo reduced Temperature
Ppc	Pseudocritical Pressure
Tpc	Pseudocritical Temperature
C*	Relative closeness to ideal solution
k	Reservoir permeability, md
S+	Separation from the ideal solution
`S-	Separation from the negative ideal solution
Fgs	Slippage factor
SS7	Songo-Songo 7
STB	Standard Barrel
q_g	Surface critical gas rate, MMscf/d
TPDC	Tanzania Petroleum Development Corporation
TOPSIS	Technique of Order Preference by Similarity to Ideal Solution
V_t	Terminal velocity, ft/sec
Mscf	Thousand standard cubic feet
$	US Dollar
VLP	Vertical lift performance
WGR	Water Gas Ratio
rw	Wellbore radius, ft

1. INTRODUCTION

Liquid loading is a common problem which occurs at any time during the production life of the gas well. This problem occurs as results of decreased gas lifting velocity to transport the produced liquid in the wellbore to surface. When the gas velocity falls below minimum lifting velocity called critical velocity, the liquid produced falls back and accumulates in the wellbore.

The accumulated liquid with time increases and creates the additional backpressure which leads to increased flowing bottomhole pressure higher than the near wellbore formation pressure. The increased bottomhole pressure higher than the formation pressure restricts the gas flow from the formation to the wellbore. With time this tendency will cause the well to cease flowing and finally the decision to abandon the well if no action to control liquid is implemented.

Due to the significant impact of liquid loading on gas wells production, the need to have the technology of handling this problem in place was important. Several liquid unloading technologies exist but each technology has different limitations for their applications depending on the well and field operating conditions. This means that not every technology is appropriate for every given well conditions but their applications needs to be evaluated depending on the existing technical and economical availability.

The Songo-Songo gas field like any other field during its production life may experience liquid loading problem. Following the rapid production decline observed in the gas well SS7 found in the Songo-Songo field, liquid loading study was initiated to find out if it was the cause for production decline.

The study to investigate and predict liquid loading problem from the historical production data recorded by the well operator (PAET) was performed during my specialization project and gave positive results (Magige, 2016). The prediction results in **Figure 31** were based on the Turner critical gas rate which was higher than actual gas production rate during the production period in 2016.

The rapid dropping of the gas production rate from the well SS7 was then anticipated to be caused by the found liquid accumulation problem. The gas flow velocity has decreased and the accumulated liquid created an additional backpressure which increased the flowing bottomhole pressure higher than the near wellbore formation pressure. The increased flowing bottomhole pressure restricted gas flow into the well leading to the observed rapid gas production decline.

The discovery of the existence of liquid loading problem in the well SS7 created a new challenge on how to remove such liquid to surface as a means of lowering the flowing bottomhole pressure. This study involved the identification of several techniques available for unloading gas wells and evaluating each method across technical and economic factors and finally to recommend the most suitable method for eradicating liquid loading problem in the well SS7. To fulfil the requirement of this study the following objectives were set.

1.1 Main Objective:

1. To determine the most suitable deliquification method for Songo Songo well SS7

1.1.1 Specific Objectives

1. To review liquid production and liquid loading problem in the well SS7.
2. Establish criteria for technical and economical evaluation.
3. Perform technical evaluation on the deliquification methods based on the identified technical criteria available for SS7.
4. Perform economic analysis for each deliquification option available using NPV.
5. Select the most suitable method based on the technical and economical evaluation results
6. Undertake a predesign of the operating parameters for the selected deliquification techniques.

1.2 Time Plan

The timeline presented using Gantt chart given in **Figure 1** was employed in achieving the objective of this master thesis study.

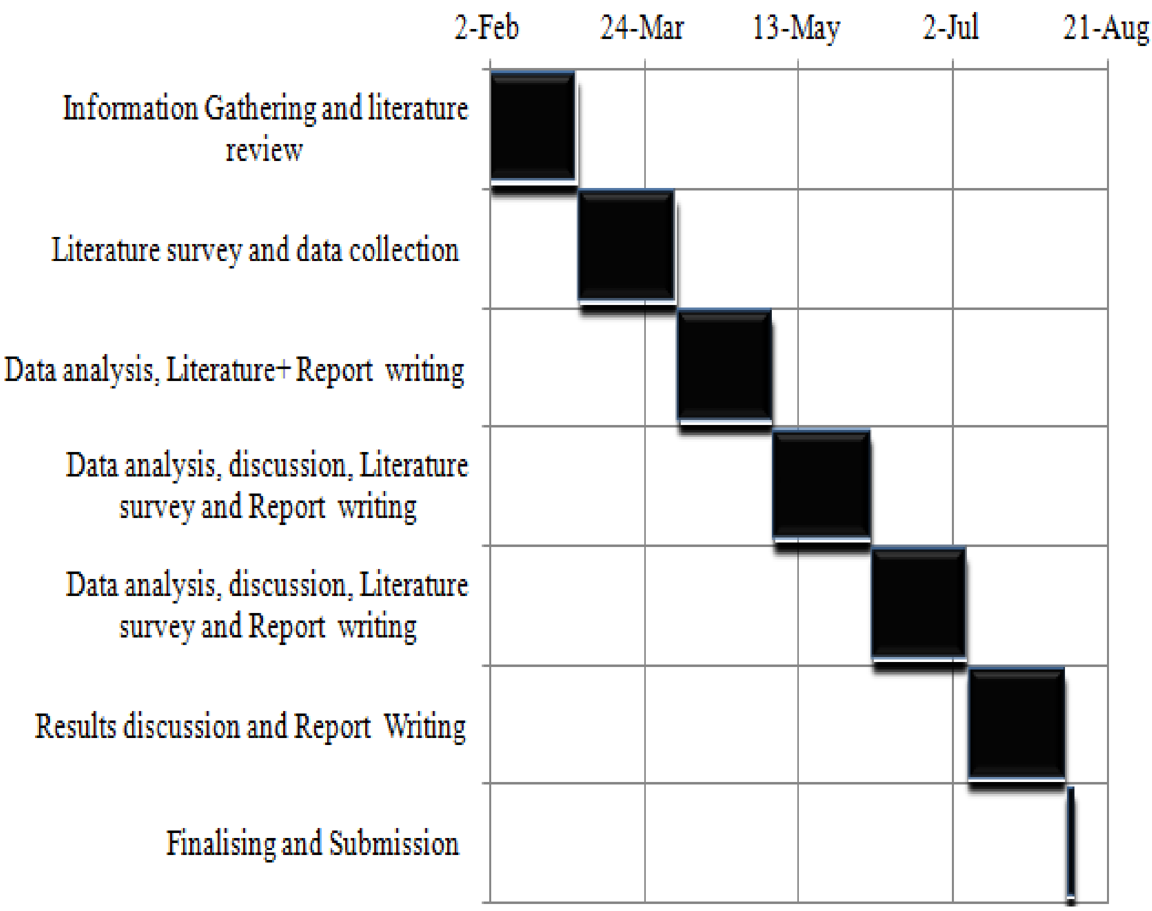

Figure 1: Thesis timeline.

2. LITERATURE REVIEW

2.1 Liquid loading

Any gas well that produces liquid during its production life will experience liquid loading problem at low gas rate. Liquid loading in gas wells is a multiphase flow phenomenon where the liquid content of the well creates backpressure that restricts, and in some cases even stops, the flow of gas from the reservoir.

The main cause of liquid accumulation in the well is the low tubing gas velocity which becomes unable to lift the produced liquid from the wellbore to surface. **Figure 2** shows the effect of gas velocity in handling the produced liquid to surface.

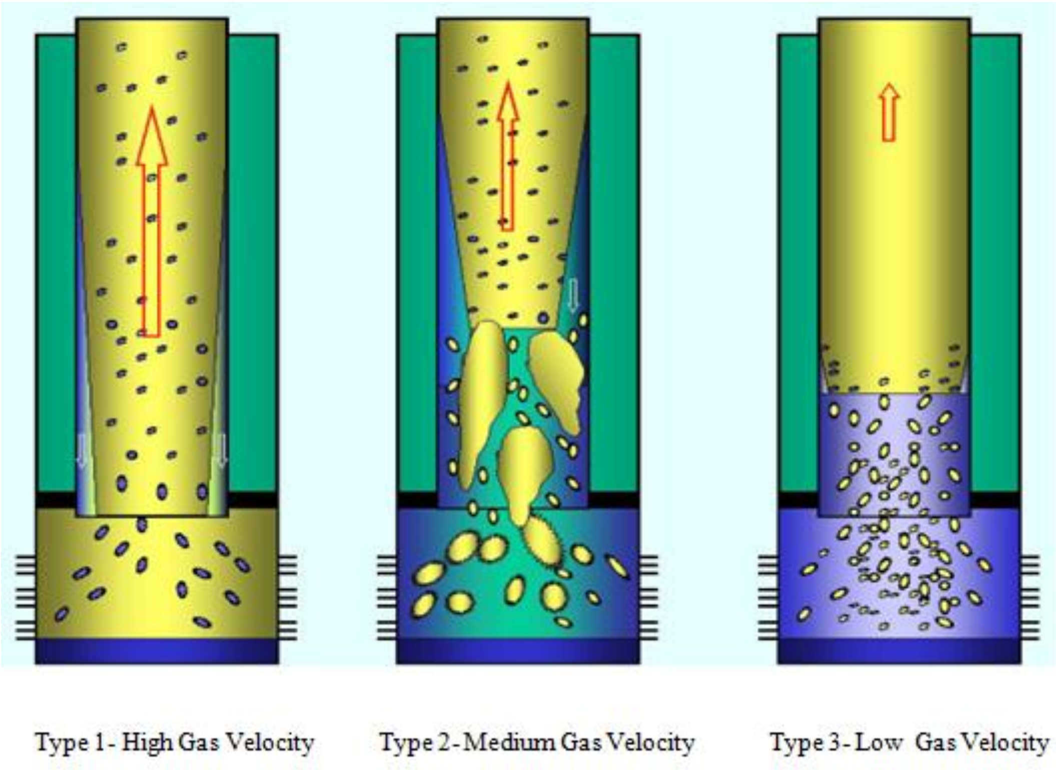

Figure 2: The three types of two phase flow in gas wells **(Rowlan, et al., 2006)**

2.2 Multiphase

Understanding how liquid and gas phases interacts in the well under the existing flowing conditions provides an idea on the flow regime changes in gas wells. The multiphase flow in a vertical conduits is usually represented by four flow regime transitions which are mist to annular, slug-annular transition, slug and bubble flow. During the production life of the gas well, any one of the flow regime or all can be experienced. As time increases and production declines, flow regime from perforation to the surface will change as the gas velocity decreases.

2.3 Sequence of Events for Liquid Loading.

Liquid loading processes pass through several sequences of events before the well stops producing (Waltrich & Barbosa, 2011). **Figure 3** describes different sequences of events which the gas well producing liquid can pass through before it is abandoned due to liquid loading problem.

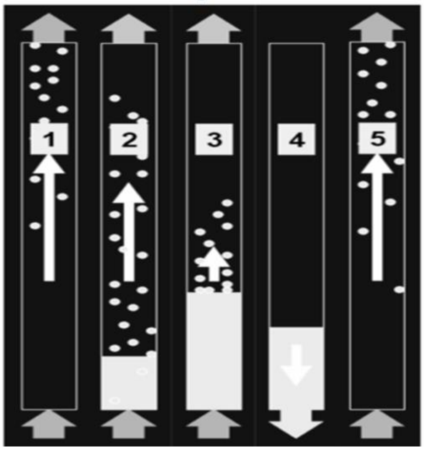

Figure 3: Sequences of events for liquid loading, **(Waltrich & Barbosa, 2011)**.

i. **Event 1:** Gas flow velocity is high enough for lifting all the produced liquid to surface.

ii. **Event 2:** Liquid began flowing back into the wellbore due to decreased gas rate.

iii. **Event 3:** Gas flowing into the wellbore becomes blocked due to increased flowing bottomhole pressure.

iv. **Event 4:** The accumulated liquid flow into the formation due to increased flowing bottomhole pressure higher than the near wellbore formation pressure.

v. **Event 5:** The liquid re-injected into the formation recharge the near wellbore pressure until it is high enough to carry produced gas and liquid to surface again.

The well ceases to flow when the reservoir becomes no longer capable of recharging the near wellbore pressure to a level of lifting gas and the produced liquid to surface (Waltrich & Barbosa, 2011).

2.4 Problem Caused by Liquid Loading in Gas Wells.

Liquid loading causes erratic, slugging flow and decreased gas production rate which can eventually lead to abandoning the well (Lea, et al., 2003).

If the liquid is not continously removed from the well due to low gas rate then the liquid will tend to flow back to the bottom of the well and accumulate. The accumulated liquid tend to create additional back pressure which increases the flowing bottomhole pressure higher than the near wellbore formation pressure. The result of the increased bottomhole pressure higher than the formation pressure is the blocking of the gas flow to the wellbore thus killing the well.

2.5 Liquid Loading Identification in Gas Field

To recognise the existence of liquid loading in the gas well, the preliminary symptoms which need to be studied from historical well production includes the following (Lea & Nickens, 2004; Joseph, et al., 2013):

i. Liquid slug produced at the surface of the well,
ii. Sharp drops in decline curve,
iii. Tubing pressure decreases as the casing pressure increases,
iv. The sharp, distinct change in pressure gradient,
v. Reduction of Liquid gas ratio.
vi. Gas production fluctuation.

2.5.1 Liquid Slug Production at the Surface.

For efficient liquid transport in the production string, the mist to annular flow regime needs to be maintained. Any flow regime changes makes liquid transports difficult. Thus production of liquid slug at the surface is the indication that gas is no longer continuous and the produced liquid has started to accumulate at the bottom of the well at low gas velocity.

The flow regime changes in gas wells are recognized by using a gas measuring flow devices called two pen pressure recorders (Schiferli, et al., 2010). **Figure 4** shows different reading recorded from the measuring device for situation with mist flow and situation with slug production. Mist flow represents situation without liquid loading and slug flow means liquid loading exists in the well.

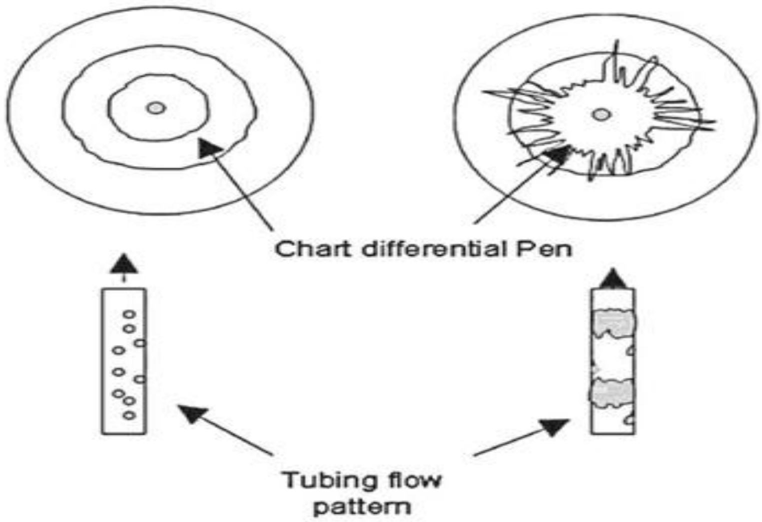

Figure 4: Differences between mist flow and the slug flow **(Schiferli, et al., 2010)**.

2.5.2 Decline Curve Analysis

The existence of liquid loading in a given well affects the nature of the forecasted decline curve. In a gas well with liquid loading the decline curve comes to abandonment at early time and sometime scattered production compared to the forecasted normal decline curve (Schiferli, et al., 2010). **Figure 5** shows the effects of the liquid loading on the nature of the decline curve.

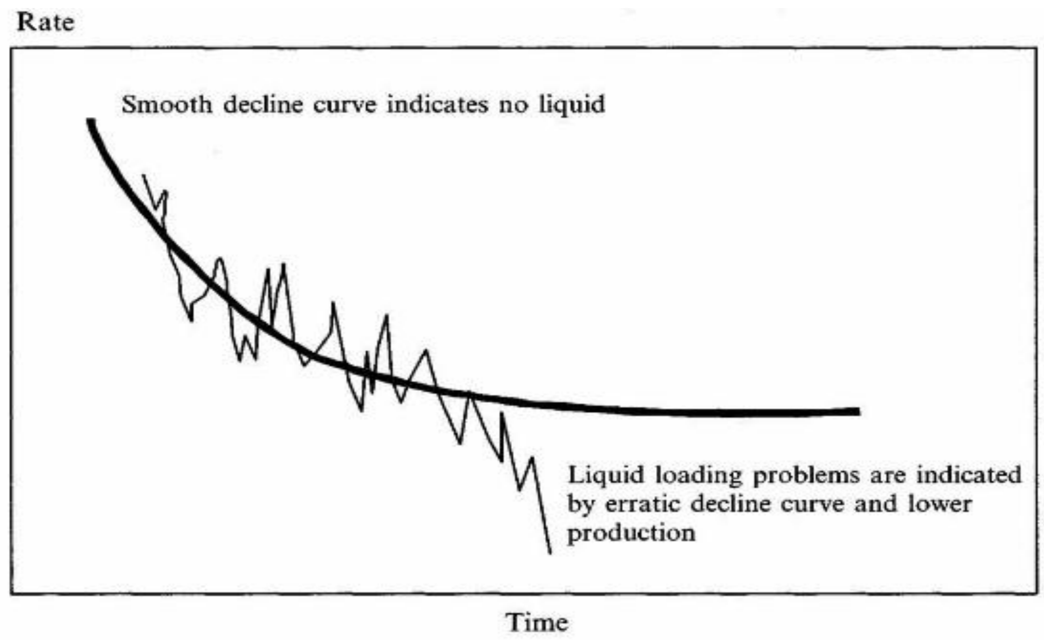

Figure 5: effect of liquid loading on decline curve **(Schiferli, et al., 2010)**.

2.5.3 Increased Pressure Difference Between Casing and Tubing.

For a packer-less completion, as the liquid accumulates in the tubing, casing pressure increases and the tubing pressure decreases with time (Lea, et al., 2008)**. Figure 6** illustrates the effects of liquid loading on the variation of casing and tubing pressure with time.

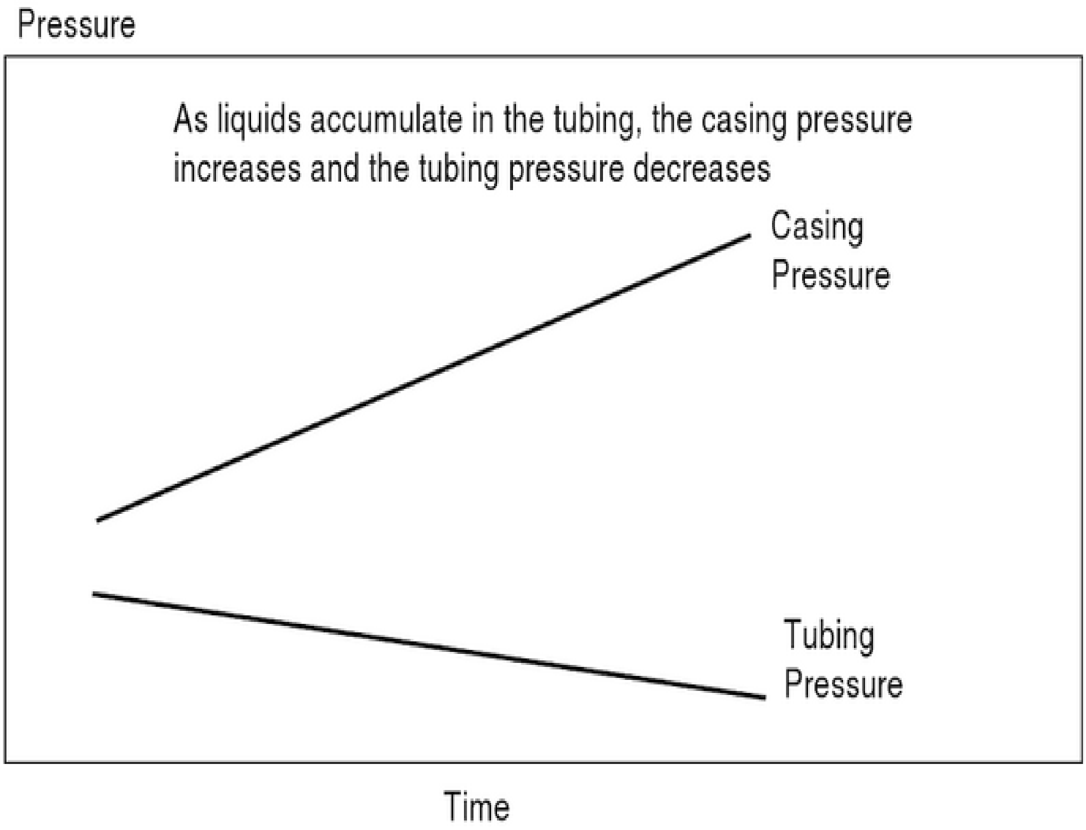

Figure 6: Pressure differences between casing and tubing with time (Lea, et al., 2008).

2.5.4 Change in Pressure Gradient**.**

Pressure gradient is affected by fluid density and depth, for a single phase gas flowing in the tubing the pressure gradient curves are always linear. When fluid changes from gas to liquid the shape of pressure gradient is affected and becomes no longer a linear curve (Lea, et al., 2008; King, 2005). Figure 7 shows the effect of fluid changes in the tubing on pressure gradient curve.

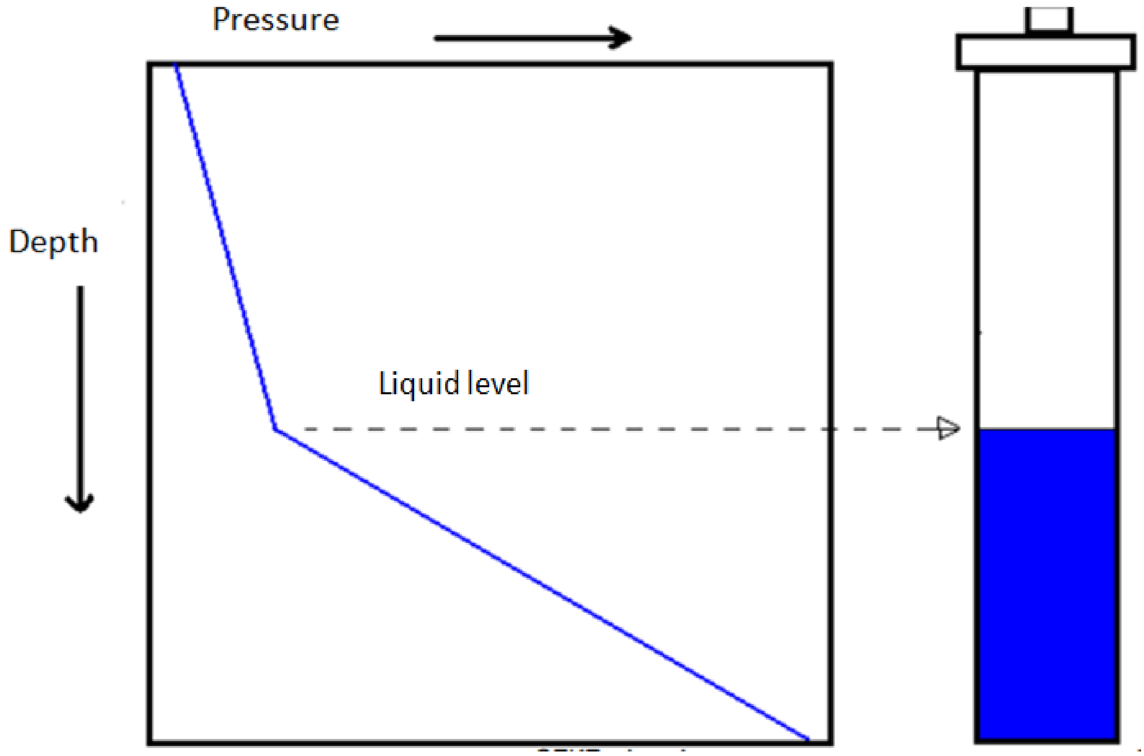

Figure 7: Typical pressure gradient curve affected by fluid changes (King, 2005).

2.6 Liquid Loading Prediction

Various liquid loading prediction methods have been published in literature but the basic method which was used as the reference were proposed by Turner. Turner developed a stand-alone model which is used to predict liquid loading using critical gas velocity. There have been several developments on Turner model depending on the requirement which resulted to other models such as Coleman model, Noisier model and LI's Model (Lea, et al., 2003; Nallaparaju, 2012).

The other available approach for predicting liquid loading in gas well was the system performance curve which involves intersecting the tubing curves with IPR curves (Lea & Tighe, 1983).

2.6.1 Turner Droplet Model.

Turner droplet model was derived from the two physical models which are (1) Liquid film model and (2) Entrained liquid droplets model, (Nallaparaju, 2012). Upon evaluation for the two physical models, liquid droplets model was proposed to best suit in predicting minimum gas velocity in field data compared to liquid film model (Nallaparaju, 2012).

The derivation of Turner droplet model was based on the force balances on the largest liquid droplet with drag force acting upwards and the weight acting downward. The terminal velocity of liquid droplet in the gas stream derived from force balance on large droplet was given by equation 1 below.

$$V_t = \frac{1.593\sigma^{\frac{1}{4}}(\rho_l - \rho_g)^{\frac{1}{4}}}{\sqrt{\rho_g}} \qquad 1$$

Where ρ_l and ρ_g stands for liquid and gas phase density respectively in lbm /ft^3.

2.6.1.1 Gas Density.

The gas density used in equation 1 depends on pressure and temperature because gas is compressible unlike liquid density which is constant at different pressure and temperature. The relationship between pressure, temperature and gas density was given by using real gas equation in equation 2 and 3 (Whitson & Brule, 2000).

$$\rho_g = \frac{P * Mg}{ZRT} \qquad 2$$

With, ρ_g = gas density, Mg = gas molecular weight.

$$\text{Gas density } (\rho_g) = 28.97 * \frac{P * \gamma_g}{ZRT} \qquad 3$$

Assuming the constant gas gravity of 0.6, Z-factor of 0.9 and gas temperature of 120^{o}F, the gas density in equation 3 can be expressed as only pressure dependent as shown in equation 4 (Nallaparaju, 2012).

$$\rho_g = 0.0031P \qquad 4$$

2.6.1.2 Gas Deviation Factor

Gas deviation factor (Z) used in equation 2 and 3 depends on pressure and temperature. For a known gas gravity, Z-factor are easily determined from standing Kartz chart in Figure 8 which are solved pseudo reduced conditions computed from pseudo condition given in equation 5 and 6 for dry hydrocarbon gases (Whitson & Brule, 2000).

$$Ppc = 667 + 15 * \gamma_g - 37.5 * {\gamma_g}^2 \quad 5$$

and

$$Tpc = 168 + 325 * \gamma_g - 12.5 * {\gamma_g}^2 \quad 6$$

Pseudo reduced pressure and temperature at the operating pressure and temperature are solved using equations 7 and 8.

$$Ppr = \frac{P}{Ppc} \quad 7$$

$$Tpr = \frac{T}{Tpc} \quad 8$$

Table 1: Liquid properties for critical gas velocity calculation (Nallaparaju, 2012)

Condensate Surface tension	20	dynes/cm
Water Surface tension	60	dynes/cm
Condensate density	45	lbm/ft^3
Water density	67	lbm/ft^3

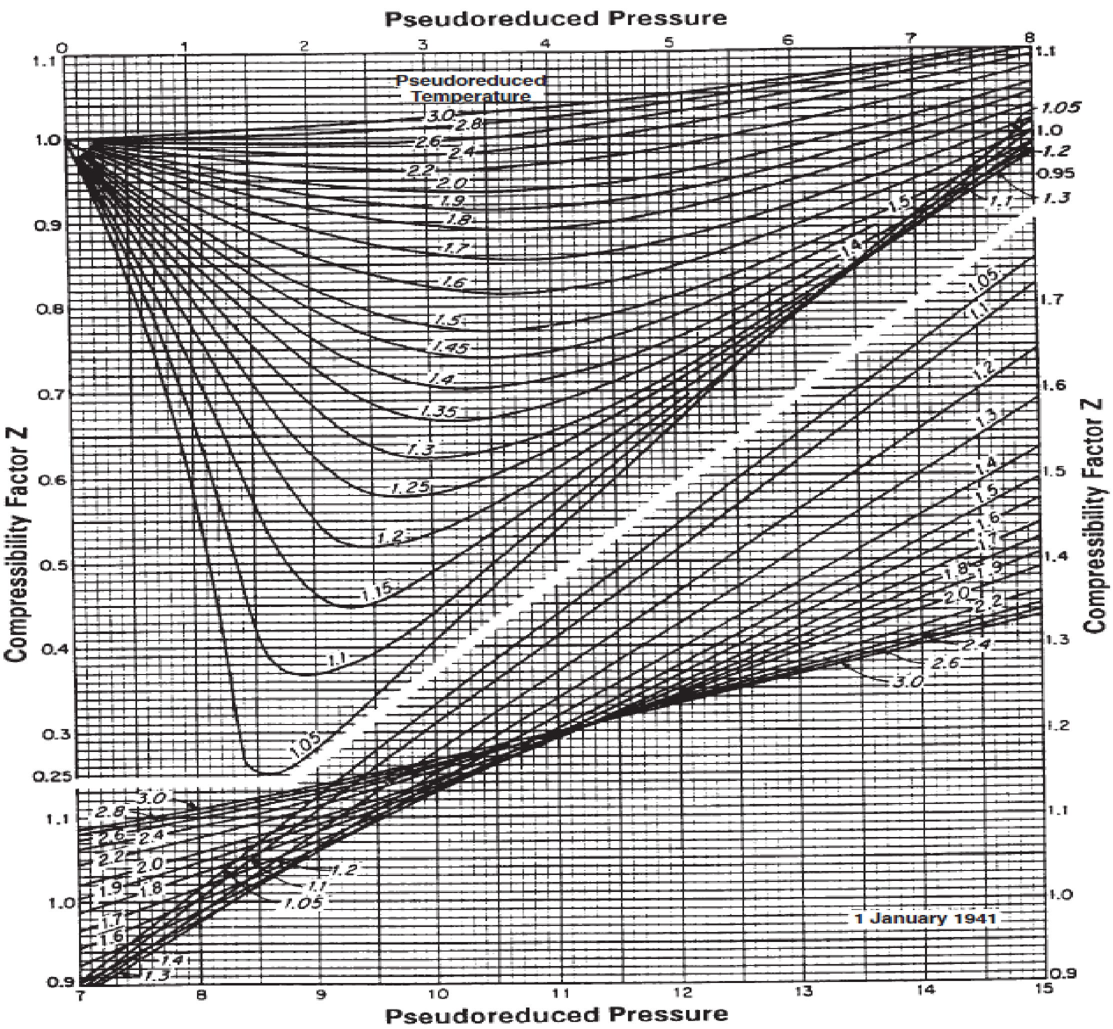

Figure 8: Standing Kartz chart (Whitson & Brule, 2000)

2.6.1.3 Critical Gas Velocity

Critical gas velocity was defined as the gas velocity below which liquid loading occurs. When the gas well flow at gas velocity above critical gas velocity all liquid tend to flow to surface but when gas velocity fall below critical velocity some liquid produced with gas tend to fall back and accumulate in the wellbore.

The derivation of critical gas velocity was based on several assumptions given in Table 1 and modified terminal gas velocity given in equation 1 to account for the type of liquid produced.

When the produced liquid is water Equation 1 was modified to equation 9 and equation 10 when the liquid is condensate.

$$V_{c,Water} = 5.304\frac{(\rho_w - \rho_g)^{\frac{1}{4}}}{\sqrt{\rho_g}} \quad 9$$

$$V_{c,Condensate} = 4.03\frac{(\rho_c - \rho_g)^{\frac{1}{4}}}{\sqrt{\rho_g}} \quad 10$$

When both water and condensate are produced from the well, water equation in 9 is preferably used in calculating critical gas velocity than condensate equation 10 because of its density being high than density of condensate (Nallaparaju, 2012).

2.6.1.4 Applicability of Turner Method

Turner droplet model can be applied using either the wellhead or wellbore conditions depending on the operating range of the flowing wellhead pressure. When operating wellhead pressure is less than 100Psia, bottomhole conditions becomes most appropriate for predicting critical velocity from Turner model otherwise Wellhead conditions are preferred (Sutton, et al., 2009). Figure 9 below shows the boundary conditions for evaluating critical gas velocity.

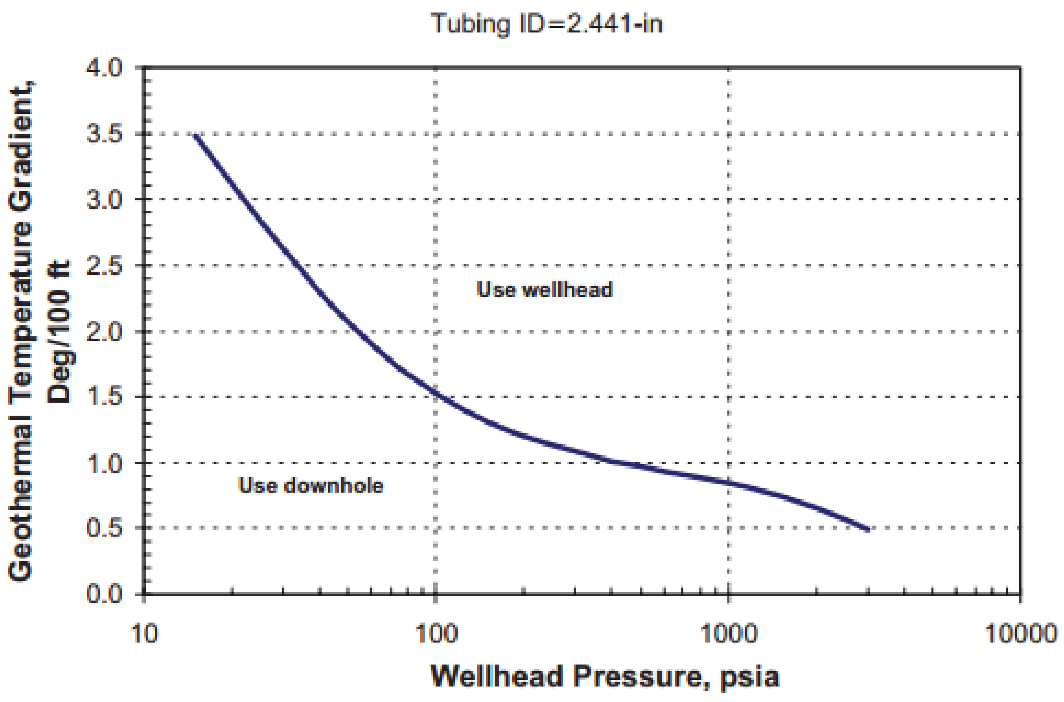

Figure 9: Boundary conditions for Turner critical velocity evaluation (Sutton, et al., 2009)

2.6.1.5 Critical Gas Rate Calculation

The calculated critical gas velocity from equation 9 and 10 can be converted to critical gas rate using equation 11 for comparison with the reported actual well gas rate. The gas rate was related to gas velocity and tubing cross section area 'A' by equation 11 (Lea, et al., 2008).

$$q_g = \frac{3.067PV_gA}{(T + 460)Z} \quad \text{MMscf/D} \qquad \textbf{11}$$

Where

$A = \frac{\pi {d_t}^2}{4x144}$, ft^2

T = surface temperature, ^{0}F

P = surface pressure, psi

A = tubing cross-section area

$d_{t\,=}$ tubing ID, inches

The constant 3.067 in the equation 11 transform velocity in (ft/sec) to ft/D (Wang, et al., 2009).

2.6.2 Prediction of Liquid Loading Conditions Using Performance Curves.

The intersecting of the IPR and the VLP curves are may be the other useful tools to predict liquid loading conditions.

2.6.2.1 The Tubing Performance Curves

The tubing performance curves is generated at a constant GLR, well depth and surface pressure and calculating the required bottomhole pressure at different gas rate (Brown, et al., 1984).

2.6.2.2 Inflow Performance Relationship Curve

IPR is generated for gas well using backpressure curve (Brown, et al., 1984) provided in equation 12 below.

$$q = C(P_R{}^2 - P_{wf}{}^2)^n \qquad \textbf{12}$$

Where

Q= gas flow rate, Mcfd

C= coefficient determined from well data, Mcfd/Psia

PR= shut in static reservoir pressure, psia

n= backpressure exponent

Intersecting tubing performance curves with the inflow performance relationship are useful in estimating the operating rate and pressure for given well which are read from their point of intersection as in Figure 10 .

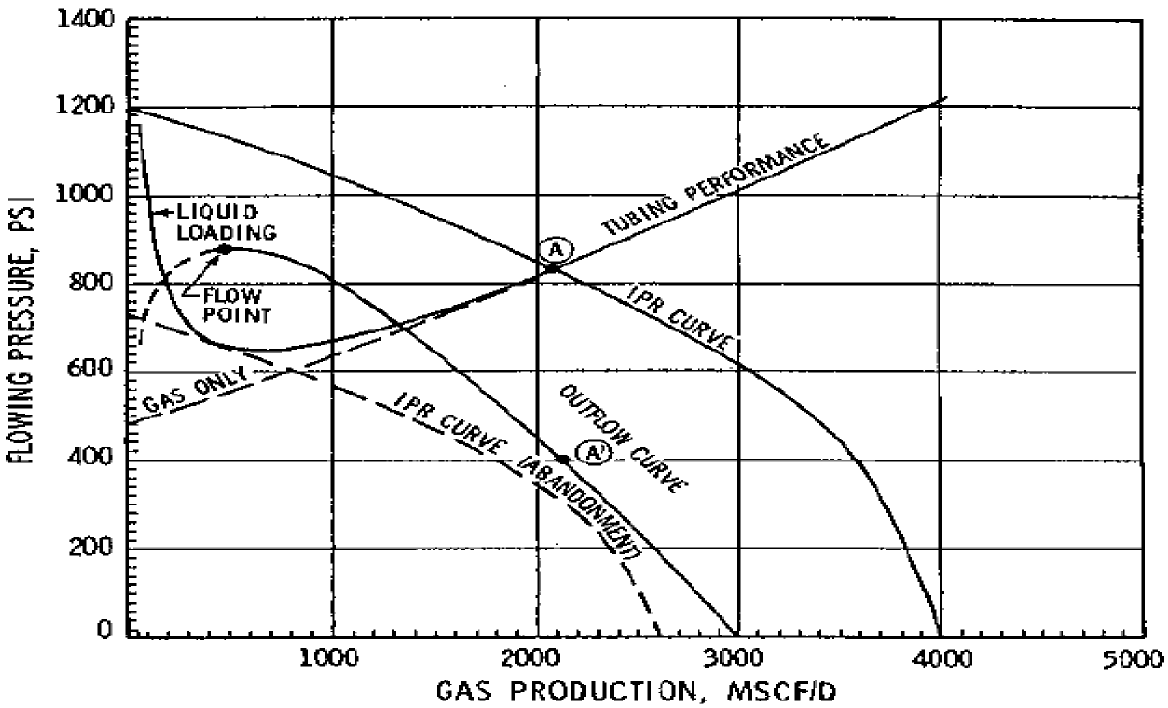

Figure 10: Example of the performance curve with some liquid productions (Brown, et al., 1984)

The performance curves can be used to predict liquid loading as for example from Figure 10 the when the IPR decline and intersect the tubing performance curve tangential this denote the abandonment because the well cannot produces unless energy is added to lift flow (Brown, et al., 1984).

Figure 10 has indicated two different tubing performance curves one affected by liquid production curves at low rate and if only gas flowing in the well the tubing performance curves becomes straight line.

2.7 Sources of Liquid in Gas Wells.

The liquid produced from gas wells may have different sources;, some may be from the aquifer which is mostly saline water, coning from the water zone above or below the production zone, liquid hydrocarbon and water vapor condensing from gas phase due to changes in pressure and temperature (Lea, et al., 2003).

A gas well producing liquid may have liquid production from all sources or from certain source depending on the production conditions. Due to changes of the well operating conditions, liquid production can be observed sometimes during the production life of dry gas well. The liquid from condensation process drop out of gas phase when the operating condions fall below dew point at any point along the production system.

2.7.1 Hydrocarbon Condensation

The gas exists as a single gas phase or dry gas only when the operating conditions is above the dew point. The heavy hydrocarbon sometimes called condensate are produced from dry gas wells when the operating conditions fall below the dew point. When the operating reservoir temperature is above cricondetherm there will be no liquids production in the reservoir but still liquids can condense out of the gas phase along the production system when the operating conditions falls below dew point (Lea, et al., 2003; Whitson, 2016).

At the initial reservoir conditions gas reservoir exists as a single gas phase. Under certain conditions of temperature and pressure these fluid will separate into two separate phases, a gas and the liquid (Whitson, et al., 2005/2006; Whitson, 2016). **Figure 11** and **Figure 12** represent the phase envelopes for dry gas and gas condensate reservoirs.

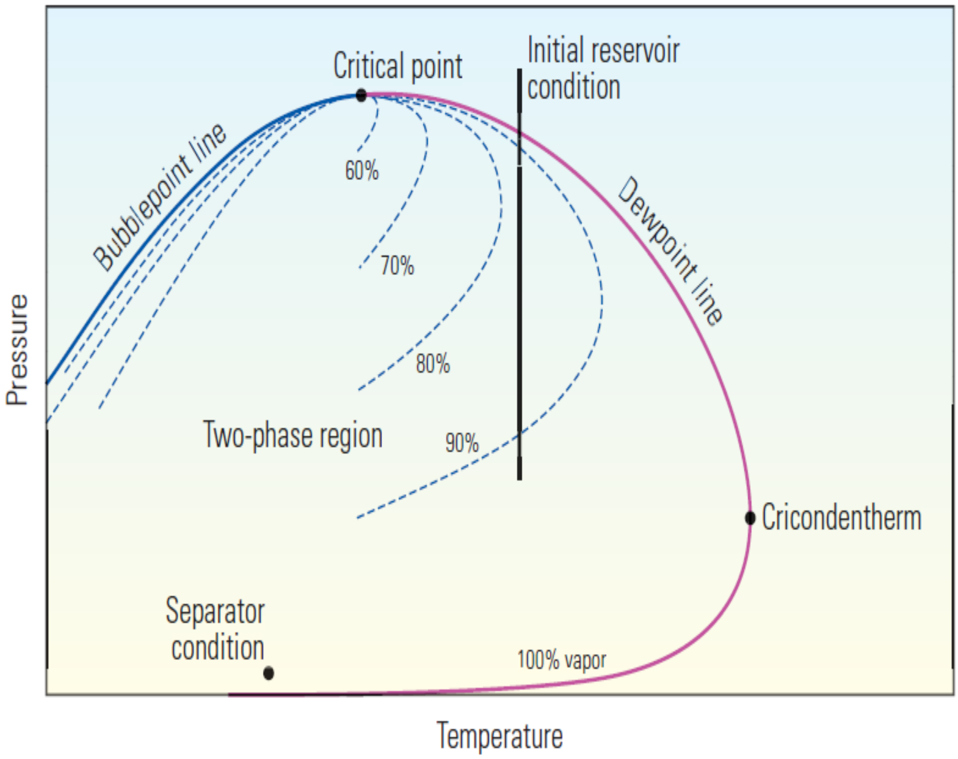

Figure 11: Phase envelope for gas condensate reservoir.

(Courtesy: Whitson et al, 2005/2006)

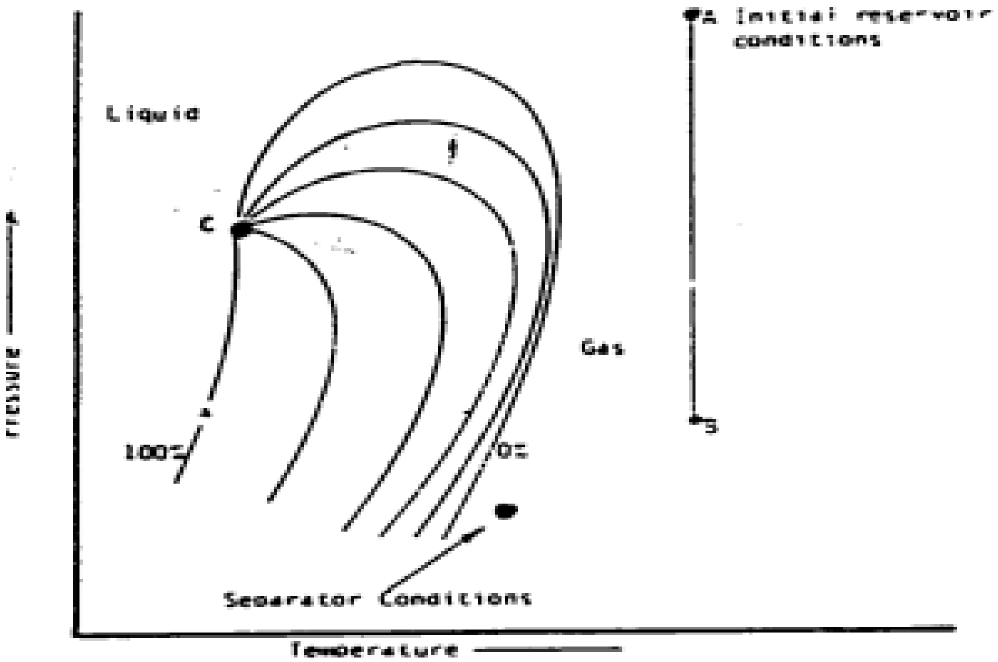

Figure 12: Phase envelope for a dry gas reservoir **(Mucharam, et al., 2006)**.

2.7.2 Condensed Water

Water vapor contained in the gas at some conditions drop out and the process of water vapor to condense from gas phase depends on pressure decline for a given reservoir temperature which is assumed constant as shown in **Figure 13**.

The effect of water vapor condensation in the wellbore is liquid accumulation over the perforation or pay zone when gas flow velocity is below critical velocity.

The other effect of water vapor condensate apart from liquid accumulation is corrosion problems which may occur at a point in the wellbore where condensation first occurs. At the surface Condensed water and the formation water are distingushed based on their salt content, condensed water has no salt content.

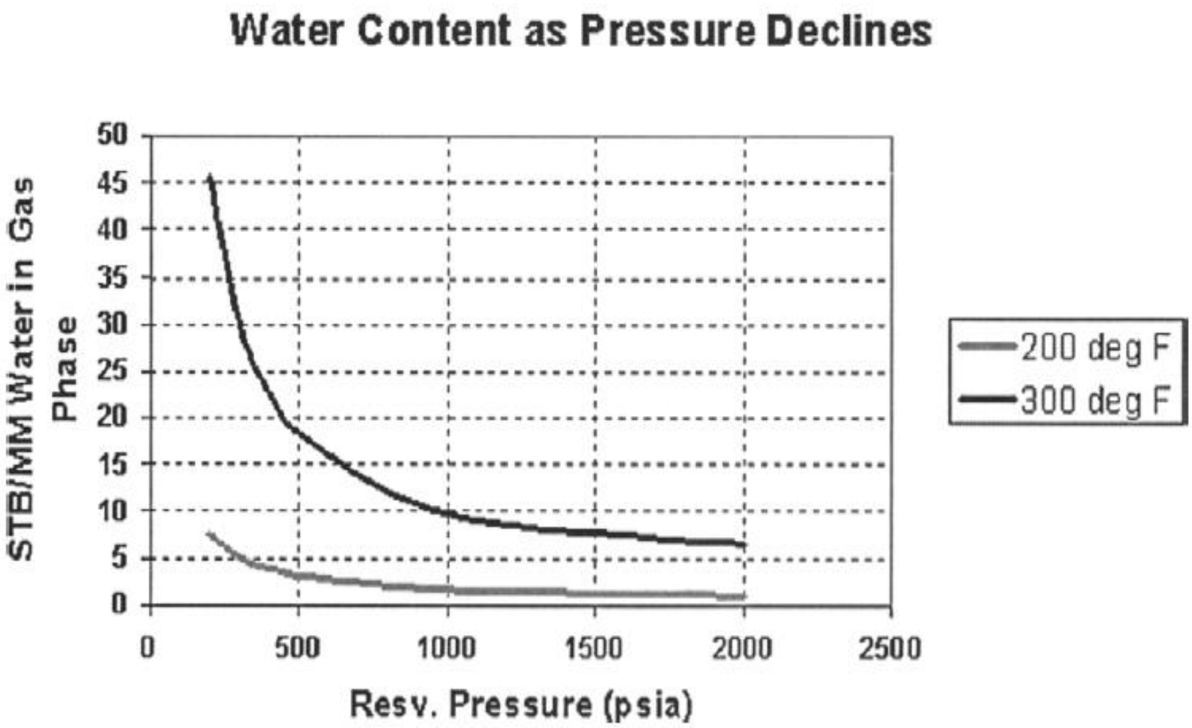

Figure 13: Solubility of water in natural gas as pressure decline.

Several correlations are available for estimating water vapor content in natural gas but the most common correlations are Bukacek correlations and Mcketta and Wehe chart which are useful for the gas well with sweet gas (Ghiasi & Bahadori, 2014).

The Bukacek correlations given in the equation 13 was derived without the correction of water salinity and gas gravity are useful in estimating the amount of water content in gas phase (Mucharam, et al., 2006).

$$W(\frac{\mathrm{lbm}}{\mathrm{MMscf}}) = \frac{A(T)}{P(\mathrm{Psia})} + B(T) \qquad \textbf{13}$$

where

$$A(T) = 10.9351 - 2949.05T^{-1} - 318.045T^{-2}, \qquad \textbf{14}$$

$$B(T) = 6.69449 - 3083.87T^{-1} \qquad \textbf{15}$$

and T is in ^{o}R.

Bukacek correlation for water content estimation in gas phase was found to be applicable at temperatures higher than 288.15K (Ghiasi & Bahadori, 2014).

Mcketta and wehe chart in Figure 14 was the other most useful means which are used in estimating the amount of water content in natural gas. The advantages of Mcketta and Wehe chart was inclusive corrections for salinity and gas gravity (Whitson & Brule, 2000; Mucharam, et al., 2006).

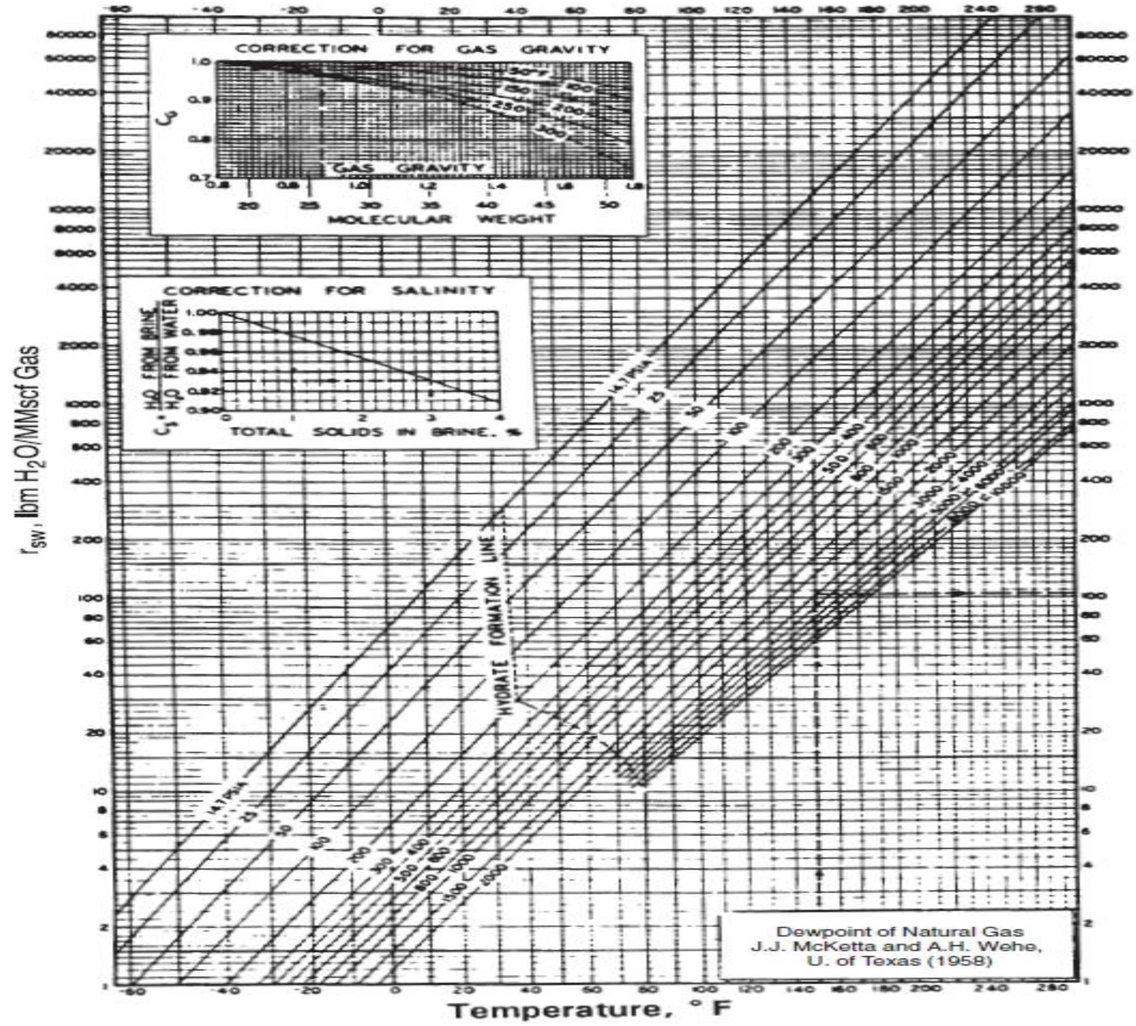

Figure 14: Water solubility in natural gases, with gas composition and salinity effects **(Whitson & Brule, 2000)**.

Figure 14 has indicated that McKetta and Wehe chart contains two charts inserts for correcting pure water solubility for salinity and gas gravity which can be given by the best fit equations 18 and 19 (Whitson & Brule, 2000).

Water vapour contents estimated from McKetta and Wehe charts can also be estimated analytically using some correlations developed from the charts (Whitson & Brule, 2000). In using these equations water content in gas estimation begins by finding the amount of condensed water in gas without considering the effect of salinity and gas gravity using equation 17 and then transforming the estimated water vapour content using equation 16 to include the effect of salinity and gas gravity.

$$y_w = y_w{}^o A_g A_s \qquad 16$$

$$\ln(y_w{}^o) = \frac{0.05227 * p + 142.3 * \ln(p) - 9625}{T + 460} - 1.117 * \ln(p) + 16.44 \qquad 17$$

$$A_g = 1 + \frac{\gamma_g - 0.55}{(1.55x10^4)\gamma_g T^{-1.446} - (1.83x10^4)T^{-1.288}} \qquad 18$$

$$A_s = 1 - (3.92x10^{-9})C_s{}^{1.44} \qquad 19$$

T in Fahrenheit, P is in psia, and Cs is in ppm or mg/L

y_w is the corrected mole fraction of water in gas and

$y_w{}^o$ is uncorrected mole fraction for water in gas

The calculation of mole fraction helps to estimate the amount of water dissolved in gas given as the ratio provided by the following equation 20 or 21 depending on the required unit;

$$r_{sw\,(\frac{STB}{MMscf})} = 135 * \frac{y_w}{1 - y_w} \approx 135 * y_w \qquad 20$$

Or

$$r_{sw}\,(\frac{lbm}{MMscf}) \approx 47300 * y_w \qquad 21$$

2.7.3 Water Coning.

Coning is a production problem in which bottom water infiltrates the perforation zone in the near-wellbore area and reduces gas production. Water coning can impact well productivity and increases water treatments requirements (Lee & Tung, 1990). Few studies have been performed in understanding the mechanism of water coning in gas wells as compared to the oil wells. Water coning in gas wells was generally understood as the term similar that occurring in oil wells (Armenta & Wojtanowicz, 2002) though there have been different responses on the behaviour of water coning for gas wells and oil wells.

For example Muskat(1982) believed that physical mechanism of water coning in gas wells was identical to that for oil wells While McMullan and Bassioni believed that water coning behaves differently in gas wells than in the oil wells (Armenta & Wojtanowicz, 2002).

Water Coning Prediction

Various literatures have published a number of coning prediction methods and most coning method predicts critical rate at which a stable cone can exist from the fluid contact to the nearest perforations. This means that at rates below the critical rate, the well will produce the desired single phase but at t rates equal to or greater than the critical rate, the second fluid will eventually be produced and will increase in amount with time (SPE, 2015)

Some of the correlations published for calculating the critical rate for predicting water coning in oil wells include;

i. Chaperon correlation given by equations 22 through equations 23 and 24.

$$q_c = \frac{4.888x10^{-4} k_h {h_c}^2 \Delta\rho q_{cD}}{B_o \mu_o} \qquad 22$$

$$q_{cD} = 0.7311 + \frac{1.843/r_{rD}}{\sqrt{\frac{k_v}{k_h}}} \qquad 23$$

$$r_{rD} = (\frac{r_e}{h_c})\sqrt{\frac{k_v}{k_h}} \qquad 24$$

$\Delta\rho = \text{density difference}, g/cm^3 = \rho_w - \rho_o$

$h_c = \text{distance from perforation to fluid contact}, ft$

ii. Meyer and Garder Correlations

Meyer and Garder developed analytical equations to determine the maximum allowable flow of oil into a well without water coning into the production well (Kuo & DesBrisay, 1983). The proposed equation 25 was the basic equation for calculating critical rate to prevent water coning.

$$q_c = \frac{1.5351x10^{-3}(\rho_w - \rho_o)(h^2 - D^2)K}{\mu_{OB_o} \ln\left(\frac{re}{rw}\right)} \qquad 25$$

iii. Schols Method

This correlation was developed based on the experimental works to calculates critical rate for preventing water coning to production zone (Kuo & DesBrisay, 1983). Equation 26 represents empirical formula developed by Schols.

$$q_c = \left[\frac{(\rho_w - \rho_o)(h^2 - D^2)K}{2049\mu_{OB_o}}\right]\left[0.432 + \frac{\pi}{\ln\left(\frac{re}{rw}\right)}\right]\left(\frac{h}{r_e}\right)^{0.14} \qquad 26$$

q_c = Critical production rate, $\frac{STB}{Day}$

h = Oil zone thickness, ft

D = Perforation interval, ft

μ_O = Oil viscosity, cp

B_o = Oil formation factor, Rb/STB

K = Reservoir permeability, md

r_e = Drainage radius, ft

r_w = Wellbore radius, ft

3. SONGO - SONGO GAS FIELD.

3.1 Field Description

The Songo - Songo field is a proven gas bearing structure located in the vicinity of Songo - Songo island, offshore Tanzania. The Island is a low relief, rough coral landmass surrounded by a broad, shallow water and intertidal coral platform and is located some 25km northeast of kilwa kivinje and approximately 160km south of dar es salaam (Kaye & Shannon, 1982).

Songo-Songo gas field was the first developed and the largest commercial producing gas field in Tanzania and East Africa (Williams, 2009).

Figure **15** is the summary of Songo-Songo field development from 1974. Based on the field development summary in

Figure 15 has indicated that the first gas was observed in 2004.

The wells in the Songo-Songo gas field were drilled both onshore and offshore as presented in Figure 16 (Bujulu, 2013).

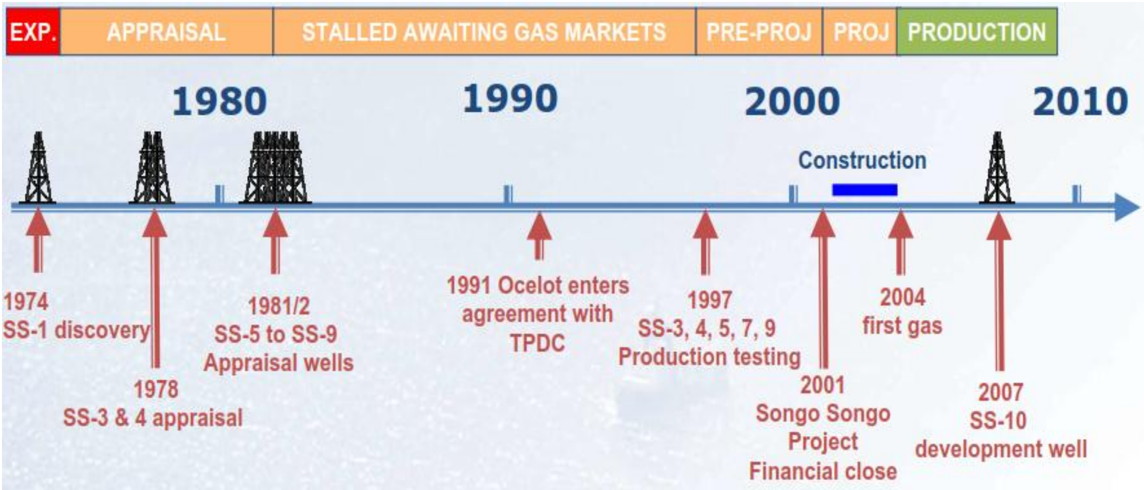

Figure 15: Songo-Songo field development summary **(Williams, 2009)**.

Figure 16: The location of the production gas wells at the Songo-Songo Island **(Bujulu, 2013)**.

3.2 Songo-Songo Gas Wells

Songo-Songo gas field have several gas wells named SS1-SS10 which was drilled from 1974 to 2007 as can be observed in Figure 15. Some additional two wells SS11 and SS12 has been discovered where SS11 is in production while SS12 is in development stage and will starts producing very soon. The well SS7 was selected for study because of the abnormal production behaviour which has been reported in the recent production period (2016). The abnormal production behaviour (rapid decline in gas production rate) observed in the well SS7 was projected to have been caused by liquid loading problem.

3.3 Gas Well SS7

SS7 was one of the several gas wells drilled on the Songo-Songo field and it was among the well exploration programme initiated to further evaluate the hydrocarbon potential of the Songo-Songo structure (Kaye & Shannon, 1982). This programme was initiated following the discovery of the gross gas column of 770 feet in the main cretaceous sand sequence.

The subsurface objectives of the location was in area where the maximum water depth were in the order of 50 ft but due to the restriction imposed by the vermillion bay of maximum water depth of 22 ft, the well was planned as a deviated well (Griffiths, 2010).

3.3.1 Well Completion

SS7 was completed with the casing diameter of 9.652inches and the tubing internal diameter of 2.992 inches from 2004 to 2015 (Kaye & Shannon, 1982). Due to declined gas production caused by increased tubing friction losses then the well operator(PAET) changed the tubing string from 2.992 inches to 3.83 inches as the means to rescure the well (Kasheshe, 2017).

The well SS7 was perforated at to an interval of 70.1ft, this perforation interval was done in phases from March, 1982 to November, 2015 as shown in Appendix X.

3.3.2 Well SS7 Historical Production

SS7 was reported to be a dry gas producer and the study done in October 2010 by Pan African Energy Tanzania to review its production status predicted the well to be producing at the gas rate of 22.3MMscfd as presented in Figure 17.

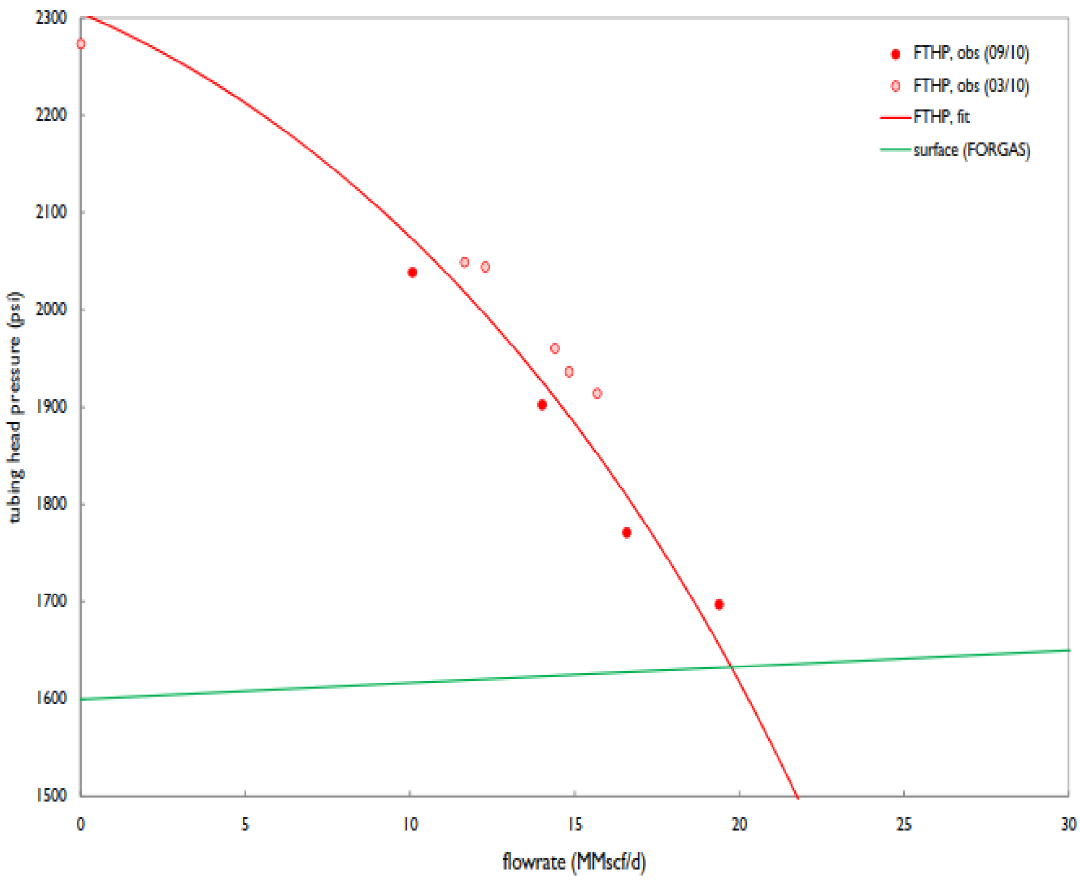

Figure 17: Tubing Deliverability Curve for SS7 (Griffiths, 2010).

The historical fluid production for SS7 gas well was reported to begin in 2004 where the only fluid produced was dry natural gas. The well continued producing only dry natural gas until in the mid 2012 when some liquid comprising hydrocarbon and water was reported to have produced (Bujulu, 2013).

The amount of the produced liquid at the surface continued to increase until when it began dropping again with the reduced gas production. Figure 18 summarises the trend of fluid production from 2012 to September 2016 based on the vendor provided historical production data.

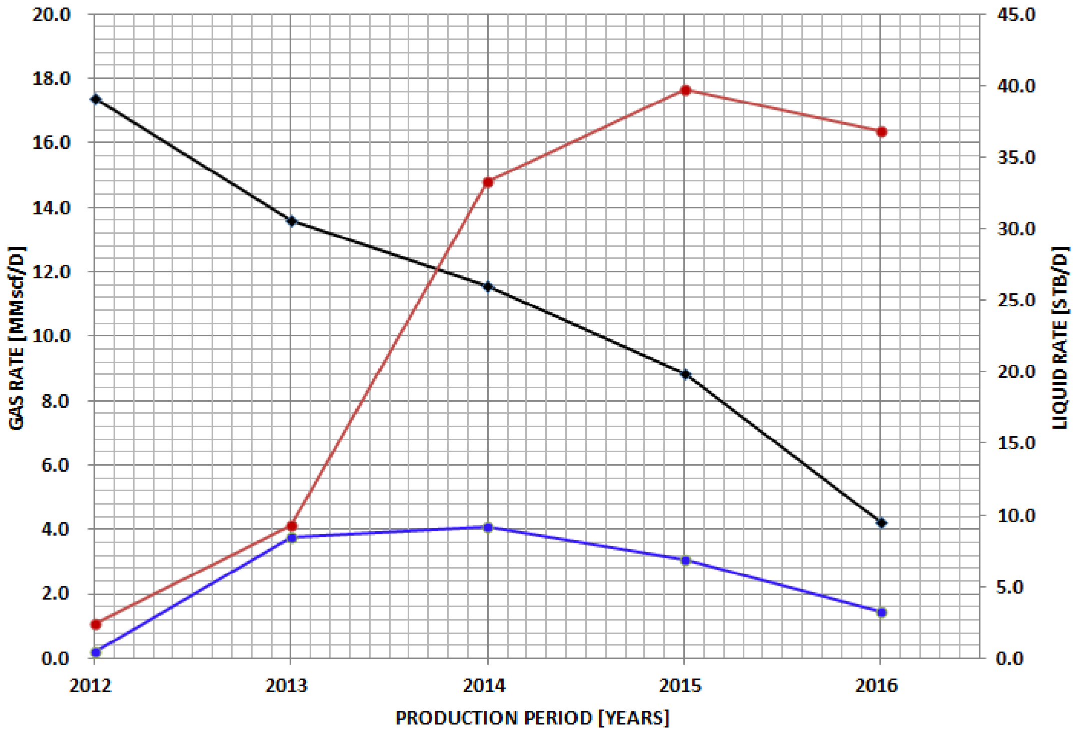

Figure 18: Historical fluid production from SS7 Gas well.

3.4 Determination of Liquid Sources in Well SS7

There exist several sources of liquid produced from any gas wells which includes Liquid from condensations processes and coning water. This study investigates the contributing sources of liquid into the well SS7.

3.4.1 Hydrocarbon Condensate

Hydrocarbon condensate dropping out of the gas is associated with changing of the production system conditions below the dew point. This investigation was based on analysing the well operating pressure and temperature against the dew point conditions. If at any production system the operating conditions fall below dew point line then the possibility of hydrocarbon condensate dropping out of gas became inevitable.

The analysis was carried out using HYSIS software to generate the operating phase envelope using the provided fluid composition in Table 2 and the operating pressure and temperature at the reservoir and wellbore.

Because the gas composition provided was recorded at the separator conditions then it was assumed that gas composition at the surface and the reservoir are the same. The generated phase envelope at the reservoir pressure and temperature of 2273.5 psia and 203^{o}F respectively computed in 2016 was presented in Figure 19.

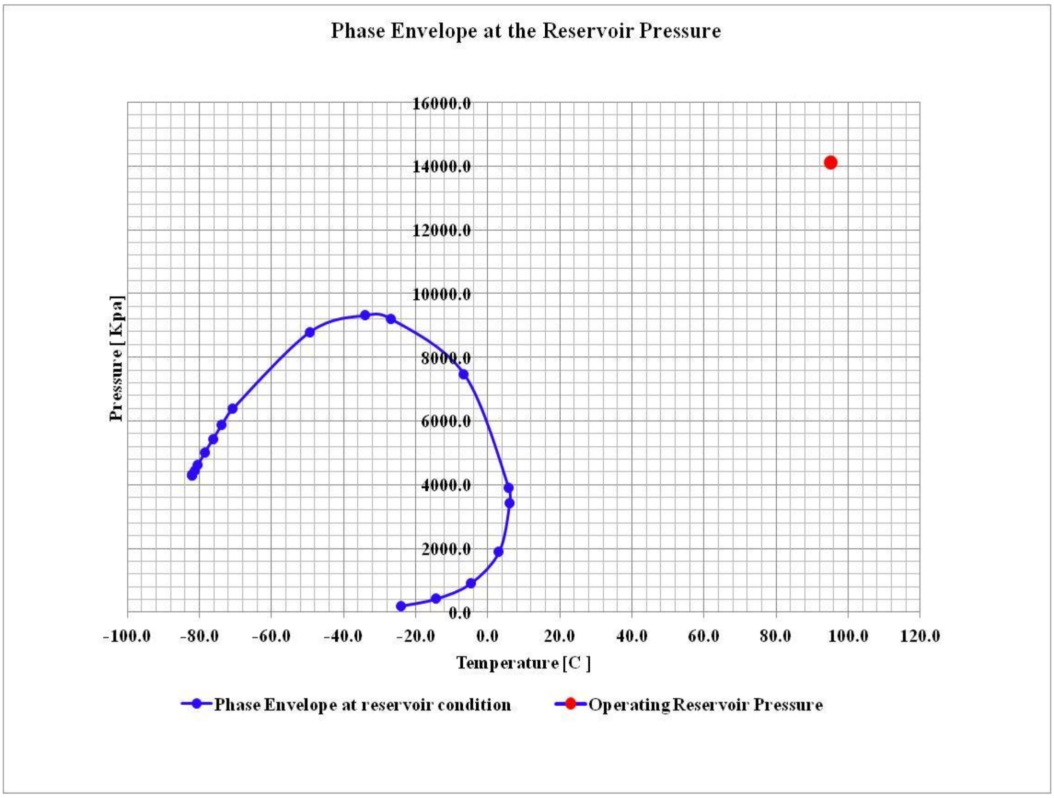

Figure 19: Phase Envelope for SS7 at Reservoir Conditions.

The red dot on the plot given in Figure 19 has indicated that only single phase gas exists at the reservoir conditions because the reservoir conditions was above the dew point line(blue curve) below which condensate exists. Hydrocarbon condensate will only drop out of gas phase when the operating pressure and temperature (red dot) falls inside the phase envelope.

Table 2: Fluid Composition from SS7 recorded during well test in 2008 (Bujulu, 2013).

Component	Well SS7 Gas Composition (%)
N_2	0.735
CO_2	0.282
C_1	97.206
C_2	1.048
C_3	0.328
$i\text{-}C_4$	0.053
$n\text{-}C_4$	0.079
$i\text{-}C_5$	0.037
$n\text{-}C_5$	0.032
C_6	0.036
C_{7+}	0.164
Total	100

Further investigation was conducted at the wellbore conditions to find out whether the reported condensate at the surface was produced from the wellbore or somewhere along the production system. This study used the wellbore pressure computed from the recorded surface tubing pressure and assumed the reservoir temperature to be the same as the wellbore pressure.

The analysis involved the generation of phase envelope using HYSYS software to determine whether the operating wellbore pressure and temperature falls in the single gas phase or in the two phase region.

The flowing bottomhole pressure of 1942psia computed from the flowing tubing head pressure of 1644psia recorded in 2016 was used in this analysis (Magige, 2016). The results of the phase envelope generated were given in Figure 20.

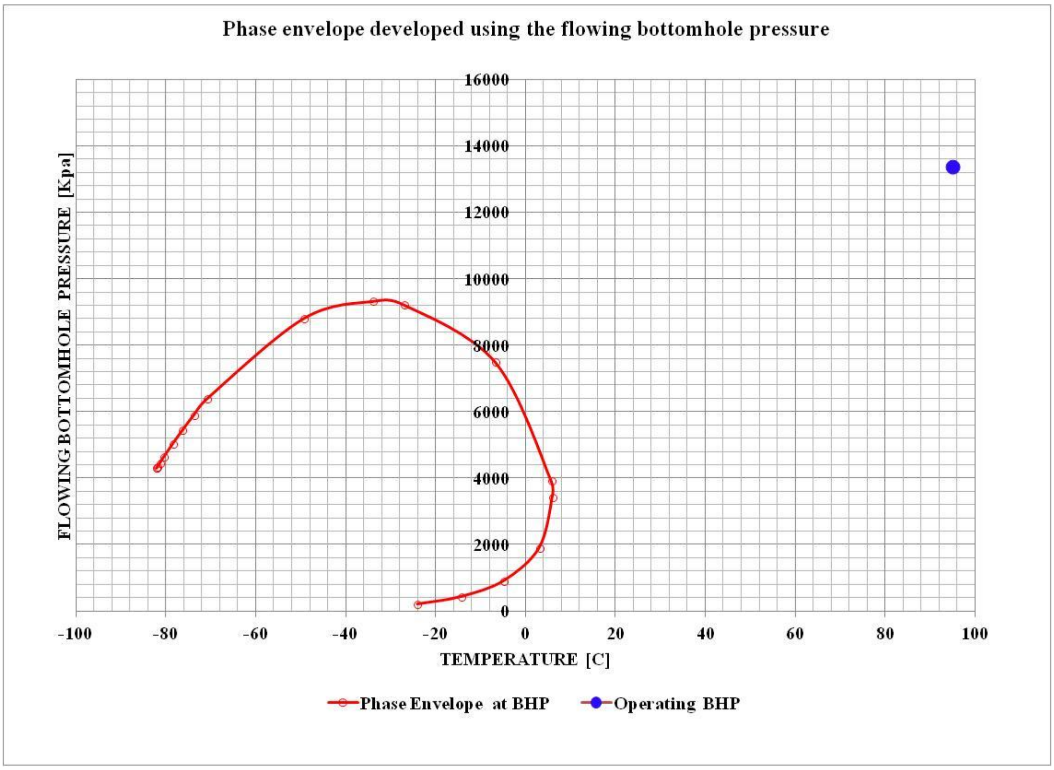

Figure 20: Generated phase envelope at the wellbore conditions (Magige, 2016).

The blue dot in Figure 20 represents the existing flowing bottomhole conditions while the red curve represents dew point line. The result has shown that the flowing bottomhole conditions are above the dew point which entails that only single gas phase exists.

The general findings of the possibility of liquid hydrocarbon to be dropping out of the gas phase at the reservoir and the wellbore conditions leads to the assumptions that the reported amount of condensate was produced at the surface.

3.4.2 Water of Condensation

McKetta and Wehe correlation was selected for analysis to determine the amount of water vapour content dropping out of the gas phase at the reservoir condition because it was the simplest and includes the effect water salinity and gas compositions.

The results estimated from McKetta and Wehe correlation was compared with the results generated from PROSPER software at the same pressure and temperature for compliances. The main inputs required in McKetta and Wehe correlation were:

a. Water salinity in % (2500ppm =0.25%)

b. Gas specific gravity of 0.586
c. Operating reservoir pressure = 2273.5 psia
d. Operating reservoir temperature of 203 ^oF

There were two analytical approaches for estimating water vapor content in gas phase and these were using McKetta and Wehe chart in **Figure 14** or solving equations 17 to 21. The following procedures were employed in estimating amount of water condensing from gas phase at the reservoir condition for SS7 using analytical equations.

i. Determination of the ratio of H_2O from brine to H_2O from fresh water (C_s) at the reported water salinity of 2500ppm (0.25%) the ratio) using the salinity correction subplot in McKetta and Wehe chart given in **Figure 14**. The value of C_s estimated was 0.994 as indicated by the red arrow shown in **Figure 21**.

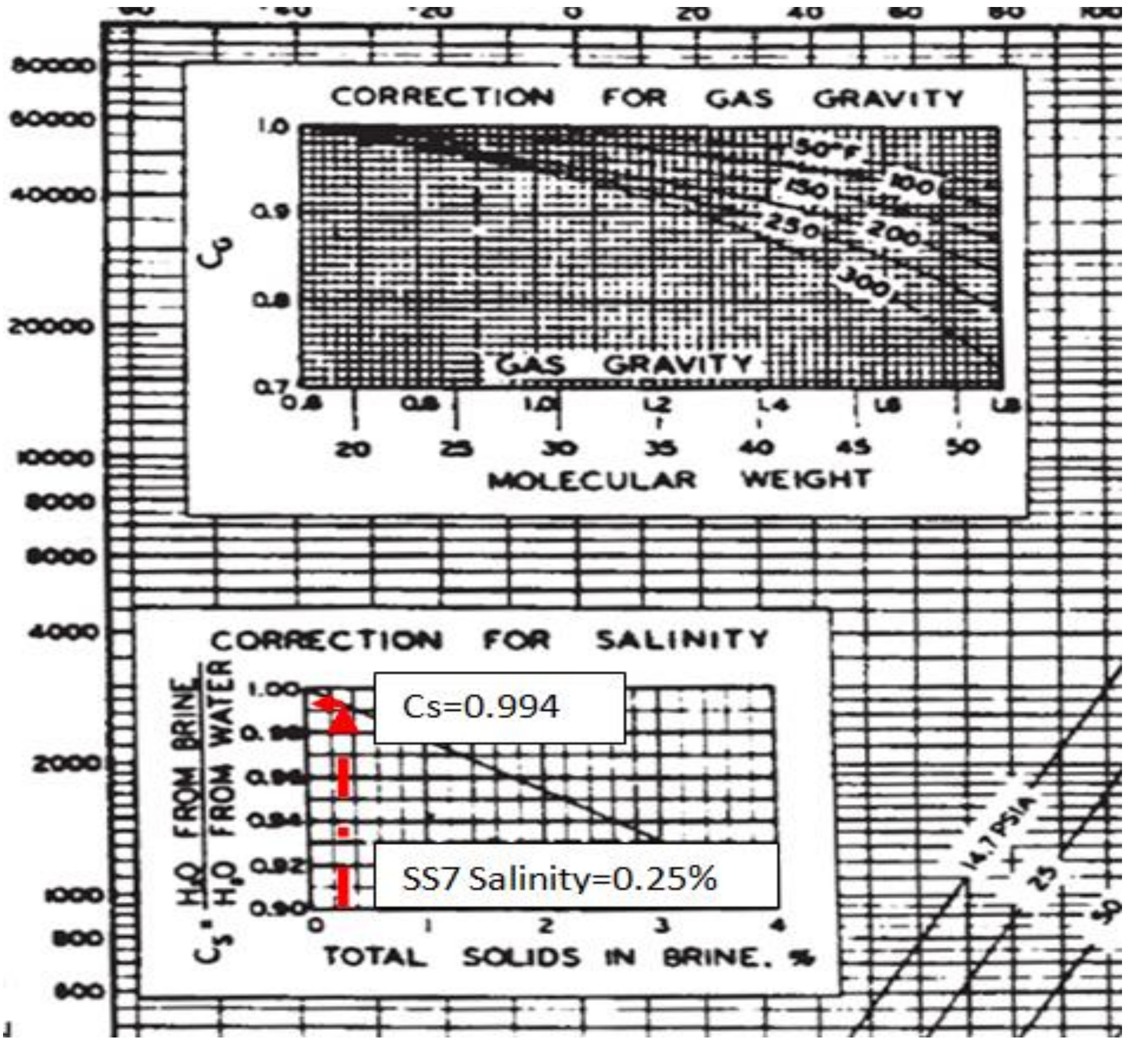

Figure 21: The estimated value of Cs for correcting the effect of water salinity.

The water salinity correction factor (A_s) was finally computed using the results in **Figure 21** using equation 19 as follows:

$$A_s = 1 - (3.92x10^{-9}) * 0.994^{1.44} = 0.999999996114 \approx 1$$

ii. Determination of gas gravity correction factor (A_g) was temperature and gas gravity dependent and it was computed using equation 18 as follows;

$$A_g = 1 + \frac{0.56 - 0.55}{(1.55x10^4) * 0.56 * 203^{-1.446} - (1.83x10^4) * 203^{-1.288}} = 0.999356$$

iii. Water mole fraction in gas $(y_w{}^o)$ given equation 17 was pressure and temperature dependent and was computed at the reservoir pressure and temperature as shown below:

$$\ln(y_w{}^o) = \frac{0.05227 * 2273.5 + 142.3 * \ln(2273.5) - 9625}{203 + 460} - 1.117 * \ln(2273.5) + 16.4$$
$$= -4.87259.$$

$$y_w{}^o = 0.007654$$

iv. The Correction of the estimated water mole fraction in gas to account for the effect of water salinity and gas gravity was done through equation 16.

$$y_w = 0.007654 * 1 * 0.9994 = 0.007649$$

The corrected water mole fraction of 0.007649 was used to compute the amount of water to gas ratio condensing out of gas phase at the given temperature and pressure.

v. The determination of water vapor content in gas for SS7 at the well operating average pressure and temperature was performed using equation 20 or 21 depending on the required units.

$$\text{Water Vapor Content in Gas} = 47300 * 0.007649 = 361.7977 \frac{\text{lbm}}{\text{MMscf}}$$

Or,

$$\text{Water Vapor Content in Gas} = 135 * 0.007649 = 1.03 \frac{\text{STB}}{\text{MMscf)}}$$

The alternative means of calculating water vapor content in gas was reading the value from McKetta and Wehe chart **Figure 14**. In this chart the uncorrected water gas ratio was directly read and then corrected for salinity and gas gravity as shown in Figure 22.

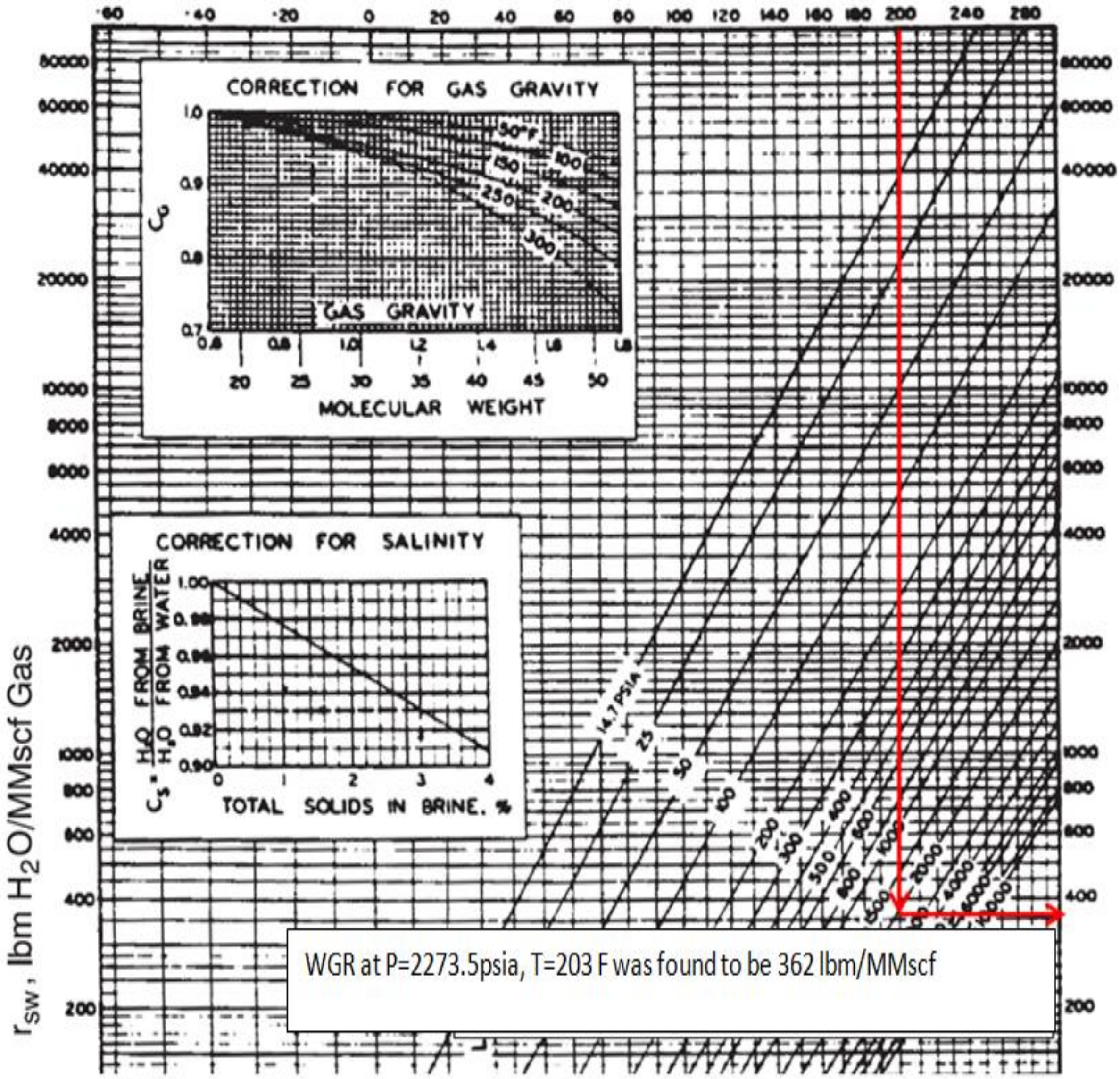

Figure 22: Reading the uncorrected water vapor content

The reading of the uncorrected water vapor content in gas from Figure 22 was found to be 362 lbm/ MMscf at pressure of 2273.5psia and temperature of 203°F. Correction factors computed from equation were used to correct the value of WGR obtained in Figure 22 and resulted to the following results to 361.78lbm/MMscf (1STB/MMscf) computed below.

Corrected water vapor content in gas $= \frac{362\text{lbm}}{\text{MMscf}} * 1 * 0.9994 = 361.78\text{lbm/MMscf}$

Both the approaches resulted to the same amount of Water vapor condensing from gas phase at the reservoir pressure and temperature. Further analysis was performed to estimate the effects of pressure decline with time on the water condensing out of gas phase. This analysis were performed using the commercial software called PROSPER as will be discussed below.

3.4.3 Effect of Pressure Decline on Water Vapor Content in Gas Phase.

The prediction of water vapor content in gas due to pressure depletion was performed in PROSPER software for the well SS7 through the following procedures.

a) Option Summary Section

The basic information required in this field was such as fluid description, well information, calculation type and well completion as given in snapshot in Figure 23.

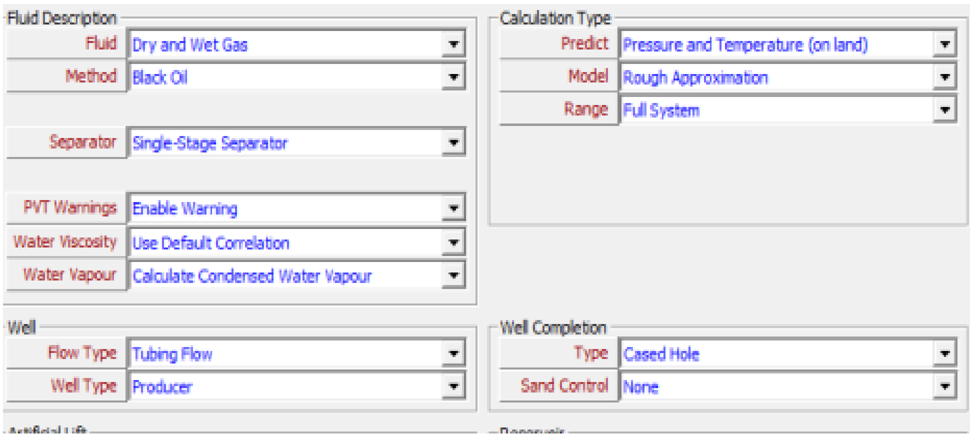

Figure 23: Option Summary Information

Under the fluid description field given in Figure 23, there was the region for water vapor content which was required to be enabled. This region was used in calculating the minimum water vapor at the specified reservoir pressure and temperature and the plot showing the variation of water vapor content with pressure at a given temperature can be generated.

b) PVT Information

The PVT input data for SS7 used in computing the minimum water gas ratio was shown in the snapshot given in Figure 24. The calculated minimum WGR resulted to a value of 0.99831 STB/MMscf which was almost similar to the value estimated from analytical equations at pressure of 2273.5Psia and temperature of 203^{o}F.

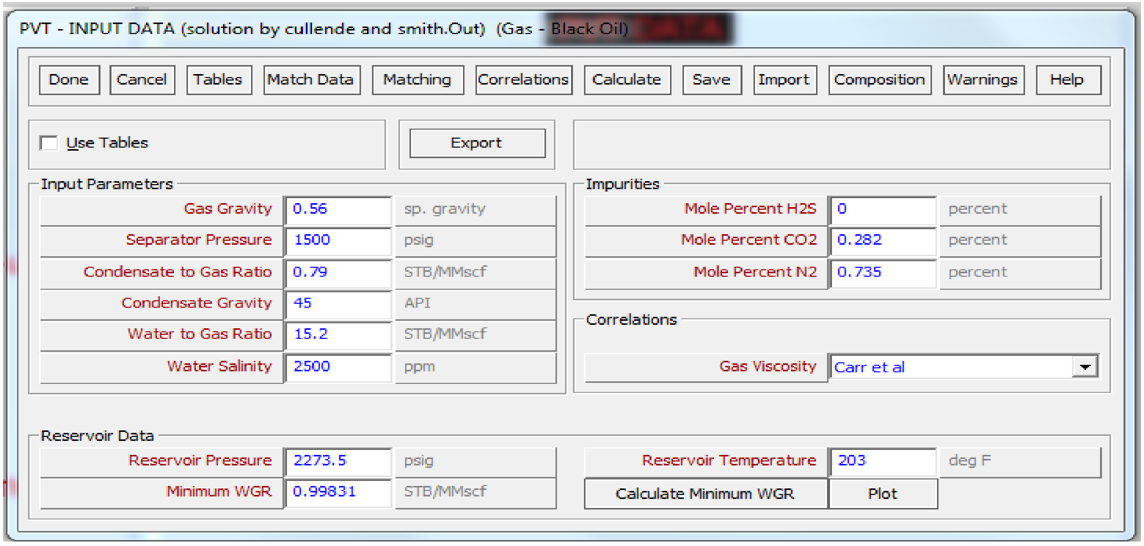

Figure 24: Input data for calculating the minimum water vapor content for well SS7.

The prediction of water vapor content condensing out of the gas due to pressure decline at a given reservoir temperature(203°F) was done in PROSPER and the results were presented graphically using a green curve shown in Figure 25.

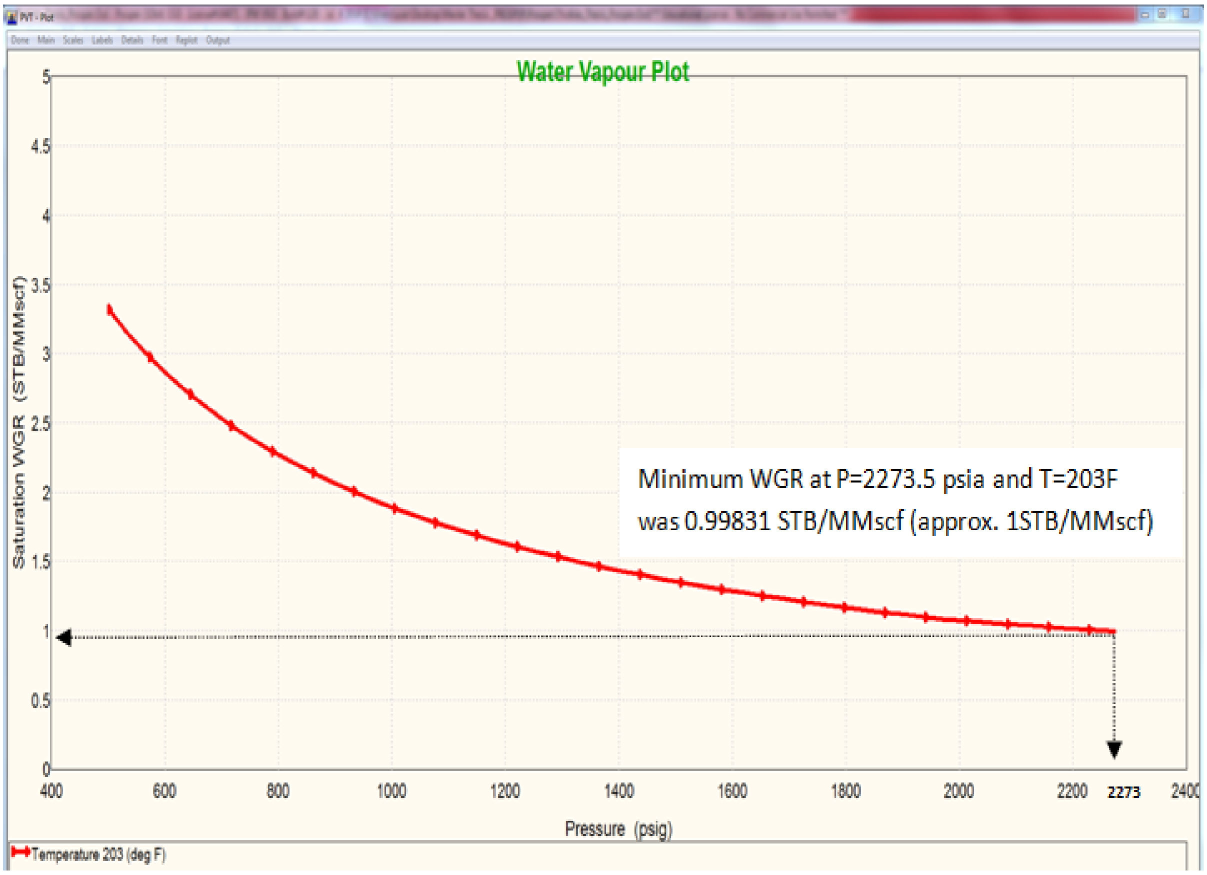

Figure 25: Water vapor content variation with pressure decline for SS7.

Based on PROSPER prediction plot in Figure 25, pressure decline has a significant effect on the amount of water condensing from gas at given reservoir temperature. The results in Figure 25 represents the situation for well SS7 and with time as pressure decline the amount of water condensing from gas will be increasing which may cause water blocking in the wellbore.

The value of the reported water gas ratio from the well SS7 was 15.2STB/MMscf high compared to the estimated condensed water gas ratio of 1.03STB/MMscf at the same well conditions. This information entails that there might be more sources of water into the well SS7 rather than condensing water due to presure decline.This provided the need to investigate the possibility of water coning into the well.

The study of water coning was a bit complex because it was reported that water gas contact was much deeper to about 80m below the SS7 well bottom perforation zone (Kasheshe, 2017).

3.4.4 Predicting Water Coning in SS7.

Several models has been developed to predict water coning into oil wells. No models has been developed for predicting the water coning in gas reservoirs and based on the Muskat (1982) study which believed that the physical mechanism of water coning in gas wells was identical to that for oil wells.

The developed water coning prediction equations for oil wells was employed in this study to predict the critical gas rate to avoid water coning in the gas well SS7. Schols equation was selected for predicting critical gas rate to avoid water coning in the well SS7 by using gas properties.

Water coning predictions involved the computation of the maximum allowable critical gas rate required to prevent water infiltration into the wellbore. The Schols model was written in excel VBA by using equation 26 and the main inputs into the equation were as follows;

i. $\mathrm{h} = \text{gas zone thickness}, \mathrm{ft} = 716\ \mathrm{ft}$
ii. $\mathrm{D} = \text{Perforation interval}, \mathrm{ft} = 230\ \mathrm{ft}$
iii. $\mu_g = \text{gas viscosity}, \mathrm{cp} = 0.01775\ \mathrm{cp}$
iv. $B_g = \text{gas formation factor}$, Rcf/Scf=6.214E-3

v. K = Reservoir permeability, md = 3.9 md

vi. re = Drainage radius, ft = 1500ft

vii. rw = Wellbore radius, ft = 0.51ft

viii. water density=1g/cc

ix. gas density=0.586g/cc

The implementation of excel VBA for Schols correlation in estimating the critical gas rate to prevent water coning was done as shown in the snapshot given below.

```
'Schols Correlations for maximum allowable gas rate(qc) to prevent water coning into the well'
'This correlation was assumed to be valid for gas well because its derivation was based on oil properties'
Function qc(rho_w, rho_g, D, h, K, miu_g, Bg, re, rw)
qc = (1 / 2049) * ((rho_w - rho_g) * (h ^ 2 - D ^ 2) * K / (miu_g * Bg)) * (0.432 + (3.14 / (Log(re / rw)))) * (h / re) ^ 0.14
''h' stands for Net Pay Thickness and 'D' stands for perforation depth in feet'
'rho_w - rho_g stands for density differences in g/cc and qc critial gas rate in SCF/D'
'miu_g in cp and Bg in rcf/scf'
're is drainage radius and rw is rhe well radius in ft
'K is the reservoir permeability, md
'Miu_g stands for gas viscosity, cp and Bg is the gas formation factor at pressure and temperature, rcf/Scf'
End Function
```

After writing the above script in the excel VBA, the calculation of the maximum allowable gas rate to prevent water coning into the SS7 gas well was done in the excel sheet by recalling the function qc and then inputing the necessary information as shown in the snapshot given in Figure 26 .

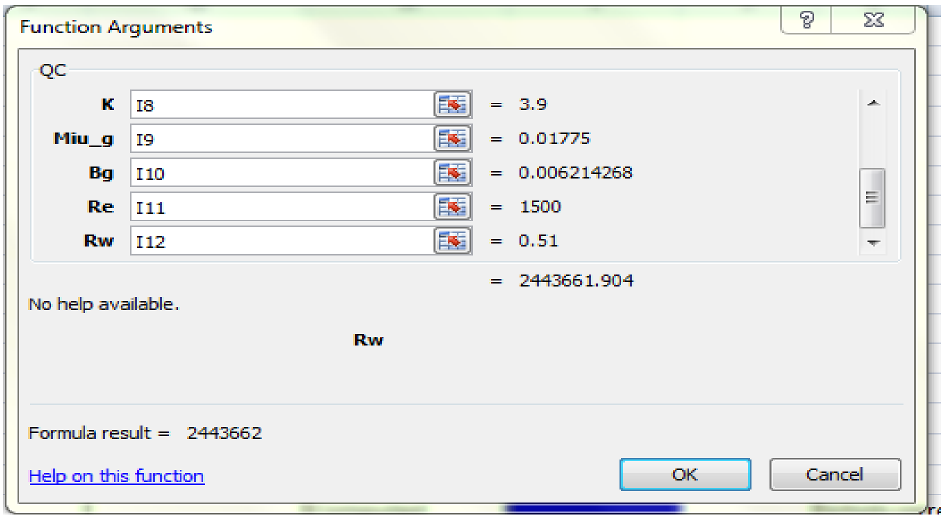

Figure 26: Function argument for critical gas rate estimation

Table 3 was the summary table from excel sheet showing all the required inputs used in Schols correlation to predict water coning by calculating the maximum allowable gas rate(q_c) to prevent water infiltrating into well SS7.

Table 3: Calculated critical gas rate for water coning prediction in SS7

SCHOLS	rho_w	1	g/cc
	rho_g	0.586	g/cc
	h	716	ft
	D	230	ft
	K	4	md
	Miu_g	0.01775	cp
	Bg	0.006214268	rcf/scf
	re	1.50E+03	ft
	rw	0.51	ft
	qc	2.44	MMscf/day
SS7_average rate	qg	4.2	MMscf/day
	Input		
	Computed		

3.4.5 Water Coning Prediction Results for Gas Well SS7.

Based on the results presented in Table 3, the computed critical gas rate to prevent water coning of 2.44MMscfd was lower than the actual average gas rate of 4.2MMscfd reported from well SS7. This gave a bad signs to the well SS7 productivity because water coning into SS7 was unavoidable. With time water coning into SS7 increases and at low gas rate more liquid will accumulate in the wellbore.

This study has only predicted the possibility of water coning into the gas well, further study which was not covered in this master thesis will be required to be carried to determine the exact location of the water which flows into the well SS7.

Generally the produced liquid reported at the surface from the well SS7 was found to having several sources including liquid from condensation as well as water coning. With time these liquid will continue to increase and at low gas rate the possibility of all liquid being lifted to surface decreases and some liquid began falling back to accumulate in the wellbore. The increased liquid fall back to the well bottom restricts gas flow from the formation to the well which causes the decreased gas production rate.

3.5 Liquid Loading Study in SS7.

Liquid loading study in the well SS7 started by investigating the sysmptoms of liquid loading problem using the historical production data collected from the well operator(PAET). Liquid loading prediction in the well was done using Turner droplet model and the performance curves generated from the commercial softawre called PROSPER.

3.5 .1 Study of Liquid Loading Symptoms for the Well SS7

Several liquid loading recognition symptoms have been published in literature to indicate the existence of liquid loading from the reported historical production history. In this study the following symptoms were analysed to understanding liquid loading problem in the well SS7.

3.5.1.1 Decline Curve Analysis.

This analysis was based on the comparison of the actual decline curve (red curve) with the predicted decline curve (blue curve). The decline curve given in Figure 27 has indicated that the actual decline curve will come to abandonment very soon as compared to the predicted decline curve.

The latest production history in 2016 has shown that there has been a wide scattering of production data (red curve) and this scattering would mean that SS7 has begun liquid loading. This was said so because prior to 2016 both the blue curve and the red curve almost fitted to each other but different behaviour was observed in 2016 were red curve gave a wide scattering of production.

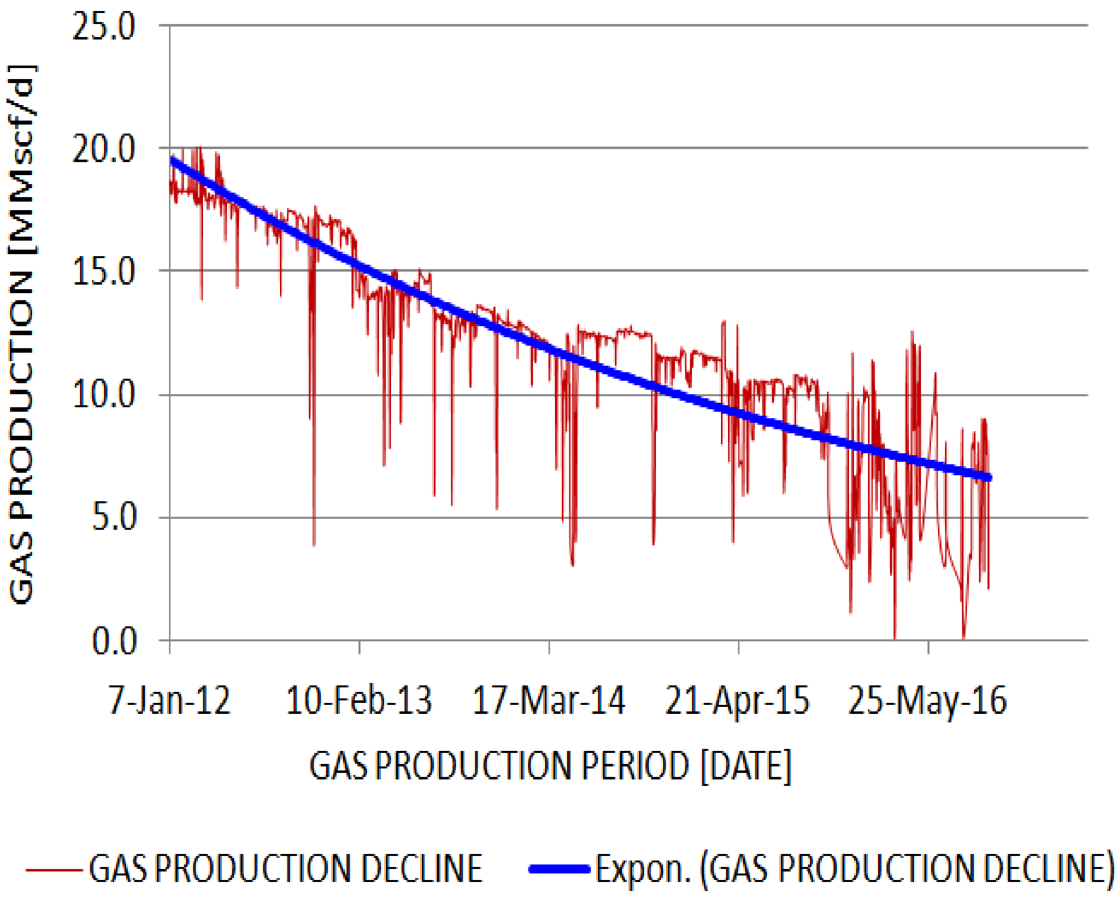

Figure 27: Gas decline curve for liquid loading onset identification ((Magige, 2016).

3.5.1.2 Liquid Production.

The study of liquid production from SS7 was performed by using the variation of water to gas ratio recorded since 2012 to September, 2016. The computed actual WGR was presented graphically in Figure 28 using the historical fluid production data recorded since when the well began producing liquid to surface.

Figure 28 has indicated that WGR has been increasing with time from 2012 to sometime in 2015 but the trend reversed where a sharp drop in WGR from 22.2 STB/MMscf to 15.2 STB/MMscf was observed in 2016.The dropping of WGR during the production period in 2016 provided an onset for liquid loading in SS7 as some liquid may have started falling back to the wellbore.

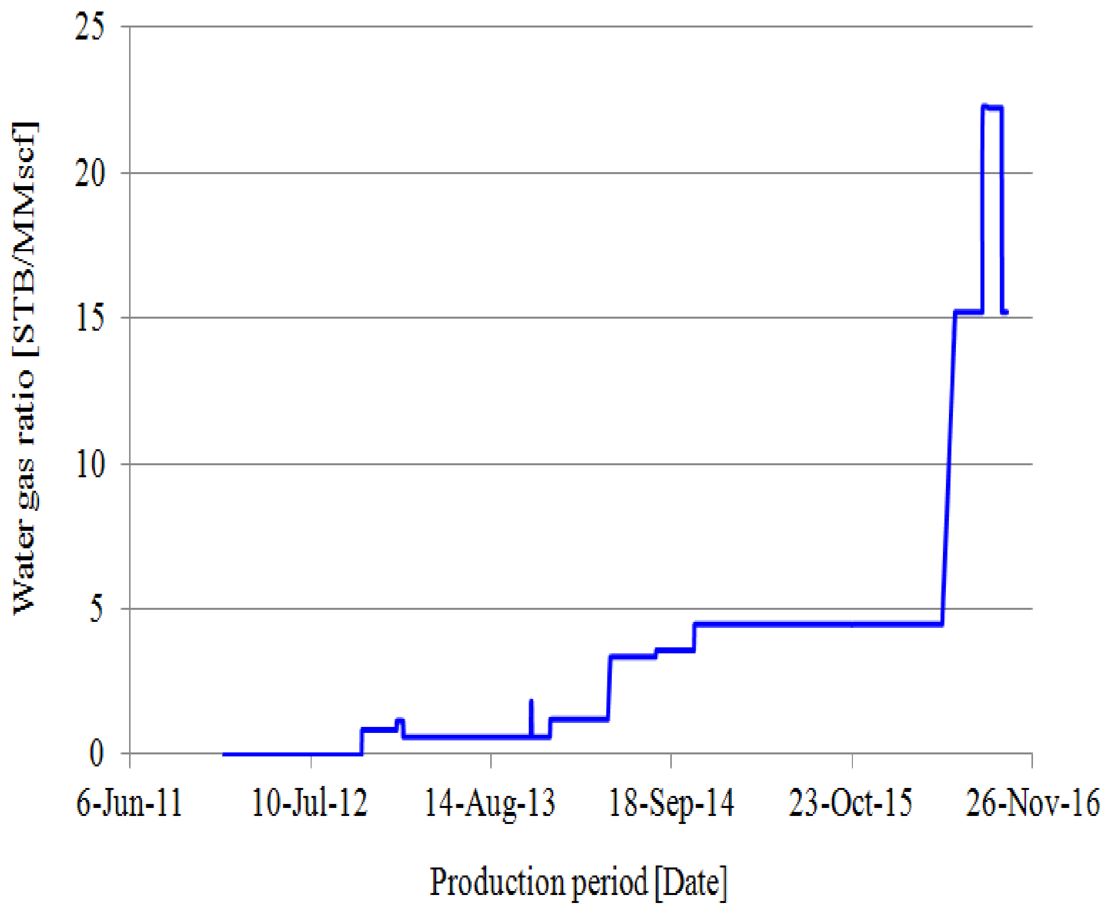

Figure 28: Water gas ratio computed from SS7 (Courtesy: Magige Project)

3.5.1.3 Liquid Holdup Study in the Production Tubing**.**

Liquid concentration in the production tubing was studied using PROSPER software during the production period in 2016 when the well WGR began dropping as in Figure 28. This study was conducted to further investigate whether the observed decline in WGR was because of liquid flowing back to the tubing bottom.

This was done when the well was producing at an average gas rate of 4.2 MMscf with flowing wellhead pressure of 1644Psia and WGR of 15.2STB/MMscf. The variation of liquid holdup with tubing depth was presented graphically in Figure 29 to investigate liquid distribution from the wellhead to the well bottom. Figure 29 was plotted in excel using the data extracted from Prosper software.

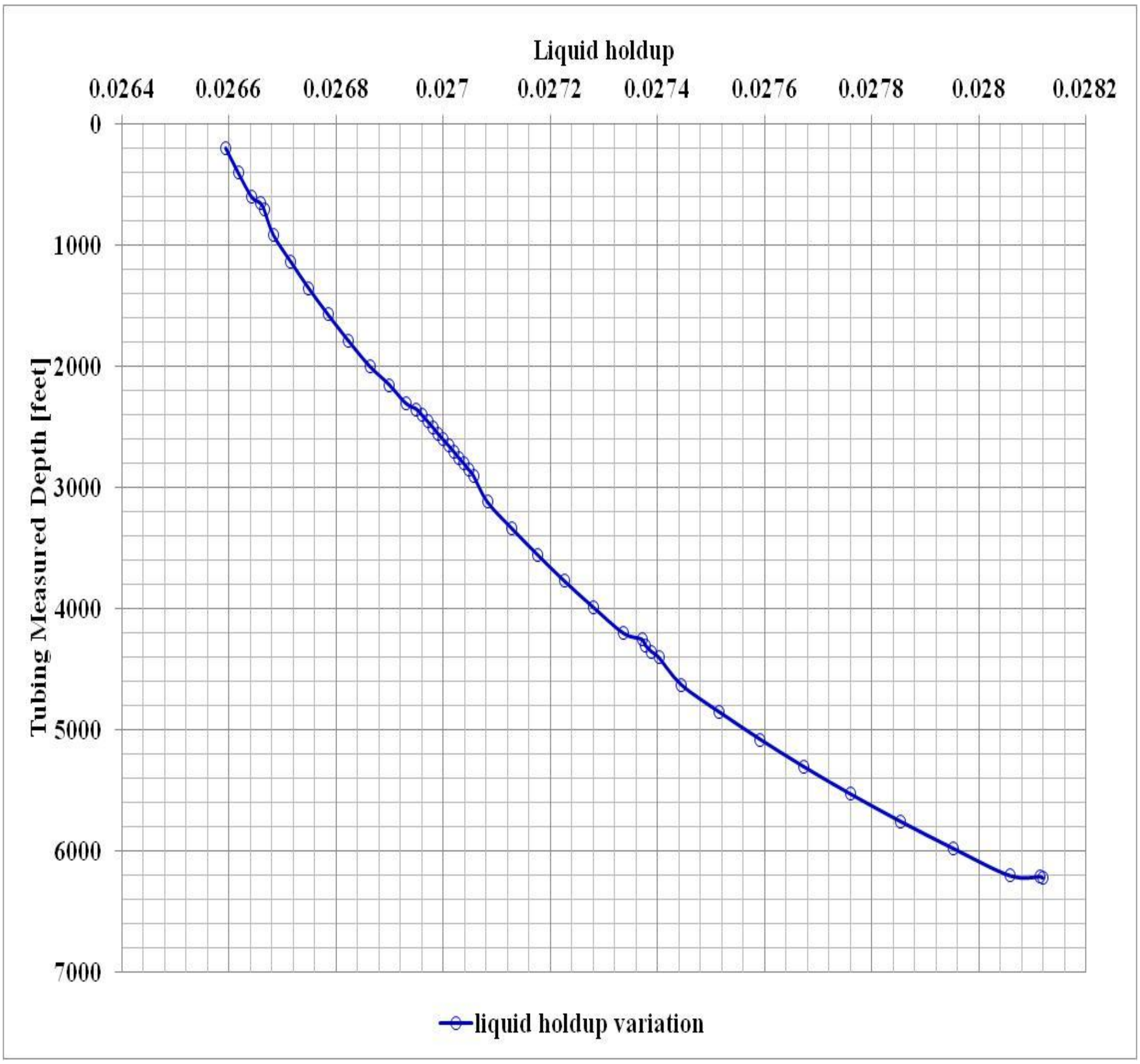

Figure 29: Liquid holdup variation with tubing depth in 2016.

An increase 5.73% liquid concentration along the production tubing from the wellhead to tubing bottom was observed from the results given in Figure 29. This increase in liquid concentration down the tubing was the other indicator of the existence of liquid loading in the well SS7.

3.5.1.4 Pressure Gradient Study for SS7

Pressure gradient depends on fluid density and well depth and it's a linear curve when a single phase fluid is flowing but changing the fluid type causes a significant effect on pressure gradient curve.

PROSPER software were used in generating the pressure gradient curves for diagnosing the well SS7 for liquid loading. The analysis of the pressure gradient curve was carried out during the production period in 2016 with an average gas production rate of 4.2MMscfd and flowing wellhead pressure of 1644psia.

The result of the generated pressure gradient in Figure 30 indicates that the pressure gradient was a linear curve to a depth of 6200ft but suddenly the curve changed to a new gradient below 6200ft. The gradient changing at a depth below 6200ft is the indication of fluid type changing and this was the very important indicator of liquid accumulating in the wellbore.

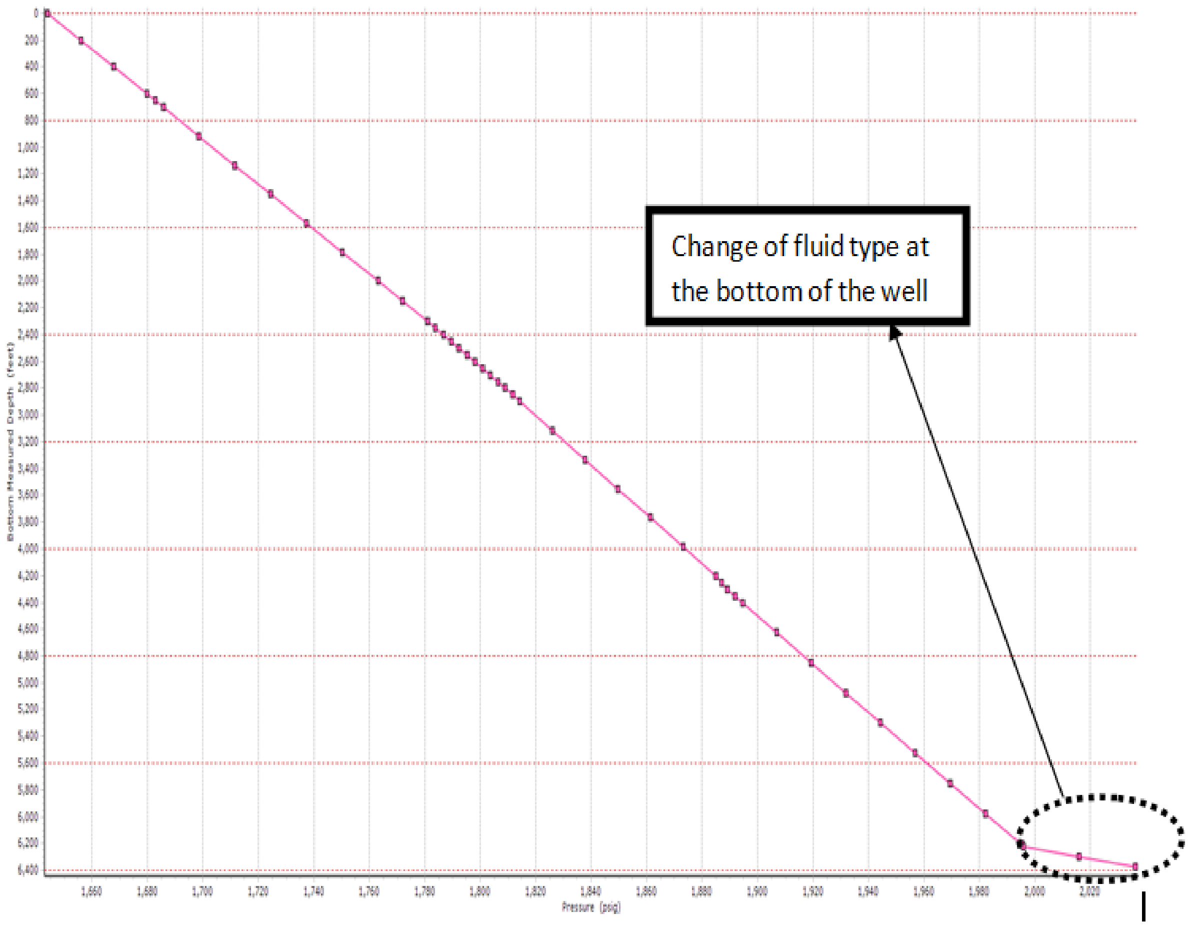

Figure 30: SS7 pressure distribution along the production tubing.

This change of slope observed in Figure 30 was because of fluid type changing from less dense to denser fluid which may be caused by liquid loading in well SS7.

3.5.2 Liquid Loading Prediction in the Gas Well SS7

The study of liquid loading symptoms has indicated the possibility of liquid loading in SS7. Further study was required to predict liquid loading in the well SS7 and it was this master thesis from two approaches.

The first approach was by using analytical models called Turner droplet model. The model predicted liquid loading in the well SS7 by calculating critical gas rate needed below which liquid loading becomes inevitable under natural flow.

The second approach was by using the performance curves developed in PROSPER during the production period in 2016. The latest historical well production data provided by the vendor was up to September, 2016. PROSPER software has inbuilt liquid loading prediction flag which applied Turner critical velocity to indicate the when the well has liquid loading problem.

3.5.2.1 Turner Droplet Model

Since SS7 produces both water and condensate, the water equation 9 was selected for calculating critical gas rate at the wellhead condition. Equation 9 was selected for prediction because when both water and condensate are produced the heaviest fluid (water) has a great influence on liquid loading than lightest.

The wellhead condition was selected to be used in calculating critical gas velocity because the average wellhead pressure recorded from the well SS7 in 2016 was 1644 psia higher than 100 psia (Sutton, et al., 2009).

Gas density used in the calculation of critical gas velocity was pressure dependent thus it was necessary compute gas densities at different pressures using equation 3 before critical gas velocity. To calculate gas density at the wellhead conditions the following were the required inputs in equation **3**.

a) Gas gravity = 0.586,
b) Wellhead pressure = 1644 psia,
c) R= 10.73, and
d) Wellhead temperature of 123^{o}F,

e) Gas deviation factor (Z) = 0.89 estimated from Standing Kartz chart in Appendix A and equations 5, 6, 7 and 8 at the wellhead condition.

$$\text{Gas density } (\rho_g) = \frac{28.97*1644 \text{ psia}*0.586}{0.89*10.73*(123+460)} = 5.013 \text{ lbm/ft3}$$

For different wellhead pressure the calculations were repeated following the above procedures. After determining the average gas density for different well head pressure, the next task was to determine the critical gas rate required in lifting the produced liquid to surface.

The calculation of the critical gas velocity from Turner model was possible after estimating gas density at the specified pressure and temperature and constant liquid density(water density) of 1073 kg/m3 (67lbm/ft3). Applying Turner model in equation 9 at the wellhead pressure of 1644 psia, critical gas velocity was computed as follows;

$$\text{Vc} = 5.304 * \frac{(67-5.013)^{0.25}}{\sqrt{5.013}} = 6.65 \text{ ft/s.}$$

The value of the critical gas velocity at various wellhead pressures reported was calculated following the same procedures described above and presented in tabular form in appendix F.

3.5.2.2 Critical Gas Rate

The critical gas rate required for comparison with the well reported gas rate was calculated from the critical gas velocity and tubing cross section area at the wellhead operating pressure and temperature using equation 11.

During the prediction period in 2016, the production tubing of internal diameter of 3.83inches, well head pressure of 1664psia and temperature of 123^{o}F was used in computing the critical gas rate as follows:

$$\text{qg} = \frac{3.067*1644*6.65*\pi*3.83^2}{(123+460)*0.89*4*144} = 5.2 \text{ MMscf/day.}$$

For different wellhead pressure the same procedures used above was employed in calculating the critical gas rate in excel and the summary of the results were presented in appendix F.

Comparing the computed critical gas rate with the actual average gas rate from SS7 the results were plotted as in Figure 31.

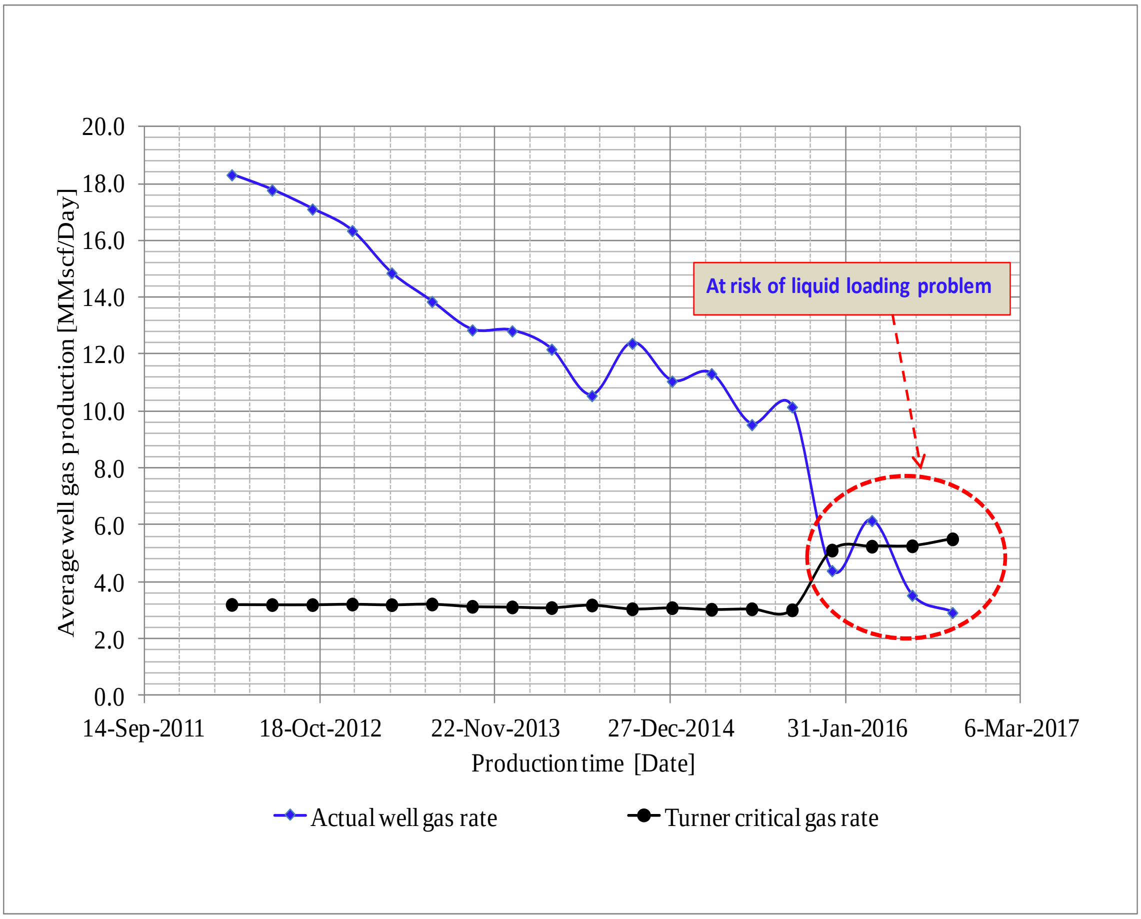

Figure 31: Comparing the Critical Gas Rate with Actual Gas Rate for Well SS7

(Courtesy: Magige Project, 2016)

Critical gas rate curve increased from the end of 2015 due to the changing of tubing internal diameter in the well SS7 from 2.992 inches to 3.83inches as the means to control increased frictional losses. The prediction of liquid loading was based on the comparison of the actual recorded production rate in blue curve with the estimated critical gas rate in black curve. The result presented in Figure 31 has indicated that the well SS7 began producing below critical early in 2016.

It was at this time when the well SS7 was predicted to have liquid loading problem and if no further control action was to be taken on the well, more liquid will accumulates and the gas productivity will continue to decrease and finally abandoning the well.

3.5.2.3 Performance Curve method.

The second approach which was identified to be used in understanding liquid loading problem in the gas wells was by using the performance curve. There exists different ways of generating the system perfomance curves but in this study a commercial software called PROSPER was employed in producing the performance curve for the well SS7 using the latest well conditions in 2016.

The system performance curve for SS7 was made by intersecting the Inflow pwerformance curve (IPR) with the tubing performance curve(VLP) using the recorded well production data.

IPR Curves

The main input data required to calculate the IPR curve for the well SS7 in 2016 were reservoir data and reservoir model data. Back pressure equation was to compute an average reservoir pressure from the estimated flowing bottomhole pressure. The flowing bottomhole pressure was calculated from the recorded flowing wellhead pressure in 2016 using Cullender and Smith method assuming only dry gas produced. The resulted average reservoir pressure input into well model in PROSPER was 2039psia and reservoir temperature of 203^{o}F.

The other reservoir data required was fluid ratios where the latest water gas ratio of 15.2 STB/MMscf and condensate gas ratio of 0.79 STB/MMscf reported from the well SS7 and were used in the generating an IPR curve. The snapshot of the reservoir data used in PROSPER was given in Figure 32 below.

Reservoir Data

Reservoir Pressure	2039	psig
Reservoir Temperature	203	deg F
Water Gas Ratio	15.2	STB/MMscf
Condensate Gas Ratio	0.79	STB/MMscf

Figure 32: Reservoir Data for Well SS7 in 2016.

Reservoir Model Data

After providing the necessary reservoir data the next were to select the appropriate model to be used in the computation of an IPR. Backpressure model was selected for calculating an

IPR curve in this study and the main inputs required were backpressure exponent ‘n’, wellbore diameter, reservoir permeability and reservoir thickness as in Figure 33.

The backpressure exponent was initially assumed to 1 and sensitivity analysis was later applied in validating the calculation with the test data to estimate the suitable value of ‘n’.

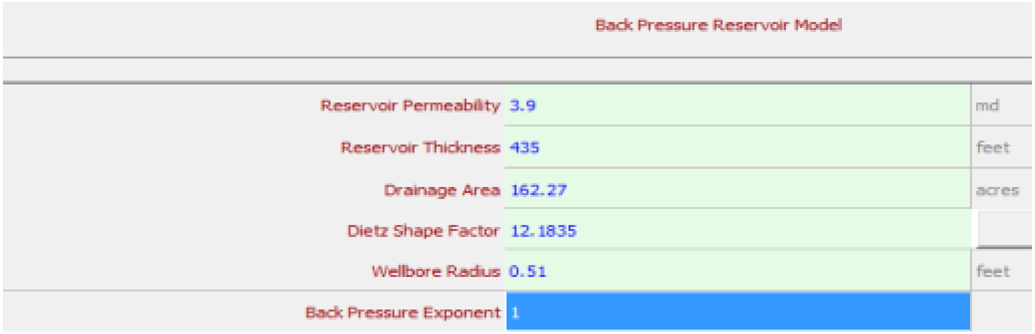

Figure 33: Input Data Required in Backpressure Reservoir Model

The generated IPR based on the provided information in Figure 32 and Figure 33 was given in Figure 34. This IPR was required to be validated using the recorded well production test data so that to find the correct reservoir pressure and backpressure exponent.

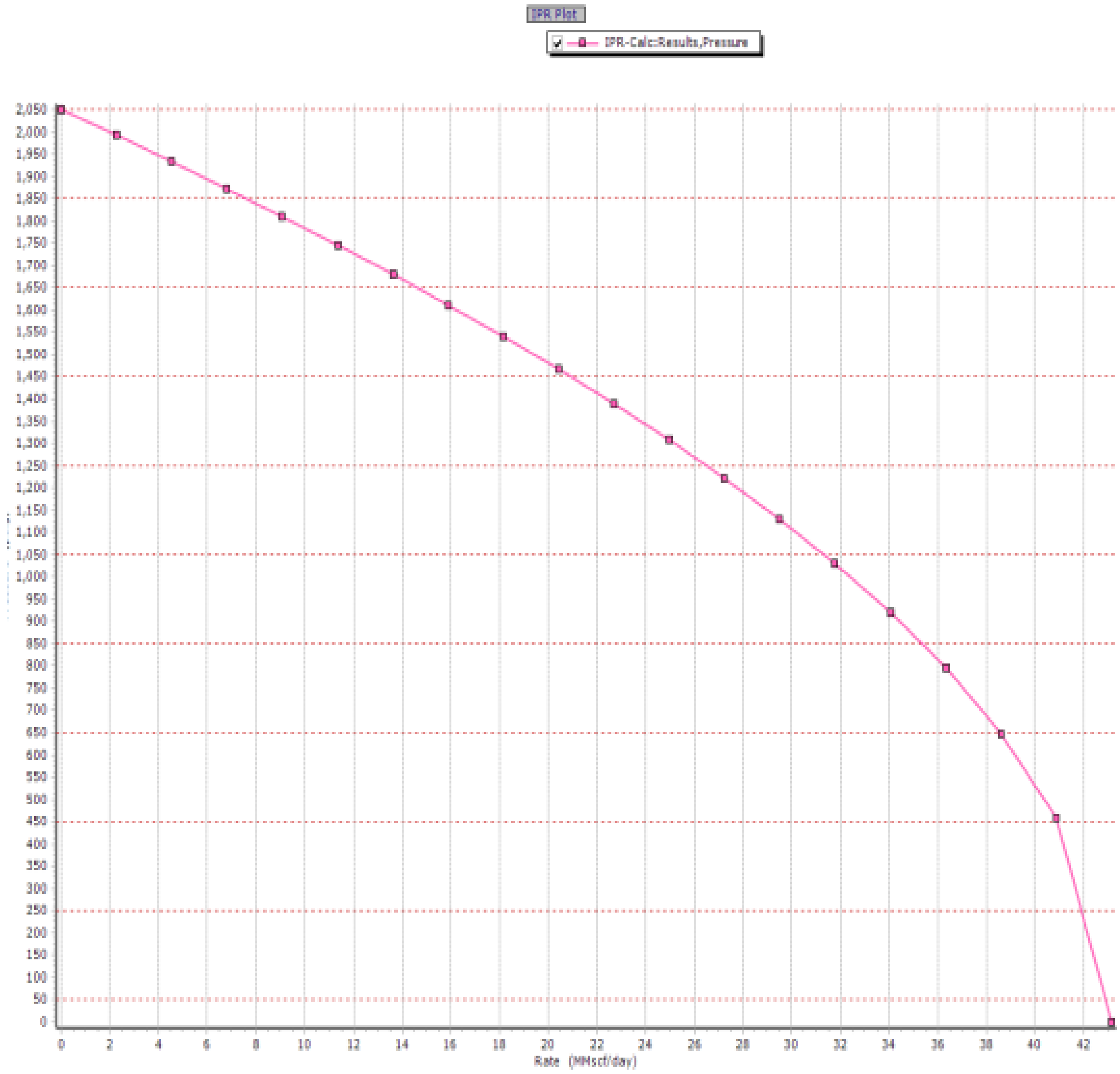

Figure 34: IPR curve for the Well SS7 computed in 2016.

3.5.2.4 Adjusting IPR to Match Well Test Data.

The recorded well test data in Table 4 was used in calculating the correct backpressure exponent ‘n’, as well as adjusting the reservoir pressure which could produce the test data. The adjustment of the reservoir pressure was necessary because the initial computed reservoir pressure from backpressure equation assumed only dry gas was produced from the well SS7.

Therefore the adjustment was done by performing sensitivity analysis for various backpressures exponent ‘n’ to fit the IPR with the reported test data. Five sensitivity cases were generated for value of n ranging from 0.5 to 1. Different IPR curves were calculated for each cases and the suitable case is the one which fitted the test data with the well IPR. Upon performing analysis it was found that the case with n=0.962 fitted the test data with SS7 IPR which meant that the model was accurate to produce test data.

After determining the correct value of backpressure exponent, the next was to adjust the average reservoir pressure at the estimated backpressure exponent using PROSPER software through several iterations to include the effect of produced liquid which was ignored by Cullender and Smith correlations.

The new calculated average reservoir pressure was applied to replace the initial used reservoir pressure and the snapshot of the new input data was given in Figure 35 and Figure 36 which has replaced input given in Figure 32 and Figure 33.

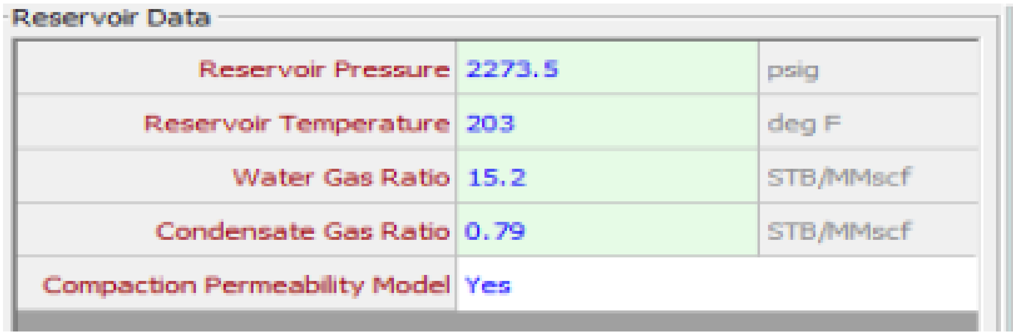
Reservoir Data

Reservoir Pressure	2273.5	psig
Reservoir Temperature	203	deg F
Water Gas Ratio	15.2	STB/MMscf
Condensate Gas Ratio	0.79	STB/MMscf
Compaction Permeability Model	Yes	

Figure 35: Adjusted Reservoir Pressure.


Back Pressure Reservoir Model

Reservoir Permeability	3.9	md
Reservoir Thickness	435	feet
Drainage Area	162.27	acres
Dietz Shape Factor	12.1835	
Wellbore Radius	0.51	feet
Back Pressure Exponent	0.962	

Figure 36: Estimated Backpressure Exponent in the Reservoir Model Data

Validated IPR

Of the reported production test data, only four test data in Table 4 was used in verifying the model and resulted to a new IPR curve Figure 37. This IPR was generated using the adjusted reservoir pressure of 2273.5psia and backpressure exponent of 0.962.

Table 4: Well Test data performed in 2016 for IPR Validation

Date	Gas Rate	Pressure (FBHP)
	[MMscf/day]	[psig]
16/03/2016	7.5	1960.8
7/4/2016	3.2	1746.8
24/04/2016	8.7	1913.3
5/5/2016	5.5	1826

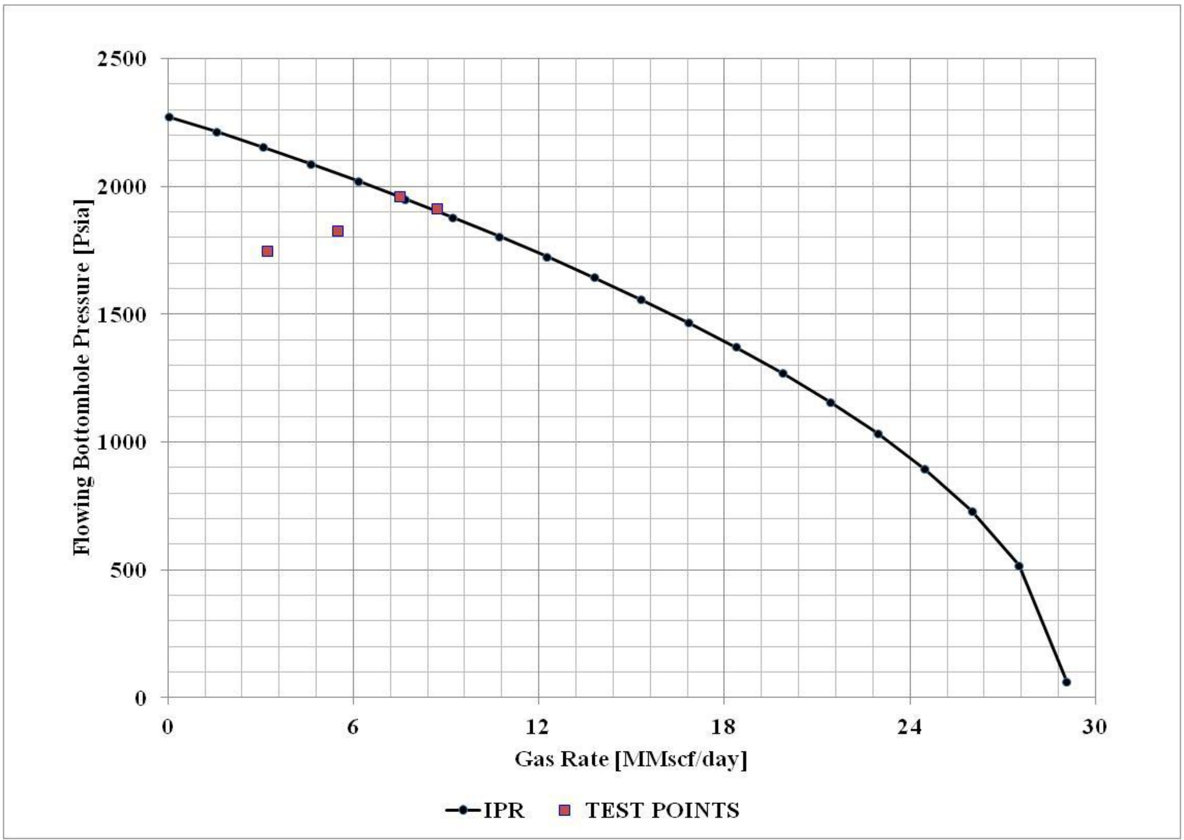

Figure 37: Adjusted IPR Curve

Tubing Performance Curve (VLP).

Tubing performance curve was generated from PROSPER software using wellhead (top node) conditions reported from the well SS7 in 2016. Figure 38 shows the top node pressure of 1644psia and temperature of 123 ^{o}F used in generating the tubing performance curve for the well SS7.

Top Node Pressure	1644	psig
Water Gas Ratio	15.2	STB/MMscf
Condensate Gas Ratio	0.79	STB/MMscf
Surface Equipment Correlation	Beggs and Brill	
Vertical Lift Correlation	Petroleum Experts 2	
Rate Method	Automatic - Linear	
First Node	1 Xmas Tree 0 (feet)	
Last Node	18 Casing 6372.95 (feet)	

Figure 38: VLP Input Data for Well SS7 (Magige, 2016).

System Performance Curve for Well SS7

The system performance curves was produced from PROSPER software by intersecting an IPR curve in Figure 37 with the VLP curves generated using data in Figure 38 .

The resulted system performance curve given in Figure 39 for the well data recorded in 2016 was used to study liquid loading in the well SS7. The study was performed based on the nature of the performance curves and also using Liquid loading flag.

Nature of the Performance Curve

The intersection of the IPR curve with the VLP curve was used in the study of liquid loading in the well SS7. Based on the results in Figure 39, the left hand intersection of the VLP and IPR curve observed was due to increased flowing bottomhole pressure caused by the existence of liquid in the wellbore. Thus liquid loading was predicted to have existence in the well during the evaluation period in 2016.

Liquid Loading Flag

Liquid loading flag was the inbuilt tools in PROSPER software for indicating liquid loading problem in gas wells. Liquid loading flag uses Turner velocity in its evaluation and has two main outputs which are **0** for no liquid loading and **1** for liquid loading. Liquid loading flag plotted on the same curve with the system performance in Figure 39 has indicated the existence of liquid loading because the flag plotted at **1**.

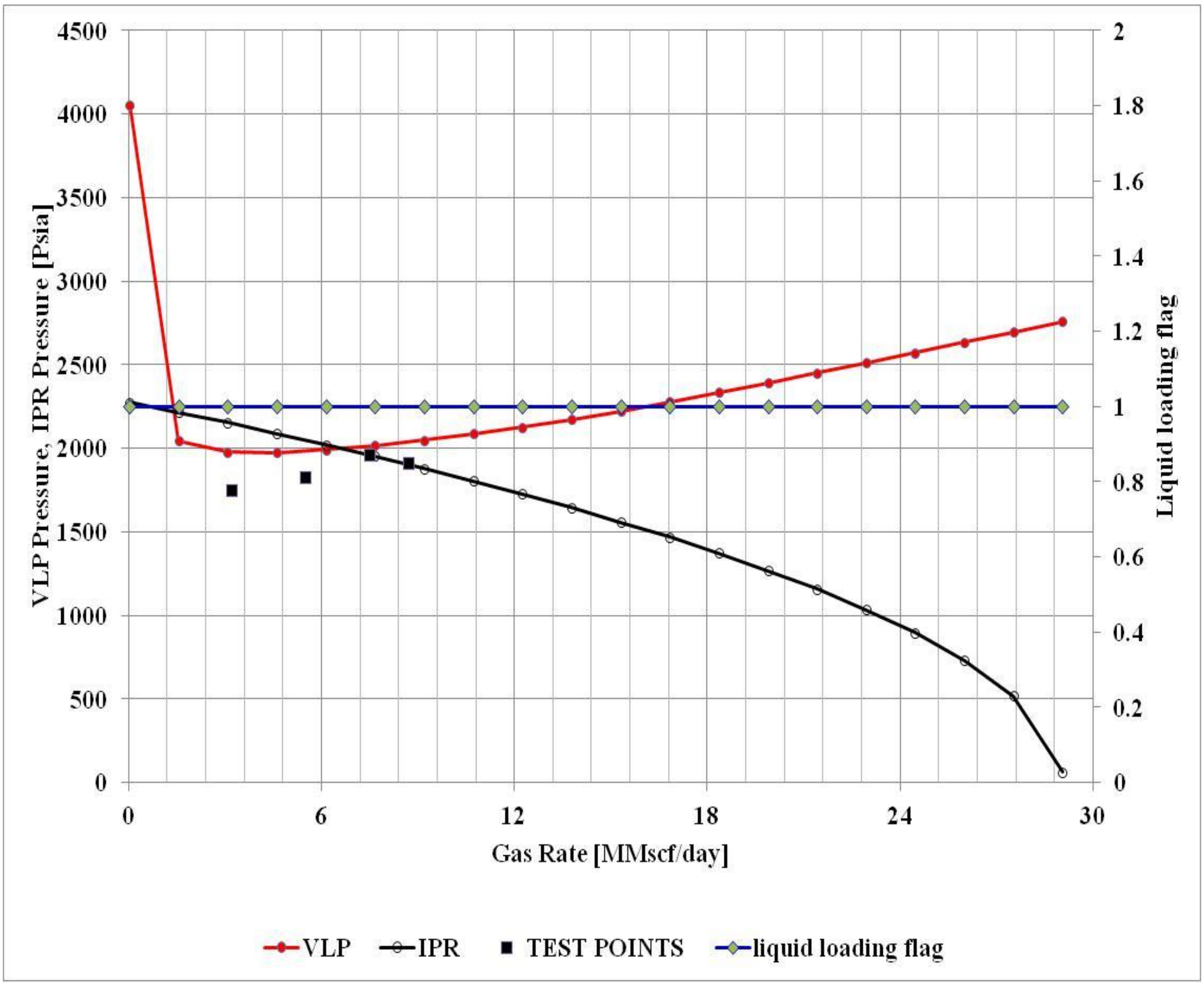

Figure 39: System performance curve for liquid loading prediction

3.5.2.5 Results of Liquid Loading Prediction.

Based on the performance curve in Figure 39 , liquid loading flag has indicated the existence liquid accumulation in the wellbore because it has plotted at 1 in the performance curve. Again the effect of liquid accumulation in the well SS7 was observed on the left hand intersection of the VLP curve with IPR curve at the low gas rate on Figure 39.

Both prediction method used in this study showed that the reported decreased gas production from SS7 in the current production period was because of liquid loading problem. The quantification of the amount of water which has accumulated in the gas well SS7 was not considered as part of this study. This will create the gap for further study to estimate the accumulation rate and establish the model which can be used as a sensor for liquid loading in the well SS7.

4. TYPICAL GAS WELLS DELIQUIFICATION METHOD

The history of liquid removal in gas wells started in the Hugoton field in Kansas when the produced water accumulated in the well as the gas rate declined over time (Hutlas & Granberry, 1972). The first options which were employed were to blowdown the well periodically so that to allow the well to build more pressure sufficient to lift the water with gas to atmosphere. A small siphon string were run in the well when the water removal were impossible by blowdown.

Currently the gas industry has developed a number of technologies which are used to deliquify gas wells experiencing liquid loading. Different methods are used depending on the well operations and the stages of liquid loading from when the well begin loading to when it becomes severe to kill the well.

The main goal of developing and installing the artificial lift technology in the gas well is to increase gas production above critical rate and prolong the life of the well as shown in Figure 40. **Figure 49** and **Figure 50** shows the limitations of applications for various artificial lift methods which have been applied in unloading liquid from gas wells in terms of the well depth and liquid handling capacity.

The terms "Deliquification methods" were derived from artificial lift method but their differences falls on their working definitions. Deliquification method is the application of energy to remove an interfering liquid in gas well to enhance gas production while artificial lift method is the application of energy to lift commercial product from reservoir depth to surface (Simpson, 2003).

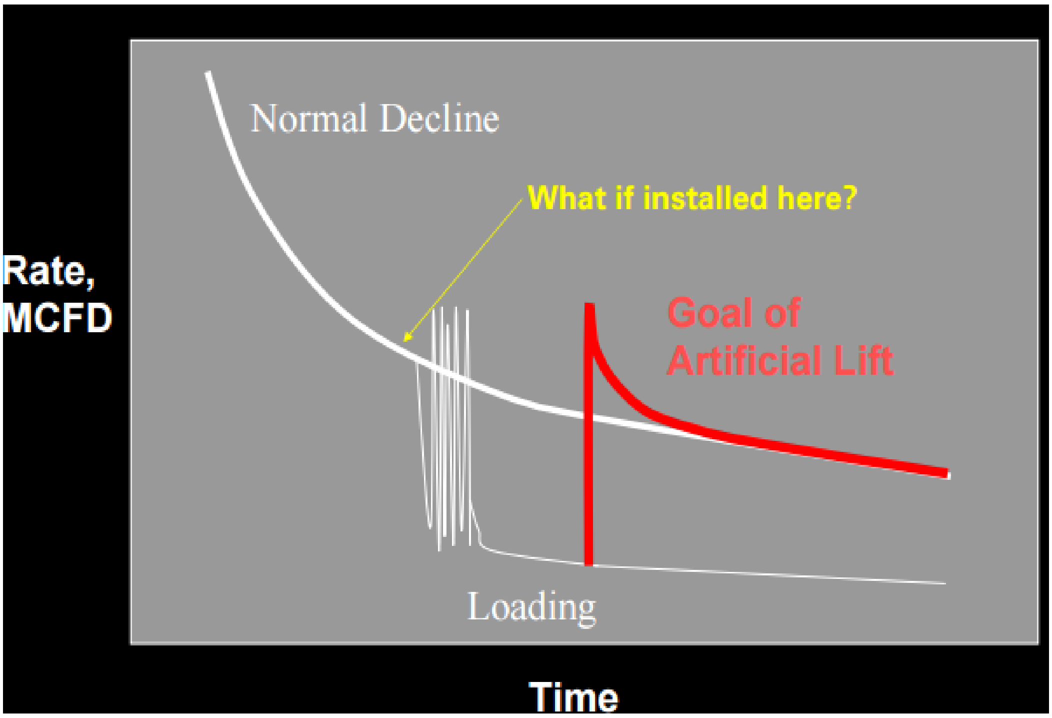

Figure 40: Effect of artificial lift on production decline **(Bondurant & Hearn, 2008)**.

4.1 Liquid Removal Technology

The methods which are used in removing the accumulated liquid from gas wells are of different varieties. There are those which use the well natural energy and those which require artificial energy in removing the accumulated liquid to surface. The following are some of these methods identified from literature.

4.1.1 Natural Energy Lifting Methods

1. Intermittent Production

When a well first begin to show signs of liquid loading, the best options is to stop the well to produce to allow pressure build up around the well and restarting the well to production again. This process of alternatively shut-in and producing the well is termed as intermittent flow. The intermittent flow are associated with other terms such as intermiting ,stop-cocking, stop clocking and blow down and its operations is by using wells natural energy (Lea & Tighe, 1983).

Intermittent flow is used as only a temporary measure to controlling liquid loading in gas well (ALRDC, n.d.; Lea & Tighe, 1983). The main disadvantages of intermitting the well as the method of dealing liquid loading is the damage of the well capability to re-inject the accumulated liquid to formation due to precence of water (ALRDC, n.d.).

2. **Small Diameter Production Tubing.**

The objective of small diameter tubing installed in gas well as the means of combating liquid accumulation is to decrease the effective flow area and increasing the gas flow velocity (Neves & Brimhall, 1989; Hutlas & Granberry, 1972; Lea, et al., 2003). The increased gas flow velocity causes the liquid to be suspended in high velocity gas phase and transported to surface.

Sometimes it becomes unnecessary to replace the whole production tubing instead a small internal diameter tubing as in **Figure 41** can be connected to the bottom of the main production tubing to decrease the required critical gas velocity (Khamehchi, et al., 2016).

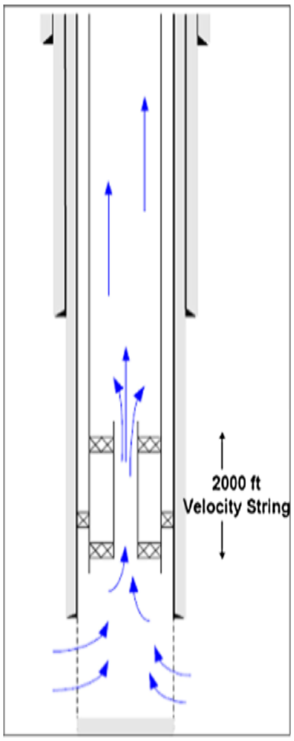

Figure 41: Schematic of the Velocity String Equipment (Khamehchi, et al., 2016).

The study by **Neves & Brimhall, 1989** has pointed out that a small tubing diameter is not the permanent means of unloading gas wells. Therefore; small tubing diameter has a limited life in its application and it has the following disadvantages once installed in the gas well (Lea, et al., 2003).

i. Pressure bombs, test tools, and coiled tubing cannot be run in the smaller strings.

ii. Small velocity string restricts the installation of other equipment such as Plunger lift.
iii. It is not easy to swab the tubing once loaded.
iv. Too small tubing size accelerates friction losses.

Evaluating the Performance of Smaller Tubing diameter.

Concept of nodal analysis is required in generating the tubing curves for various tubing sizes and obtaining some information from the shape of the tubing curve (Lea, et al., 2003).

The other method which may be used in analysing tubing size is by using the concepts of critical flow which need the velocity in the tubing to be greater than critical velocity that reduce the holdup.

Small Tubing String Applications.

The application of small diameter tubing as the means to deliquify the gas well is on a low liquid volume producing wells with low bottomhole pressure (Lea & Tighe, 1983). The selection of small tubing diameter as the deliquification method also depends on the costs of tubing as well installation costs which involves some workover costs. Depending on the availability of the tubing string sometimes the used tubing can be less cheap than purchasing the new tubing of equal size (Neves & Brimhall, 1989).

3. Plunger Lift System

Plunger lift method uses a free travelling piston that fits tightly within the production tubing to remove the accumulated liquid in the wellbore. The travelling mechanism of the Plunger lift depends on the well pressure for upward movement of Plunger to surface and gravity for moving the Plunger back to well bottom.

Gas wells with Plunger lift do not depend on critical gas velocity for lifting liquid to surface as for the case of natural flow (Lea & Tighe, 1983; SPE, 2012). Natural flow can only lift the liquid to surface once the gas flow velocity is higher than critical gas velocity but well with Plunger lift system it can be produced to a very low gas velocity without liquid loading.

Plunger Lift Equipment

There are several components that make up a Plunger lift system. Figure 42 is a typical Plunger lift installation with all its components (Bondurant & Hearn, 2008). The following are the most common components of Plunger lift system.

i. Downhole bumper spring allow the Plunger to land more softly downhole.

ii. Free travelling Plunger along the tubing depth.

iii. Wellhead designed to catch the Plunger and allow flow around the Plunger.

iv. Controlled motor valve to open and close the operation line sensor to sense the arrival of the Plunger.

v. An electronic controller: Contains logic that determine the cyclic operation of Plunger for better production.

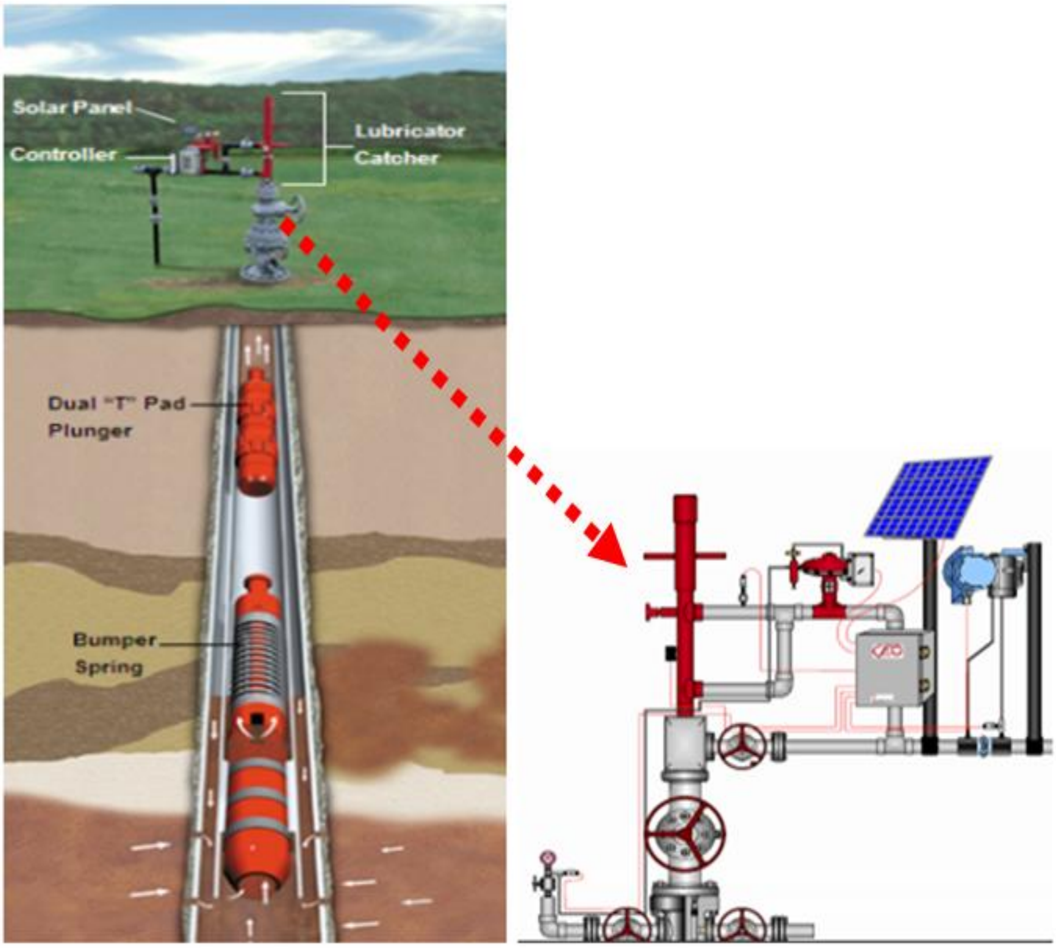

Figure 42: Plunger Lift Operations and Equipment **(Bondurant & Hearn, 2008)**.

Figure 43 are different types of pieces of the equipments used in the Plunger lift system described in Figure 42 above.

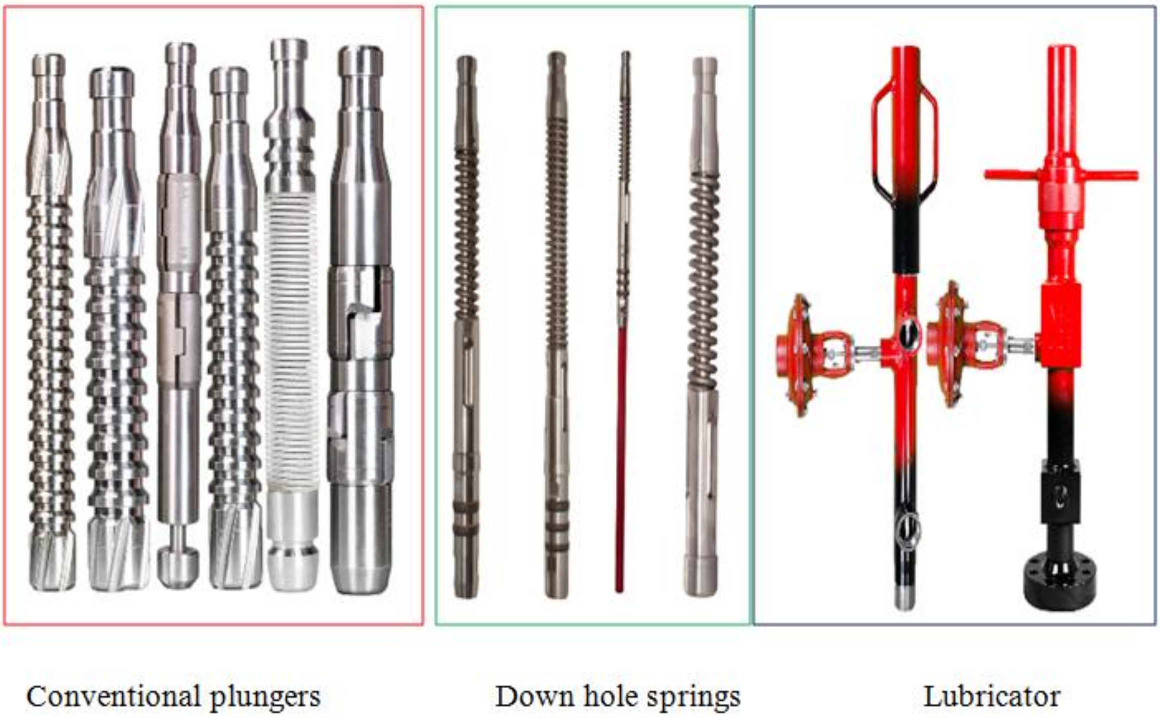

Figure 43: Different Types of pieces of equipment in Plunger lift taken from (http://www.epiclift.com/Plunger-lift).

Types of Plunger System

The following are different types of Plungers depending on the ability of the well to flow once loaded with liquid (Hearn, 2010).

a) Continuous Flow Plunger uses energy from the produced gas in raising the Plunger and needs velocity higher than 10 ft/s to continuously arrive to the surface.
b) Conventional Plungers uses the pressure stored in the well and in the annulus for the Plunger to arrive at the surface.
c) Staged Plunger system uses multiple Plungers system in the same well transfer fluid from stage to stage.

Plunger Lift Operation.

The operation of Plunger lift is a cyclic operation as it involve alternatively shut-in and flow. During shut in the Plunger falls back to the bamper spring first through gas and then through some accumulated liquid. Based on the Foss and Gaul model the fall velocity of Plunger through gas is 2000ft/min and through the accumulated liquid fall velocity was 172ft/min (SPE, 2012).

Falling of Plunger to the bumper spring is followed by gas build up which aids in lifting the Plunger and some accumulated liquid to surface and the well is open to production again (Lea, et al., 2008). The well remain flowing with the Plunger at the surface until when the gas production rate becomes less than critical rate and the well is closed and the Plunger fall to the bottom and the process is repeatitive (Lea, et al., 2008). Figure 44 summarise the Plunger lift cyclic operation using pictorial diagrams.

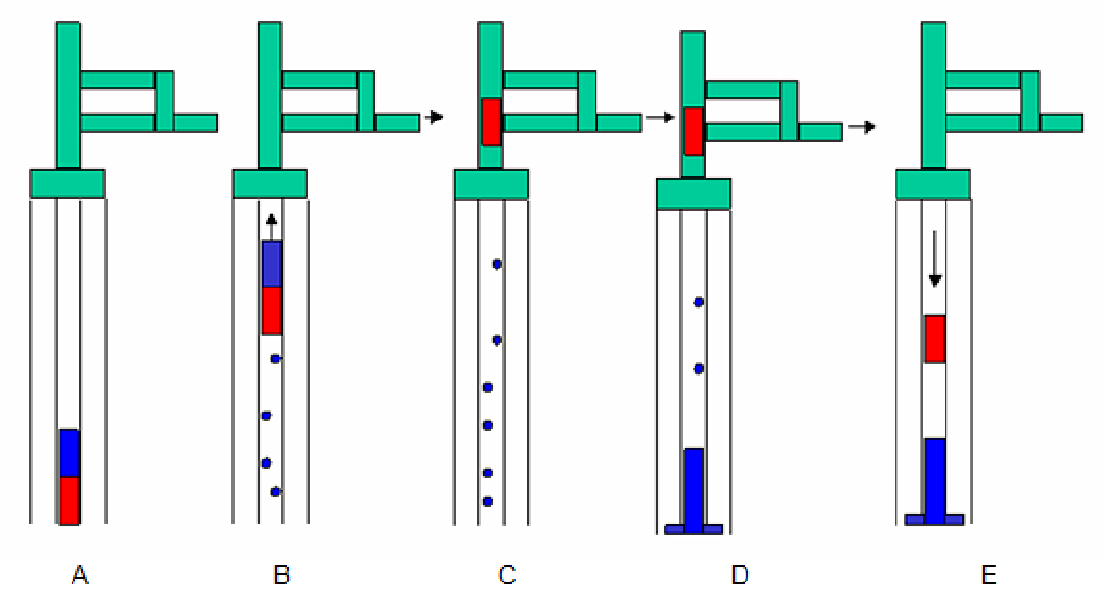

Figure 44: Description of Plunger lift cycle events **(ALRDC, n.d.)**

A - Plunger at the bottom with some lliquid above Plunger, surface valve closed

B - Surface valve opens and Plunger rises with liquid above it

C - Well flows at high rate for a while

D - Well begin to liquid load

Plunger Lift Modelling and Design.

The engineering design of Plunger lift installation in gas well involves the estimation of casing pressure required to lift the liquid slug weight and the minimum required volume of

Plunger lift gas at that pressure (Lea & Tighe, 1983). The other parameter which is very important to estimate during Plunger lift design is the maximum number of cycles required for Plunger lift operation (SPE, 2012).

Several correlations have been developed to estimate the Plunger parameters and the basic models which are mostly used to determine the Plunger lift operating range is the Foss and Gaul model. Foss and Gaul model was associated with several assumptions and the following are their basic assumptions:

i. The pressure effect of the Plunger frictions against the tubing wall was neglected,
ii. Small pressure differences between the tubing and the casing annulus,
iii. The pressure effect of the fluid entry beneath the Plunger is neglected
iv. The casing-tubing gas friction pressure loss is neglected and

Estimating the Casing Pressure Build up

Foss and Gaul model provided the basic equations that are used to estimate the casing pressure build up during Plunger lift operations. Equation 27 represent the minimum casing build up pressure was proposed as the basic equations from which other casing pressure at different location of the tube can be estimated (Mower, et al., 1985; SPE, 2012).

$$P_{Cmin} = [P_t + P_P + 14.7 + (P_{ln} + P_{lf}) * S]\left(1 + \frac{D}{K}\right) \quad 27$$

Where

P_t = Surface tubing pressure, psi

P_P = Pressure to lift Plunger = $\frac{\text{Plunger weight}}{\text{tubing area}}$, psi

Plunger weight = 10lbs

$P_{lh}+P_{lf}$ = pressure of liquid head(P_{lh}) and flowing friction(P_{lf}), psi

($P_{lf} = 1.3P_{lh}$)

D = Tubing Depth, ft

$K = \text{Constant to account for flowing gas friction}$

For given tubing size the value of 'K' and $''\mathbf{P_{lh}}+\mathbf{P_{lf}}''$ are constants and Table 5 summarises those constants for different tubing internal diameter (SPE, 2012; Lea & Tighe, 1983).

Table 5: Approximations of K and Plh+Plf for various tubing sizes

Constant	**Value**	**Tubing size, in**	Plh+Plf Psi/bbl.
K	27, 000	1.61	
K	33,500	1.995	165
K	45,000	2.441	102
K	57,600	2.992	63

The maximum casing build up pressure, tubing cross section area 'A_t' and casing area 'A_a' was estimated using equation 28, 29 and 30 (Mower, et al., 1985; SPE, 2012).

$$P_{c\,max} = P_{c\,min} * (\frac{A_t + A_a}{A_a}) \tag{28}$$

Where

$$A_t = \pi * \frac{{d_t}^2}{4 * 144}, ft^2 \tag{29}$$

$$A_a = \frac{\pi}{144 * 4} * \left[{d_c}^2 - {d_t}^2\right], ft^2 \tag{30}$$

And

$d_t = \text{tubing internal diameter, inches}$

$d_c = \text{casing internal diameter, inches}$

The estimation of the average casing build-up pressure ($P_{c\,avg}$) was given by equation 31 below (SPE, 2012).

$$P_{c\,avg} = P_{c\,min} * (1 + \frac{A_t}{2 * A_a}) \qquad 31$$

Gas Required per Cycle

The minimum gas lift required to lift the slug is calculated as the gas in the tubing just before the well is open to cycle (Lea & Tighe, 1983). This gas rate required in lifting the Plunger and the liquid above to surface was estimated using equation 32 (Lea & Tighe, 1983; SPE, 2012).

$$Q_C, \frac{Mscf}{cycle} = F_{gs} * P_{c\,avg} * (\frac{V_t}{14.7})(\frac{520}{(T_{avg*}Z)}) \qquad 32$$

Where

V_t = Actual tubing volume, cuft $= A_t * \frac{(D - S * L)}{1000}$

F_{gs} = Slippage factor $= 1 + \frac{0.02 * D}{1000}$

$P_{c\,avg}$ = Average casing build up pressure, psia

T_{avg} = Average wellbore temperature, R

Z = Gas deviation factor at Pcavg and Tavg

D= Plunger depth

S= Slug size

L = Tubing inner capacity $= \frac{5.615}{A_t}, \frac{ft}{bbl}.$

Maximum Cycles

The maximum Plunger cycles (C_{max}) stands for the maximum possible cycles on the basis of Plunger velocities used **(SPE, 2012)**. Therefore the well is always expected to operate below C_{max} because well shut-in time is required to build any casing pressure. The estimation of the maximum possible number of Plunger cycles per day was given using equation **33**.

$$C_{max} = \frac{1440}{\frac{D - SL}{v_{fg}} + \frac{D}{v_r} + \frac{SL}{v_{fl}}} \qquad 33$$

Where

$\mathbf{v_{fg}}$ = Average velocity of Plunger falling through gas, ft/min (200 − 1,200 ft/min)

$\mathbf{v_{fl}}$ = Average velocity of Plunger falling through liquid, ft/min (50 − 250 ft/min)

$\mathbf{v_{r}}$ = Average rise velocity of Plunger , ft/min (typically 400 − 1,200 ft/min).

Restriction on Plunger Lift design parameters

The following are some of the restrictions identified from literature for Plunger lift designed parameters (Mower, et al., 1985).

a) If the calculated maximum casing build up pressure becomes greater than the well shut in pressure then production is not possible.
b) If the estimated gas liquid ratio is too low then production is not possible.

Production is only possible once the well GLR becomes higher than the produced GLR for each cycle. (Mower, et al., 1985).

c) The time to produce must exceed the well shut in time.

Applicability of Plunger Lift.

Plunger lift can work for several different set of well conditions given below.

a) GLR Rule of Thumb

Plunger lift becomes the best candidates for gas well with higher GLR of atleast 400scf/bbl for every 1000ft (Lea, et al., 2008). The GLR of 400scf/bbl for every 1000ft well depth were used as the rule of thumb in estimating the minimum GLR as compared to the reported well GLR.

b) Feasibility Charts.

The other means to estimate the minimum GLR in a well is by using the feasibility charts in Figure 45. The main input into the chart in estimating the minimum GLR are operating pressure and the well depth (Lea, et al., 2008). Plunger lift becomes the best candidates for a given well if the well measured GLR is greater than or equal to chart GLR.

c) Maximum liquid produced with the Plunger

Plunger lift application can tolerate a certain volume of liquid produced for a given well depth and tubing sizes (Lea, et al., 2008). Figure 46 relates the relation between the tubing sizes, well depth and the maximum liquid volume required for Plunger operation.

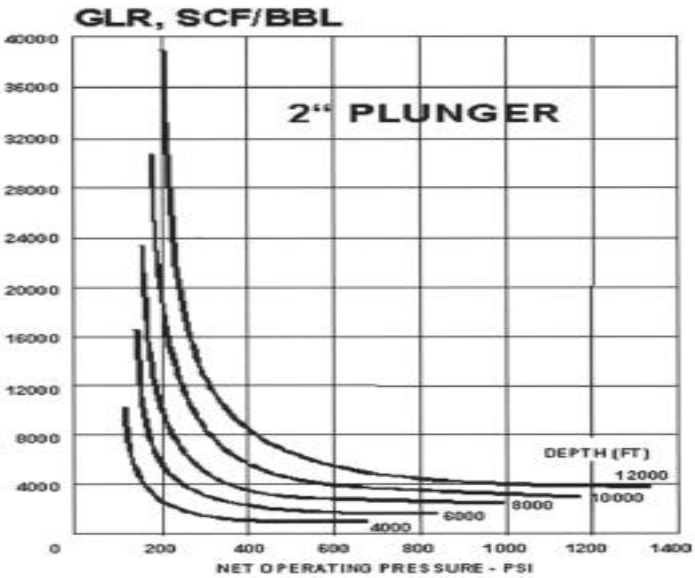

Figure 45: Feasibility Charts of Plunger Lift for 2-3/8's Inch Tubing **(Lea, et al., 2008)**.

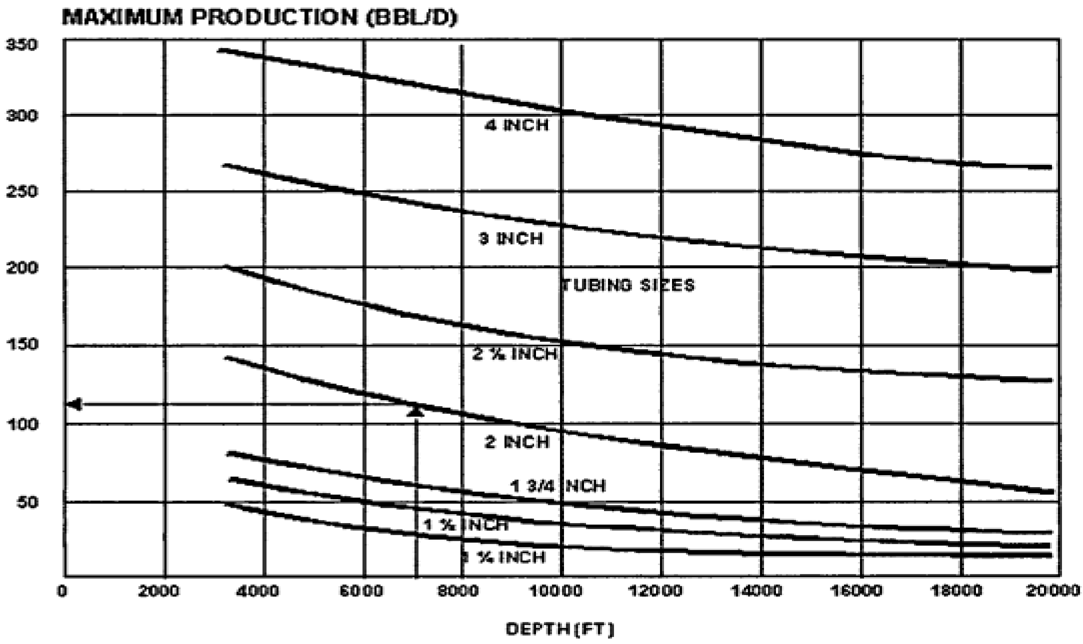

Figure 46: Liquid Production Estimates for Plunger Lift **(Lea, et al., 2008)**.

d) Well Completion.

The well completion type can limit the applicability of Plunger lift in gas well. Plunger lift becomes more efficient and preferable in a packerless completion. For a well completed with packers to use Plunger lift will require a re-perforation of the tubing above and near the packer so that to allow communication between the tubing and the annulus (Lea, et al., 2003; Lea, et al., 2008). Figure 47 compares the performance of the Plunger lift with and without packers in the well.

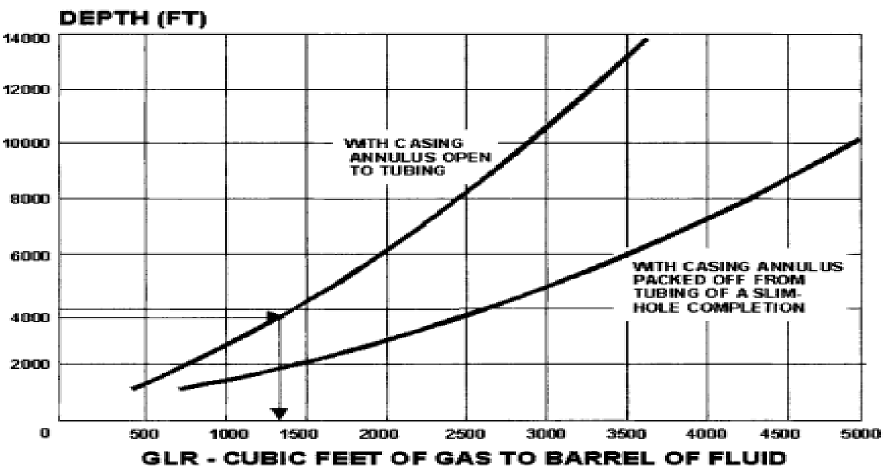

Figure 47: Gas Needed for Plunger Lift with or without a Packer in the Well **(Lea, et al., 2008)**

Advantages and disadvantages of Plunger lift system.

Plunger lift system method has several advantages and disadvantages in unloading the gas well (James, et al., 2002) and the following are the advantages of Plunger lift.

i. Only uses natural well energy.
ii. Can produce the well to economic depletion
iii. Produced gas can go to sales if no venting required
iv. Can easily be automated
v. Low maintenance costs
vi. Is good for well deviation up to 60^o
vii. Used to control paraffin and scale build up in the well.

Disadvantage of Plunger lift

a) Well shut-in time is required and gas sales are not continuous
b) Tubing must have consistent ID for Plunger to work
c) Swabbing may be required periodically to assist in some aplications
d) Wells with production packers or small casing annulus must have higher GLR.

4.1.2 Estimating Production Rate

There are several approaches which can be used to determine the production increases from Plunger lift system in the gas well. Decline curve analysis is the simplest and sometimes the most accurate method employed in predicting the natural decline of gas production rate expected in the gas well (SPE, 2012). When liquid loading occur in a given well there is an abrupt decline in gas production which mark the deviation of the actual decline curve from the normal expected decline curve.

The intention of the Plunger lift is to return the deviated actual production to the normal production forecasted by the normal decline curve as shown in **Figure 40** to keep the well from liquid loading.

4. Gas Lift

Gas Lift Systems is one of the artificial lift methods which use the external source of high pressure gas injected through the downhole valve to assist the formation gas in removing the accumulated fluid from the bottom of the well to surface. The primary consideration in selecting gas lift for unloading gas well is the availability of external source of gas and the cost associated with gas compression to design pressure (Schlumberger, 1999).

The working mechanism of the gas lift in gas well is by decreasing the hydrostatic head above the injection point and increasing gas velocity to lift the liquids to the surface (Neves & Brimhall, 1989).

For dewatering the gas wells, the volume of injected gas is designed such that the combined formation and injected gas will be above the critical rate for the wellbore especially for lower liquid producing gas wells (Lea, et al., 2008).

Applicable Conditions for Gas Lift (Lea, et al., 2008; Winkler, 1987)

i. Gas lift is more efficient when GLR exceeds 500scf/bbl

ii. Gas lift is excellent in handling solids.

iii. Gas lift is the solution for lifting the accumulated liquid in deviated gas wells.

iv. Gas lift is easily adapted to reservoir condition changes.

Gas lift limitations

Though gas lift was found to be the most efficient means of dewatering gas wells as well as handling the produced solids. It has several limitations in their applicability and the primary limitations includes lack of formation gas or external source of gas, wide well spacing, and available space for installing the compressor on offshore platforms (Winkler, 1987).

Gas Lift System Components

The following are the components which are required for the complete gas lift system (Lea, et al., 2008). Figure 48 describe different components which make the complete gas lift system.

i. A gas source

ii. Surface injection system such as compressors, pipes and control valve.

iii. Producing well completed with downhole gas lift injection valves and mandrels.

iv. Surface processing system such as separators and control valves.

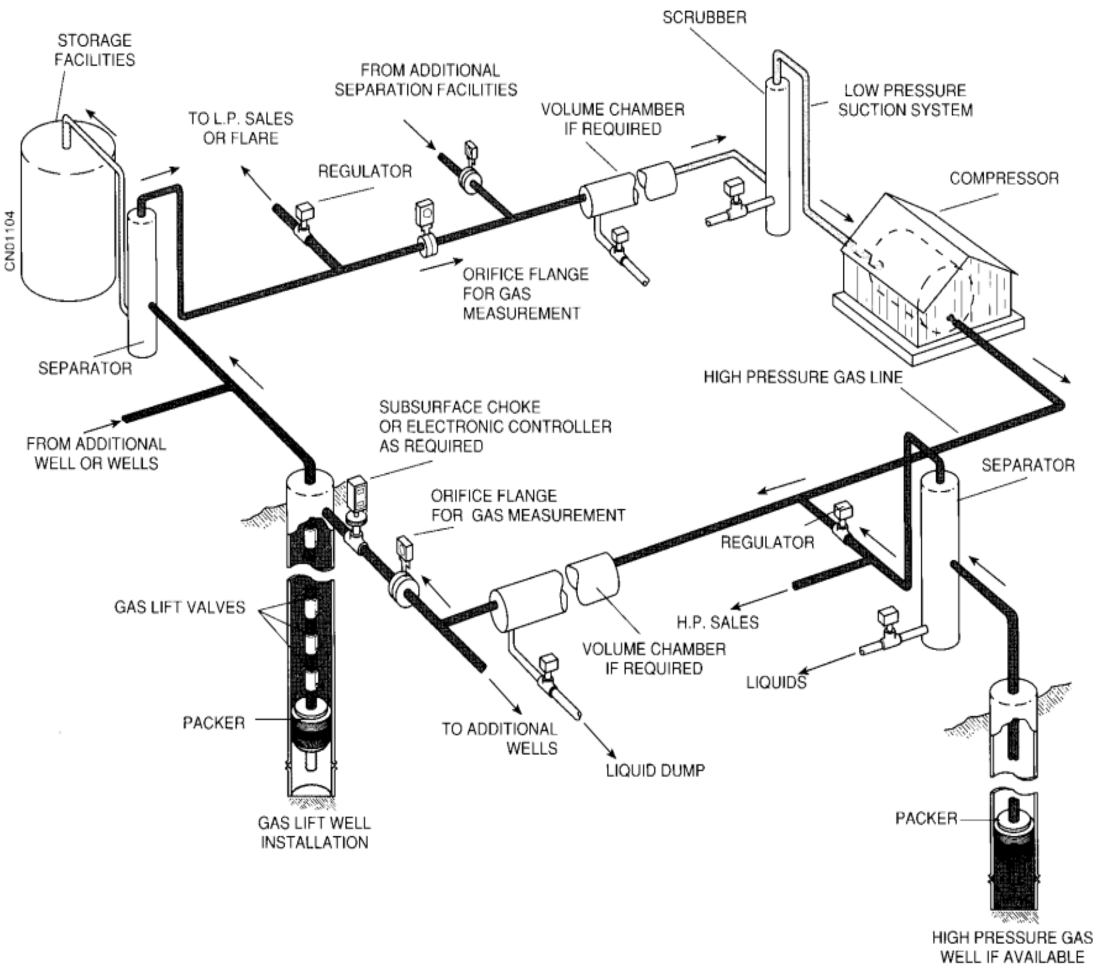

Figure 48: Basic components for gas lift systems (Schlumberger, 1999).

Gas Injection Pressure.

Injection pressure at depth is very important factor to be estimated in the design of the artificial gas lift system. Equation 34 was developed to be used in the calculation of static gas injection pressure at depth

$$P_D = P_S\, e^{\left(\frac{\gamma_g D}{53.34TZ}\right)}$$ 34

Where

$P_D =$ Operating injection gas pressure at depth D, psia

$P_S =$ Operating injection gas pressure at surface, psia

$D =$ True vertical depth, ft

$\gamma_g =$ Gas specific gravity

$T =$ Average Temperature in oR

$Z =$ Gas deviation factor

Injection Gas Volume Calculations.

The calculation of gas volume required to lift the liquid slug from gas well during gas lift operation can be calculated by applying the gas equation in 35.

$$PV = nZRT$$ **35**

Where,

P= presssure in psia

T= Temperature in ^oR

Z= gas deviation factor at P and T

R= Gas constant 10.73 psia-cu ft/lbm-mol-^oR

The volume of gas required to fill the conduit can be calculated from equation 36 (Winkler, 1987).

$$V_g = V_C \frac{PT_{SC}}{zP_{SC}T} \quad (36)$$

Where

$V_g =$ Gas volume injected at the standard conditions, scf

$V_C =$ Conduit volume, cu ft

$T_{SC} =$ Surface temperature, 520R

$P_{SC} =$ Standard pressure, 14.7 psia

$T =$ Average temperature, R

$P =$ Average gas pressure, psia

$z =$ Average gas compressibility at P and T

The implementation costs for gas lift method will range from $25,000 to $40,000 depending upon the compressor size (Neves & Brimhall, 1989).

4.1.3 Pumping Method

Pumping unit may be defined as the machine which cause the up and down motion through the sucker rod string, to the subsurface pump (API, 2000). Different pumping method will have different extenal driving energy added to the system to increase its lifting capacity as described in Table 8.

Pumping method for removing liquid from gas are depends on the volume of liquid produced and well depth as shown in **Figure 49** and **Figure 50**. The gas wells which are either not producing or producing at very low rate and low flowing bottomhole pressure due to large amount of liquid accumulation downhole are the best candidates for pumping method. The application of pump in deliquifying gas wells does not depend critical gas rate thus it can be used to drain the well until the reservoir are depleted (Hutlas & Granberry, 1972).

There exist several types of pumping units which has been installed in wells for removing the produced liquid from gas well. These pumping units were such as Hydraulic pumping, ESP, Rod pumping, Progressive cavity pump and Beam pumping.

1. **Hydraulic Pumping**

The driving energy when using Hydraulic pumping to unload the gas wells are either electric motor, diesel engine or gas engine (Lea, et al., 2003). Hydraulic pumping is highly tolerant to sand and other particles and is capable of producing up to 500bpd of liquid (Lea, et al., 2008).

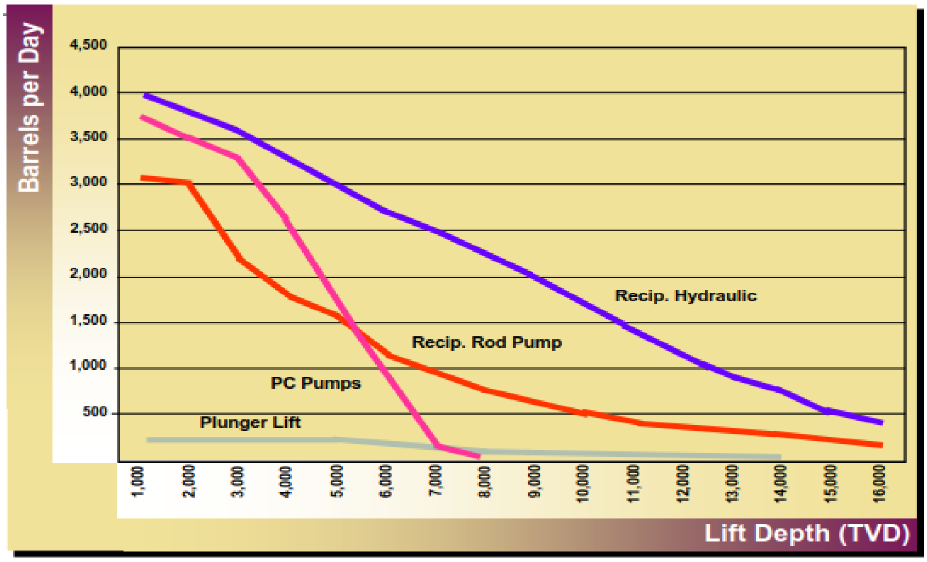

Figure 49: Lower volume gas lift methods **(Bondurant & Hearn, 2008)**

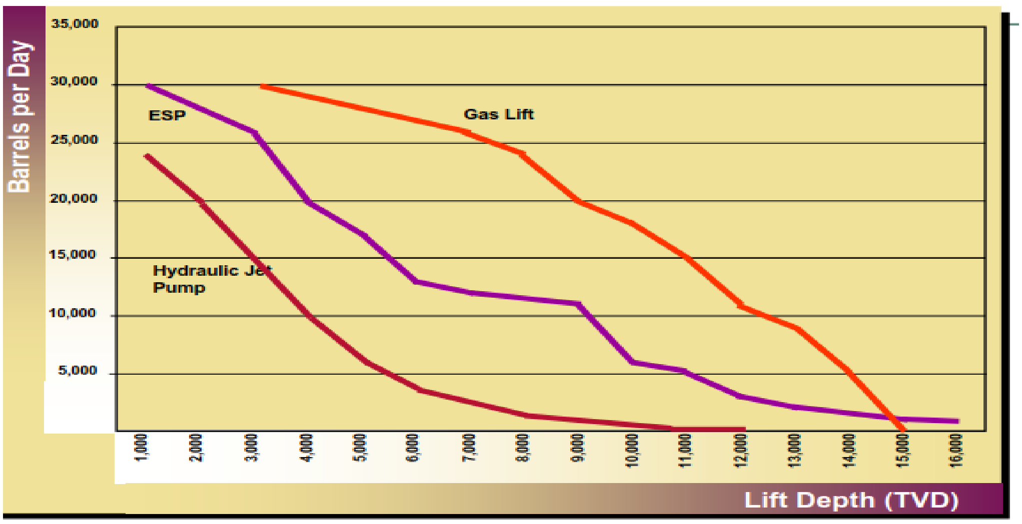

Figure 50: High volume artificial lift mechanisms **(Bondurant & Hearn, 2008)**.

2. Beam Pump or Reciprocating Rod Pump

Beam pumping is likely the most common method used to remove liquids from gas wells. Figure 51 is the arrangement of different components which are installed in the well and lift the produced liquid to surface.

Beam pumps are highly affected by the amount of gas passing through it, to avoid gas interference in dewater gas wells special attention should be taken like to set the pump below the perforation and flowing the gas up the annulus (Lea, et al., 2003).

Pump – off Controller

POC are used to stop the pump from operating when the liquid level is too low and the main advantages of having POC in the system is to reduce the well maintenance and energy usage (API, 2000). The minimum design liquid rate required to operate the pump to avoid pumping off was given by equation 37 (Lea, et al., 2008).

$$\text{Design rate} = \frac{\text{max inflow capacity x 24hrs/day}}{\text{pump volumetric efficiency x hours pumped/day}} \qquad 37$$

Lea, et al., 2008, suggested 20 hrs/day pumping time as a good rule of thumb.

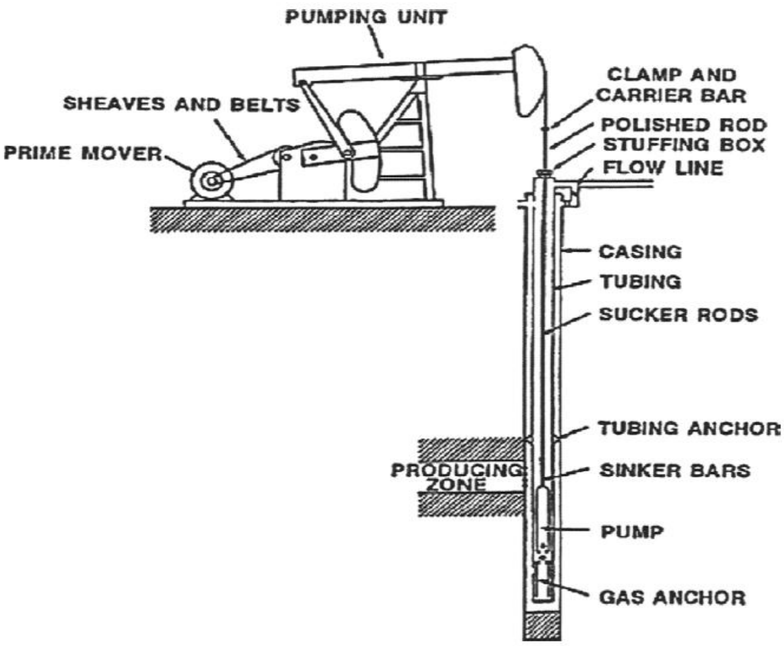

Figure 51: Schematic of Beam Pumping System **(Lea, et al., 2008)**.

3. Progressive Cavity Pump

Progressive Cavity Pump and gas lift are the most useful methods in a sand producing wells because they are more competent in handling solids, liquid and gases. **Table 6** is the typical range of well conditions in the application of PCP to unload gas wells. PCP can handle a significant amount of gas if enough liquid flows through the pump to carry away heat of compressions (Simpson, 2006). Heat of compression is result of gas present in the pump being compressed from low pressure up to pump discharge pressure.

Table 6: The General Application Envelope for PCPs System **(Lea, et al., 2008)**

Conditions	Typical Range	Maximum
Operating depth	1000-5000ft	9800ft
Operating Volume	5-2500BPD	5000BPD
Operating Temperature	65-170F	300F
Wellbore deviation	N/A	Less than 15 Deg / 100ft
Solid handling	Excellent	
Corrosion handlling	Good	
Gas handling	Excellent	
Fluid Gravity	Below 45 API	
Servicing and Repair	Require Workover or Pulling the Rig	
Prime mover type	Electric Motor or Internal Combustion Engine	
Offshore application	Good	

4. Electrical Submersible Pump (ESP)

ESP are applicable when the produced flow is primarily liquid. As indicated in Figure 50 ESP can work in the well with high liquid volume up to 30,000bbls and can operate in a deep well.

The efficiency of ESP are highly affected by the precence of the amount of gas flowing across the pump. High volume of gas in this pump can cause gas intereference or severe damage if ESP is not properly installed. To avoid the effect of gas on the pump, gas are produced through the casing and liquid through the tubing or downhole separation may be required (Lea, et al., 2003).

ESP Components

Figure 52 is the schematic diagram of gas well with ESP installation showing different components required for its operations.

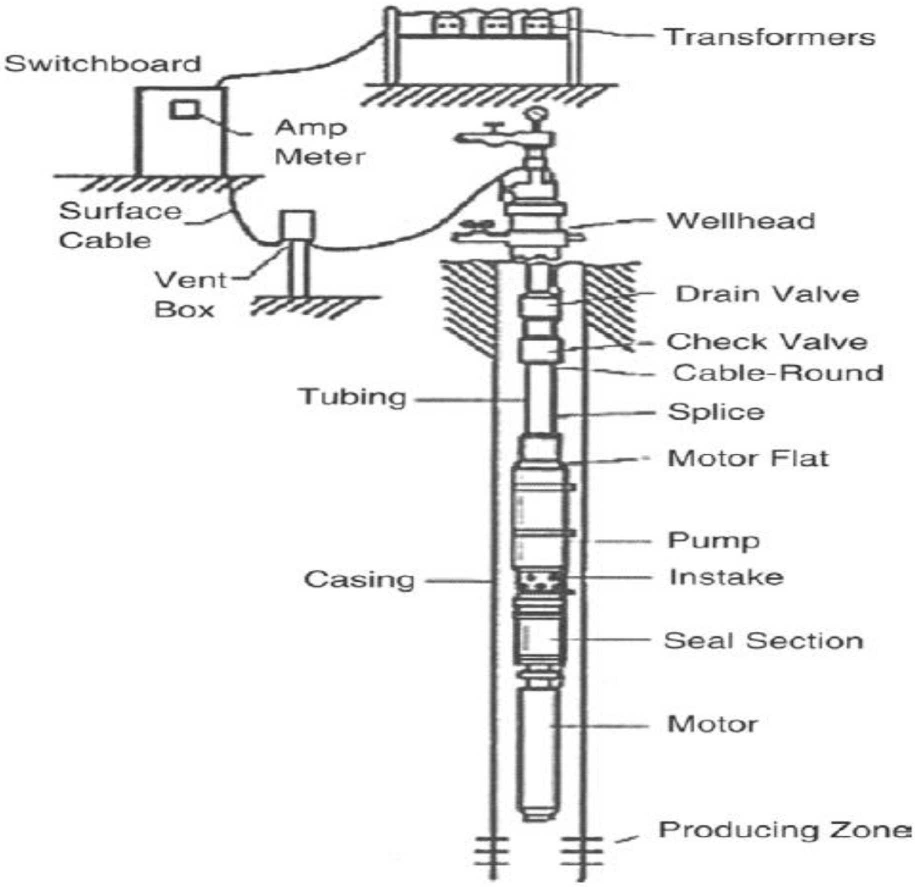

Figure 52: Typical ESP System **(Lea, et al., 2003)**

ESP require external source of energy to operate, so from Figure 52 the transformer at the surface is required to generate electricity which is caries to the motor below the pump.

5. Foam for Gas Deliquification

Foam has many application in the gas and oil industry. It may be used as the drilling fluid, fracturing fluid and for enhanced oil recovery . Apart from that foam is considered the least expensive method of gas well dewatering at low gas rate (Yang, et al., 2006).

The working mechanism of foaming in unloading gas well is by changing the liquid into a bubble film which decreases the density of the liquid, decrease surface tension, increases the exposed surface area and finally lowered critical gas velocity (Hearn, 2010).

The addition of surfactant leads to decrease of the surface tension and formation of foam that has much lower density than the bulk liquid as in Figure 53. The decreased fluid density facilitate the deliquification of the gas wells as they lead to increased effective gas lifting force (Heuvel, et al., 2010; Yang, et al., 2006).

There are several factors that may affect the performance of foam in removing the accumulated liquid to surface. These factors has a negative effect on foam generation are they are such as the precence of brine, hydrocarbon condensate and high temperature downhole (Yang, et al., 2006).

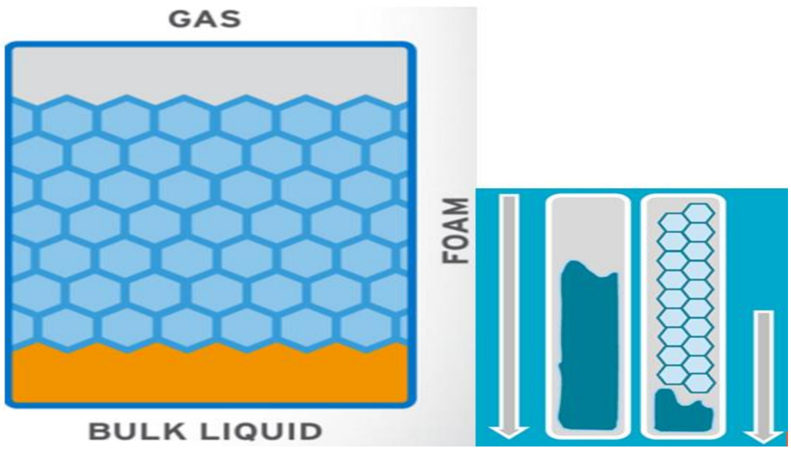

Figure 53: Working Principle of Foam in Lifting Liquid **(Heuvel, et al., 2010)**.

Effect of Brine on Foam Performance

The presence of brine (NaCl) in solution has two effects on foam unloading of water (Yang, et al., 2006).

i. Brine reduces thickness of foam film leading to decreased volume fraction of water in foam and
ii. Brine forms denser adsorption layers which results in film rupturing.

Effect of Hydrocarbon Condensate

Hydrocarbon condensate acts as antifoam and forms emulsion which reduces the effectiveness of surfactant as foamer (Yang, et al., 2006). The relationship between foam unloading and hydrocarbon condensate are shown in Figure 54. The presence of condensate in the well may limit the applicability of foam as the deliquification method.

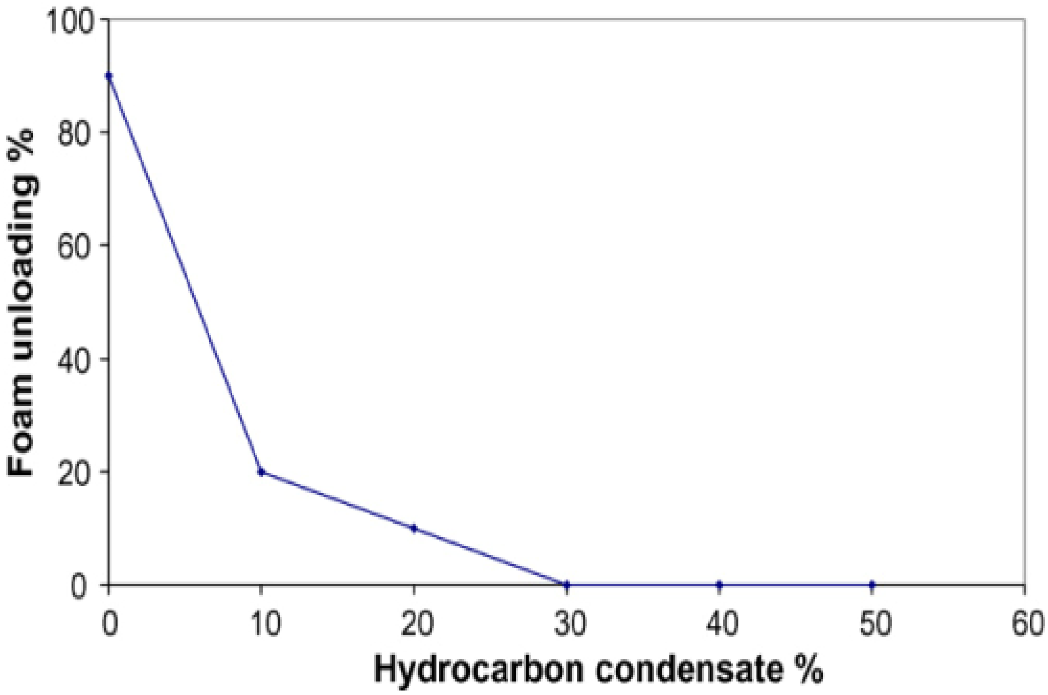

Figure 54: Effect of hydrocarbon condensate on foam unloading (Yang, et al., 2006)

Effect of High Bottomhole Temperature on Foaming

High downhole temperature in gas wells has a negatve effects on foam unloading. The performance of foamer in unloading gas wells was studied in the laboratory at high temperature as in Figure 55 below and gave the results that at high temperature foam height was low and short half life (Yang, et al., 2006).

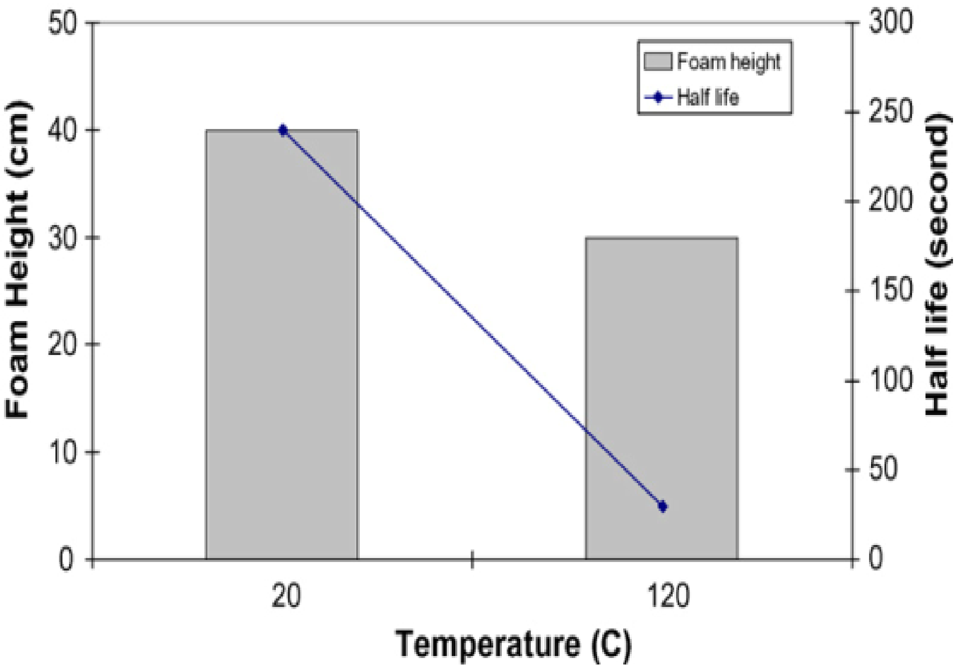

Figure 55: Effect of temperature on foam unloading (Yang, et al., 2006).

The best application of foaming as the deliquification method for loaded gas well is with gas well with higher GLR between 1000 and 10000 cf/bbl where agitation necessary exists and in higher water cut greater than 50% (Hearn, 2010).

5. LIFT SELECTION PROCESS.

The application of various deliquification methods identified above depends on the existing field and well operating conditions. Each method is suitable for certain well conditions. The selection of which method to install in the well for lifting the accumulated liquid in gas well is not always an easy task because the methods need to be selected based on a broad range of conditions.

The suitability of the deliquification method in gas well is usually evaluated on the basis of their technical and economic factors. Technical and economical evaluations are so important because different liquid unloading techniques have different technical limitations as well investment cost.

The evaluations are performed based on the decision matrix which is done in stages from primary screening of the technical viability of each method to final selection (Park, et al., 2009). The stages for evaluation of the deliquification methods in gas wells to select the most optimum method based on technical and economic factors were presented in Figure 56.

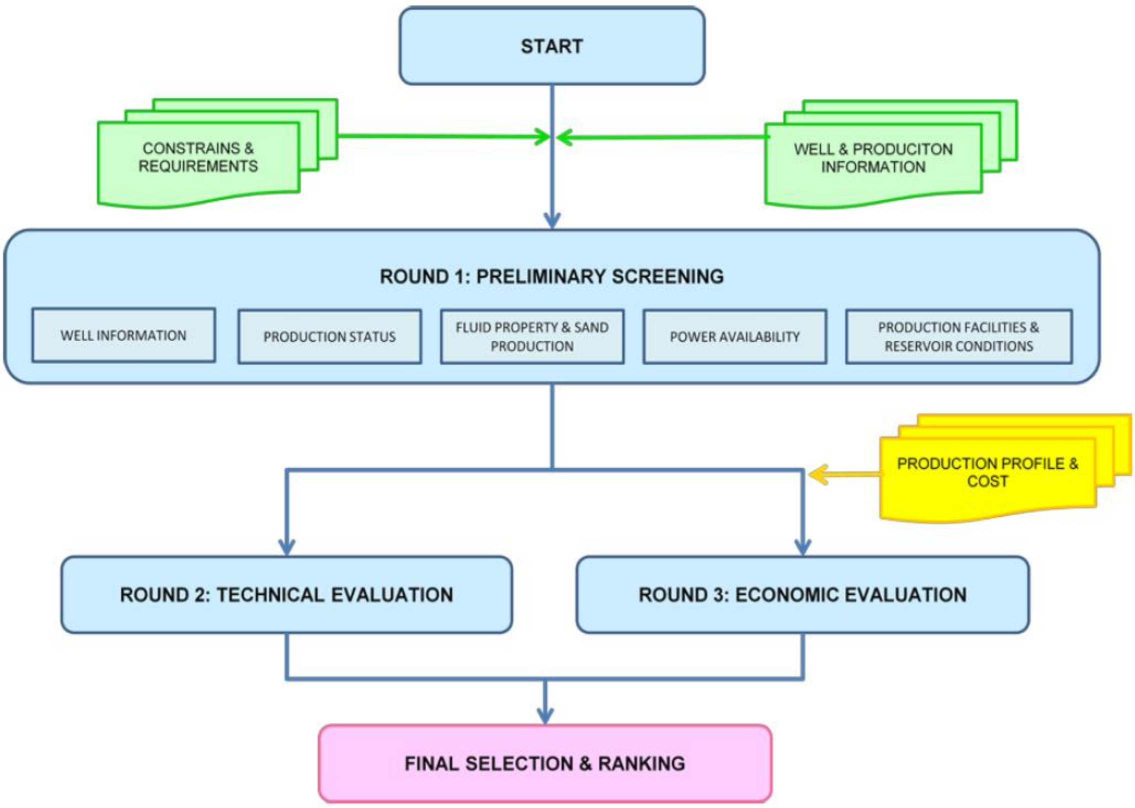

Figure 56: The workflow of the liquid unloading decision matrix (Park, et al., 2009).

The following were the different technical and economic factors which are considered in evaluating the suitability of the deliquification method in gas wells (Neves & Brimhall, 1989).

a) Equipment Cost.

Different artificial lift methods involve the installations of the equipment in the well and their selection may be limited by the availability of fund though it might be technically feasible for given well conditions.

b) Operating Costs

Nerves & Brimhall, 1989 defined the operating costs in four categories which are personal costs, material costs, maintenance costs, and energy costs. Operating costs in the selections of the deliquification methods are very important factor to be considered because once the methods has been installed in the well it needs to be maintained for its productivity.

c) Equipment Availability.

Sometimes a certain artificial lift method may be suitable for removing the liquid from the well but its selection may be hindered by the equipment availability in storage (Neves & Brimhall, 1989).

d) Existing Equipment.

The installed surface and subsurface equipment in gas well can dictates the selection some artificial lift for unloading the gas well. The gas well completed with packer, small tubing string can limit the operator choice for the optimum method.

The methods such as Plunger lift, Foaming agent, Rod pumping and intermitting are highly affected by the presence of packer completion which sometime may require additional cost to re-perforate above the packers (Neves & Brimhall, 1989).

e) Well Location

Well location may limit the selection of a certain deliquification methods because of the shortage of space for equipment installation. For example Plunger lift and gas lift are never employed when the wells are located offshore.

f) Gas Liquid Ratio (GLR).

GLR is very important factor to be considered in the design and application of the artificial lift methods. Most of pumping method can operates more effectively for the well which produce low GLR otherwise separation equipment is required to separate gas before entrance into the pump.

g) Liquid Production Rate.

The total volume of liquid to be produced from the well is important factors governing the selection of artificial lift method. Different artificial lift methods are useful to different liquid production in gas wells as classified in **Figure 49** and **Figure 50**.

h) Well Deviation.

Well deviation has a significant effect on the selection of the artificial lifting methods. A highly deviated well presents operating problems when using rod pumping and Plunger lifts for removing liquid from the wellbore but gas lift is more viable means of producing highly deviated wells (Park, et al., 2009). **Figure 57** is the operating range and the maximum well deviations required for different liquid unloading methods.

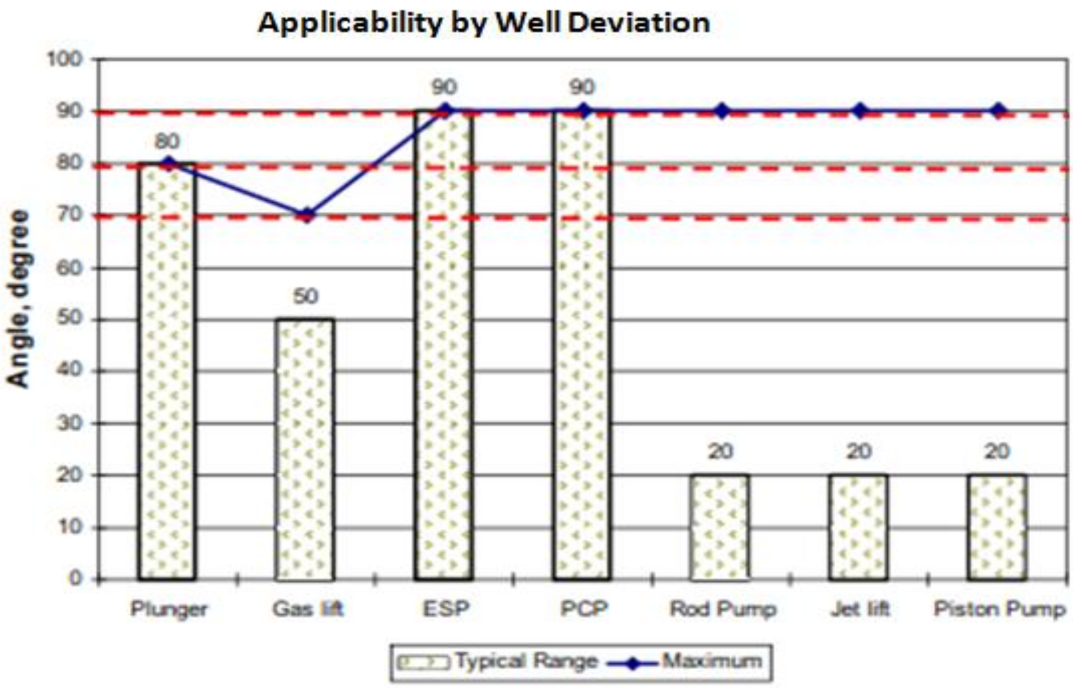

Figure 57: Application of Technical Remedial by Well Deviation **(Park, et al., 2009)**.

i) Existing Reservoir Pressure.

Depending on the operating range of the reservoir pressure, liquid unloading methods are applicable to a certain range of the existing reservoir (Lea, et al., 2008). Table 7 shows the operating reservoir pressure range applicable for various liquid unloading methods in gas well.

Table 7: Pressure Range for Selection of Deliquification Method (Lea, et al., 2008).

Range of Pressure	Possible Method Applied
P_R>1500 Psi	❖ Evaluate natural flow of the well ❖ Use nodal analysis, evaluate tubing size for friction and future loading effect.
500<P_R<1500 psi	❖ Plunger lift ❖ Small tubing ❖ Gas lift ❖ Reggular swabbing for short flow period ❖ Pit blow down ❖ Surfactants- injection.
150<P_R<500 Psi	❖ Plunger lift-operate with large tubing ❖ Small tubing ❖ Surfactant ❖ Rod pump or PCP is severe sand ❖ Gas lift ❖ Swabbing ❖ Jet pumping
PR<150 Psi	❖ Rod pumps ❖ Plunger in some cases ❖ Siphon strings ❖ Intermitent gas lifts, chamber lifts. ❖ Jet pump ❖ Swabbing ❖ Sufactants

j) Power Availability

Different deliquification methods are driven by different sources of energy which ranges from natural energy to external added energy such as electricity and gas. The selection of the deliquification must consider the cost and availability energy.

The low cost power availability is the critical factor in chosing the efficient liquid deliquification method for gas well. **Table 8** shows different sources of energy for different unloading method.

Table 8: Power Sources of Artificial Lift Methods (Park, et al., 2009).

Deliquification Method	Prime Mover Type (Driving energy)
Plunger Lift	Natural energy of the well
Gas Lift	Pressurized gas (Compressor w/electric motor or gas engine)
ESP	Electric Motor
PCP	Gas engine or electric motor
Rod Pump	Gas engine or electric motor
Jet Lift	Multi-cyclinder hydraulic pump w/electric motor or gas engine
Piston Pump	Multi-cyclinder hydraulic pump w/electric motor or gas engine
Velocity string	Natural energy of the well

5.1 Evaluation of Liquid Deliquification Method

Based on the evaluation flow chart given in Figure 56 the following four steps are used as the guide during the selection of the most optimum method for removing liquid from the gas well (US EPA, 2011)**.**

i. Determine the technical feasibility of various artificial lift options.
ii. Determine the cost of various options.
iii. Estimate the natural gas savings and production increase.
iv. Evaluate and compare the economics of artificial lift options.

Following the above steps the evaluation processes is usually done in three round namely round 1, round 2 and round 3 (Park, et al., 2009). For each round, different criteria are considered where by the evaluation through round 1 and 2 are done for technical feasibility while round 3 is based on using the estimated costs to find the economics of various methods. **Table 10** has indicated the most useful information evaluated in each round for the selection of the most optimum method from various methods available.

5.1.1 Technical Feasibility of a Fluid Removal Method

Figure 56 has indicated that technical feasibility study need to be performed in two stages or round which are round 1 and round 2. In executing this step various data and criteria need to be gathered.

The most important information required for technical evaluation are such as well IPR curves, Reservoir Pressure, Gas and liquid production flow rates, fluid levels in the well, the desired flowing bottomhole pressure and casing pressure, production tubing size and the downhole condition of the well (US EPA, 2011).

Round 1: Preliminary Screening

The evaluation of the deliquification method through round 1 was called the preliminary screening of different method based on their technical viability (Park, et al., 2009). During preliminary screening the unsuitable methods are rejected by technical criteria.

Several criteria have been developed to be used in selecting the appropriate liquid unloading method for gas wells (Weatherford, 2014).

Table 9 represents the technical screening criteria developed by Weatherford to be used in evaluation of liquid unloading methods for gas wells. Round 1 screening process will involve the comparison of the reported well conditions with the operating range of each method proposed in

Table 9 to find out if a certain method can operate for a given well conditions (Park, et al., 2009).

Table 9: Technical Selection Criteria for Liquid Removal Methods **(Weatherford, 2014)**.

Form of lift	Rod Lift	PCP	Gas Lift	Plunger Lift	Hydraulic Lift	Hydraulic Jet	ESP	Capillary Technologies
Maximum operating depth, TVD (ft/m)	16,000 4,878	12,000 3,658	18,000 4,572	19,000 5,791	17,000 5,182	15,000 4,572	15,000 4,572	22,000 6,705
Maximum operating volume (BFPD)	6,000	4,500	50,000	200	8,000	20,000	60,000	500
Maximum operating temperature (°F/°C)	550° 288°	250° 121°	450° 232°	550° 288°	550° 288°	550° 288°	400° 204°	400° 204°
Corrosion handling	Good to excellent	Fair	Good to excellent	Excellent	Good	Excellent	Good	Excellent
Gas handling	Fair to good	Good	Excellent	Excellent	Fair	Good	Fair	Excellent
Solids handling	Fair to good	Excellent	Good	Fair	Fair	Good	Fair	Good
Fluid gravity (°API)	>8°	<40°	>15°	>15°	>8°	>8°	>10°	>8°
Servicing	Workover or pulling rig		Wireline or workover rig	Wellhead catcher or wireline	Hydraulic or wireline		Workover or pulling rig	Capillary unit
Prime mover	Gas or electric	Gas or electric	Compressor	Well's natural energy	Multicylinder or electric	Multicylinder or electric	Electric motor	Well's natural energy
Offshore application	Limited	Limited	Excellent	N/A	Good	Excellent	Excellent	Good
System efficiency	45% to 60%	50% to 75%	10% to 30%	N/A	45% to 55%	10% to 30%	35% to 60%	N/A

Table 10: Consideration factors for evaluation of the deliquification method **(Park, et al., 2009)**.

Consideration factors		Round 1	Round 2	Round 3
Producing characteristics	L_{iquid}	√	√	
	GLR	√	√	
Fluid properties	Viscosity	√		
Hole characteristics	Depth	√	√	
	Deviation	√	√	
Operating problems	Sand	√	√	
	Paraffin		√	
	Corrosion		√	
Well locations	Offshore or onshore	√	√	
Power availability	Electricity or natural gas	√	√	
Economic concern	CAPEX			√
	OPEX			√
	Fuel cost			√

Round 2: Ranking the Alternatives

After the primary evaluation of the alternatives across several criteria, ranking of the alternative in order of their performance for each criterion is necessary. Literature has identified several multi-criteria ranking methods for decision making in data analysis.

TOPSIS was among the methods which are used by decision maker to select the best alternatives using several available attributes (Khamehchi, et al., 2016). The selections of the best method by TOPSIS are based on the minimum distance from ideal solution and maximum distance from negative ideal solution (Khamehchi, et al., 2016; Triantaphyllou, et al., 1998).

In this context, the term “Ideal alternative” refers to the alternatives which have the best level for all attributes considered and "negative ideal alternative” refers to the alternative which has the worst attribute values.

In this master thesis study TOPSIS will be used in selecting the most effective deliquification option which are in accordance with the SS7 conditions. The main input into the TOPSIS method is the list of options to be evaluated and the criteria which the methods are to be selected across. TOPSIS firstly assumes that there are ‘**m**’ alternatives (options) and ‘**n**’ attributes/criteria and also assumes the score for each option across each criteria used to rank the alternatives (Triantaphyllou, et al., 1998).

If X_{ij} is the score of option ‘i’ with respect to criterion ‘j’ then we have $X = (X_{ij})$ mxn matrix. If J are set of positive attributes or criteria and J' are the set of negative attributes or criteria then TOPSIS analysis are performed following steps (Triantaphyllou, et al., 1998).

Step 1: Construct normalized decision matrix.

This step transforms various attribute dimensions into non-dimensional attributes, which allows comparisons across criteria. Transformation is done using equation **38** which normalizes the scores or data.

$$r_{ij} = \frac{x_{ij}}{\sum_i {x^2}_{ij}}, \text{for } i = 1, \dots., m\ ; j = 1, \dots.., n \tag{38}$$

Step 2: Construct the weighted normalized decision matrix.

Assume we have a set of weights for each criterion w_j, for $j = 1, \dots., n$

Multiply each column of the normalized decision matrix by its associated weight which results to an element of new matrix as in equation 39.

$$V_{ij} = w_j r_{ij} \tag{39}$$

Step 3: Determine the ideal alternatives and the negative ideal alternatives.

Ideal alternative V_j^*.

$$A^* = \{V_1^*, \dots \dots, V_n^*\}, \text{where}$$

$$V_j^* = \{\max(V_{ij}) \text{ if } j \in J;\ \min(V_{ij}) \text{ if } j \in J'\}$$

Negative ideal alternativesV_j';

$$A' = \{V_1', \dots \dots, V_n'\}, \text{where}$$

$$V_j' = \{\max(V_{ij}) \text{ if } j \in J;\ \min(V_{ij}) \text{ if } j \in J'\}$$

$J =$ associated with the criteria having a positive impact and,

$J' =$ associated with the criteria having a negative impact

Step 4: Calculate the separation S_i measures for each alternative.

The separation S_i^* from the ideal alternative is:

$$S_i^* = [\sum_j (V_j^* - V_{ij})^2]^{\frac{1}{2}}, \text{for } i = 1, \dots, m$$

Similarly, the separation $S_i'$from the negative ideal alternative is:

$$S_i' = [\sum_j (V_j' - V_{ij})^2]^{\frac{1}{2}}, \text{for } i = 1, \dots, m$$

Step 5: Calculate the relative closeness to ideal solution C_i^* using equation 40

$$C_i^* = \frac{S_i'}{S_i' + S_i^*}, 0 < C_i^* < 1, i = 1, 2,3 \dots \dots m \qquad 40$$

$C_i^* = 1$, If and only if the the given deliquification alternative has the best conditions and

$C_i^* = 0$, If and only if the alternative has the worst conditions.

Step 6: Ranking the alternatives

Depending on the performance of a given alternatives, ranking of the alternatives will depends on the estimated preference rank order of C_i^*. Usually select the alternatives that give C_i^* close to 1. Therefore, the best alternative is the one that has the shortest distance to the ideal solution.

5.2 Cost Estimates for Various Liquid Deliquification Methods

The very important costs estimate required for economic evaluation of the artificial lifting alternatives are CAPEX, OPEX and Fuel costs as presented in Table 10. The presented costs estimates are very important in performing the cash flow analysis which is useful in determining the alternative worth before the final decision to install in the given gas well. Table 11, Table 12 and Table 13 gave different costs estimates for various lifting options used in gas wells by different companies.

Economical evaluation in gas deliquification techniques is performed after estimating the required alternative costs and based on Figure 56 it is performed in round 3 for the selected technical viable alternatives.

Round 3: Economical Analysis of Technical Viable Method

The economics of several liquid removal methods from gas wells which are technically proven to be viable need to be evaluated before the final decision to install in the well (Hutlas & Granberry, 1972).

Each lifting option's capital cost, maintenance cost, and fuel cost will be determined and they will be used in performing the cash flow analysis to estimate the option's NPV and its corresponding payback period (Park, et al., 2009; US EPA, 2011).The economic analysis for various deliquification options are evaluated using the generated NPV and payback period for the given options.

Table 11: Lift System Installation Cost Analysis **(Weatherford, 2014)**

BHT (°F)	Depth	Capital Installation Cost $000 - All usual automation included: Plunger	Capillary	Gas Lift	RRP	PCP	ESP	HYD
100	0-2,500	$8.0	$13.0	$16.0	$59.0	$38.0	$33.0	$84.0
150	2,500-5,000	$8.0	$15.0	$20.0	$82.0	$44.0	$52.0	$84.0
175	5,000-7,500	$10.0	$16.0	$26.0	$128.0	$53.0	$66.0	$134.0
200	7,500-10,000	$10.0	$19.0	$30.0	$153.0	N/A at these temps	$80.0 marginal at rates and temp	$134.0
250	10,000-12,500	$10.0	$44.0	$36.0	$175.0	N/A at these temps	N/A at these rates	$158.0
300	12,500-15,000	N/A at these rates	$52.0	$40.0	$234.0	N/A at these temps	N/A at these rates	$177.0

Table 12: Economical analysis costs for different alternatives (Khamehchi, et al., 2016)

Method	**CAPEX ($)**	**OPEX ($/Year)**
Velocity string	1, 300,000	500,000
Gas lift	5,000,000	1,000,000
Sucker rod pump	2, 623,000	500,000
ESP	2,325,000	500,000
Hydraulic pump	2,503,000	1,500,000

Table 13: Cost of artificial lift used for gas wells from Chevron (Soponsakulkaew, 2010)

Artificial Lift Type	Sucker Rod Pump		ESTSP	Hydraulic reciprocating piston pump-closed loop	Conv. PCP (<250F)	I-PCP (<250F)	Mechanical lock PCP (upto 300F)	Metal-Metal PCP (>300F)
Pump description	Sucker Rod Pump with Beam Pumping Unit		Electrical Sumbersible Twin Screw Pump	3 tbg in the well connected to piston pump through BHA, closed loop power fluid (PF)	tubing retrievable PCP	rod retrievable PCP (Insert-PCP)	Mechanical lock PCP	Metal-Metal PCP
Flow Rate (gross)	200	500	500	500	500	500	500	500
Fluid Density (90% cut, 12 degree API)	0.993	0.993	0.993	0.993	0.993	0.993	0.993	0.993
Depth (ft)	2,000	2,000	2000	2,000	2000	2000	2000	2000
Downhole Pump Cost	$26,500	$46,500	160,000	$70,300	$55,000	$53,000	$56,300	
Driver Cost (e.g., pumping unit, VFD, etc.)	$50,000	$50,000	$60,000	$38,000	$0	$0	$0	$0
Tubing/ Sucker rod/ Shaft/ CT Cost	$10,000	$10,000	$0	$0	$0	$0	$0	$0
Rig/ CTU/ Crane Costs	$5,000	$5,000	$5,000	$2,500	$5,000	$5,000	$5,000	$5,000
Surface Facilities Cost (pad, controls)	$15,000	$15,000	$7,500	$15,000	$7,500	$7,500	$7,500	$7,500
Total Installed Cost	**$106,500**	**$126,500**	**$232,500**	**$125,800**	**$67,500**	**$65,500**	**$68,800**	**$12,500**
Estimated Mean Time Between Failures	2	2	2.85	0.8	2.5	2.5	2.5	2.5
Estimated Pump Repair Cost	$10,000	$10,000	$64,000	$5,100	$13,900	$12,500	$15,400	$15,900
Estimated Hoist / Rig/ CTU Cost	$5,500	$5,500	$5,500	$2,750	$5,500	$2,750	$5,500	$5,500
Average pull costs per year	$7,750	$7,750	$24,386	$9,458	$7,760	$6,100	$8,360	$8,560
Pumping System Overall Efficiency (%)	45.0%	45.0%	40%	70%	65%	65%	65%	45%
Annual Electrical cost @ $.08 / kw-hr	$3,394	$8,485	$9,545	$5,455	$5,874	$5,874	$5,874	$8,485
Total Annual Operating Cost + Prod Loss	**$11,144**	**$16,235**	**$33,931**	**$14,912**	**$13,634**	**$11,974**	**$14,234**	**$17,045**
NPV @ 10% over 10 years	**$181,822**	**$236,232**	**$461,843**	**$226,593**	**$159,653**	**$146,433**	**$165,009**	**$127,706**

5.2.1 Cash Flow Analysis.

There are several methods which may be used to measure the investment worth and these methods are such Net Present Value (NPV), Internal Rate of Return (IRR) and discounted payback period and return on investment (Strøm, 2016).

i. Net Present Value (NPV).

In order for a project to be accepted net present value should be positive and nothing has been said about its magnitude. When several investments are to be compared on the basis of their NPV the optimum method to be selected is the method with the highest positive NPV (Strøm, 2016).

ii. Internal Rate of Return (IRR)

Internal rate of return in **Figure 58** is defined as the discount rate when the project NPV equal to zero (Strøm, 2016). The projects worth measurement on the basis of the internal rate of return are performed by comparing the internal rate of return with the project discount rate. If the project discount rate is higher than the estimated internal rate of return then the project are rejected, the lower the IRR the better the project (Strøm, 2016).

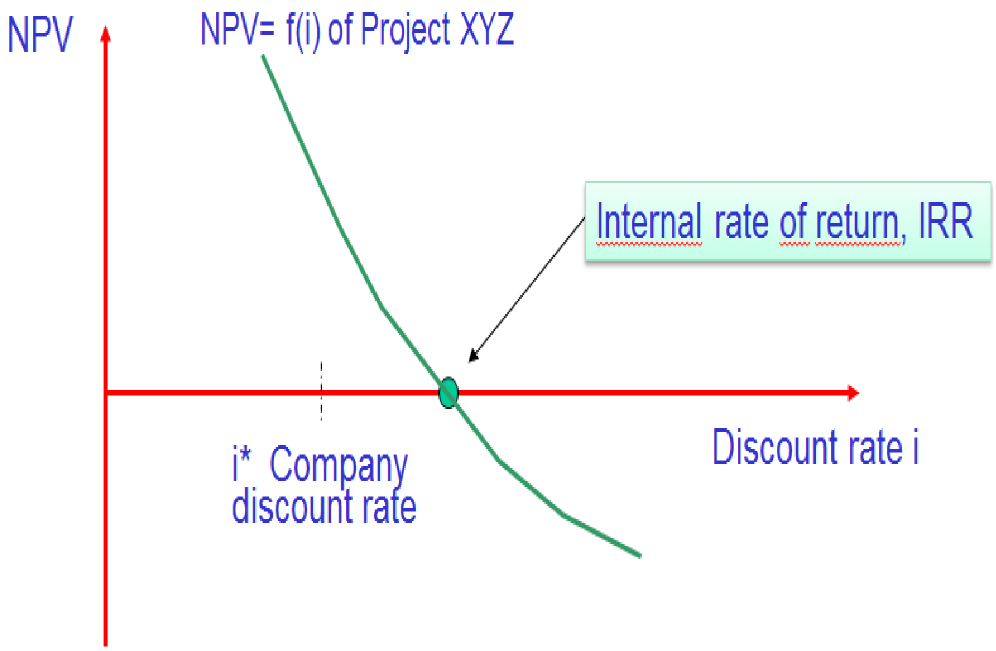

Figure 58: Graphical Estimation of IRR **(Strøm, 2016)**

iii. Discounted Payback Period

Payback period is the length of time required for the cumulative cash flow to turn positive (Strøm, 2016). Equation 41 is used to estimate project payback period.

$$\text{Payback Period} = \frac{\text{Initial Investment}}{\text{Net Cash Inflow}} \qquad 41$$

The computed payback period above is also called simple payback period and one of its major disadvantages is that it ignores the time value of money.

To account for the time value of money limitation an alternative procedure called discounted payback period was proposed (Jan, 2011 - 2013). The time values of money are encountered by discounting the cash inflows of the project and the discounted payback period are estimated using equation 42.

$$\text{Discounted Payback Period} = \text{A} + \frac{B}{C} \qquad 42$$

Where,

A =Last period with a negative discounted cumulative cash flow,
B = Absolute value of discounted cumulative cash flow at the end of the period A and
C = Discounted cash flow during the period after A.

The selection using payback period considers the alternative that gives the shortest length of time to recover the investment cost thus the shorted the payback period the better the alternative.

6. EVALUATING THE DELIQUIFICATION METHODS FOR SS7

Various deliquification methods used in gas well has been published in literature and their evaluation to select the most optimum method to be used in unloading SS7 was performed following the procedures in Figure 56. Figure 56 has indicated that the evaluation processes goes through three stages which involves technical and economic analysis.

Technical evaluation was based on screening operating conditions for SS7 against the established alternative operating range of the well conditions. Weatherford developed the screening criteria for technical evaluation of different deliquification methods in gas wells. Table 9 shows the technical screening criteria proposed by Weatherford.

Based on data availability several screening criteria for SS7 were established and it was used during evaluation by comparing it with the reference criteria established in Table 9. To establish the screening criteria for SS7 various data was gathered such as well information, production status, liquid volume produced and reservoir operating pressure.

6.1 Information Gathering

The information used in this study was the secondary data recorded from SS7 by the well operator which was Pan African Energy Tanzania (PAET). Based on the identified criteria on Figure 56 and Table 10 collected data required to establish the new evaluation criteria for SS7 will depend on the data availability.

Technical and economic data was gathered both from the internet and from well operators to enhance evaluation process and the following was the brief descriptions of the data collections processes for SS7.

6.1.1 Technical Information Gathering

The following were the gathered information for SS7 from Pan African Energy Tanzania (PAET) which was the company which was operating SS7.

a) Well Location

As was described in literature well location was very important to understand during evaluation processes because it has a significant impact on the selection of suitable liquid unloading method. Some method has excellent applicability onshore and some have limitations when offshore. Figure 16 indicated that the well SS7 was located in shallow offshore.

b) Liquid Production

The produced liquid rate from SS7 was mainly composed of water and small amount of condensate. At the current well condition which was used in liquid loading prediction the recorded hydrocarbon condensate was at an average of 5.95 STB/day and water estimated from the performance curve in Figure 59 was produced at an average rate of 115.999 STB /day.

The total liquid rate produced from SS7 was found as the sum of water and condensate rate. Therefore the estimated liquid produced from SS7 was at an average rate of 121.95 STB/day which was the same as the results reported from the well model created in PROSPER in APPENDIX G. The total liquid rate obtained above was used in the evaluation deliquification alternatives on SS7.

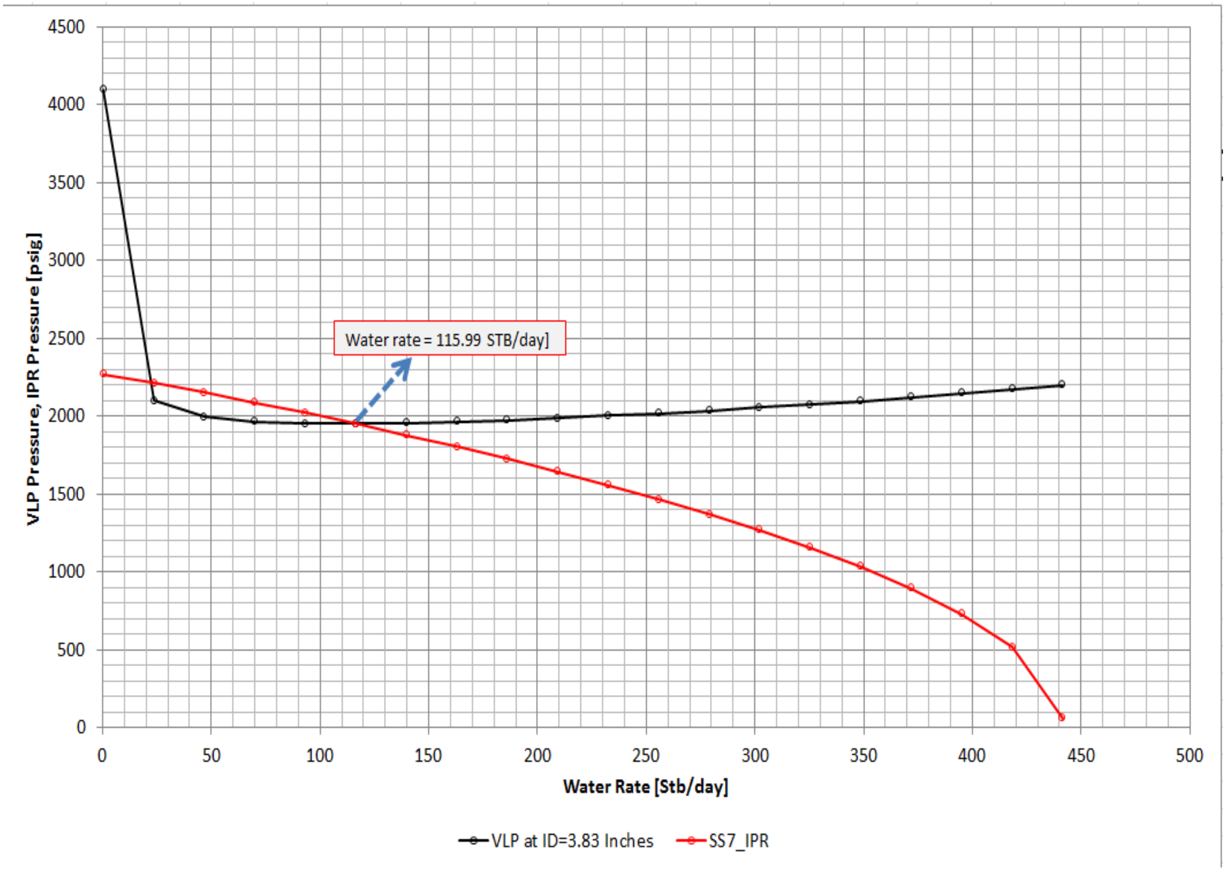

Figure 59: SS7 Water production rate

c) Well Information

The basic well information necessary for evaluation of the deliquification methods were well depth and well deviation. This information was provided by the well operator which reported that the total depth of well SS7 was 7400 ft. The well architecture for SS7 provided from the company which gave the well depth was presented in Figure 62.

Based on the provided well survey data with measured well depth and true vertical depth, the well trajectory in Figure 60 was established in PROSPER to estimate the well inclination and it was found that SS7 was inclined to an average angle of 29^{o}.

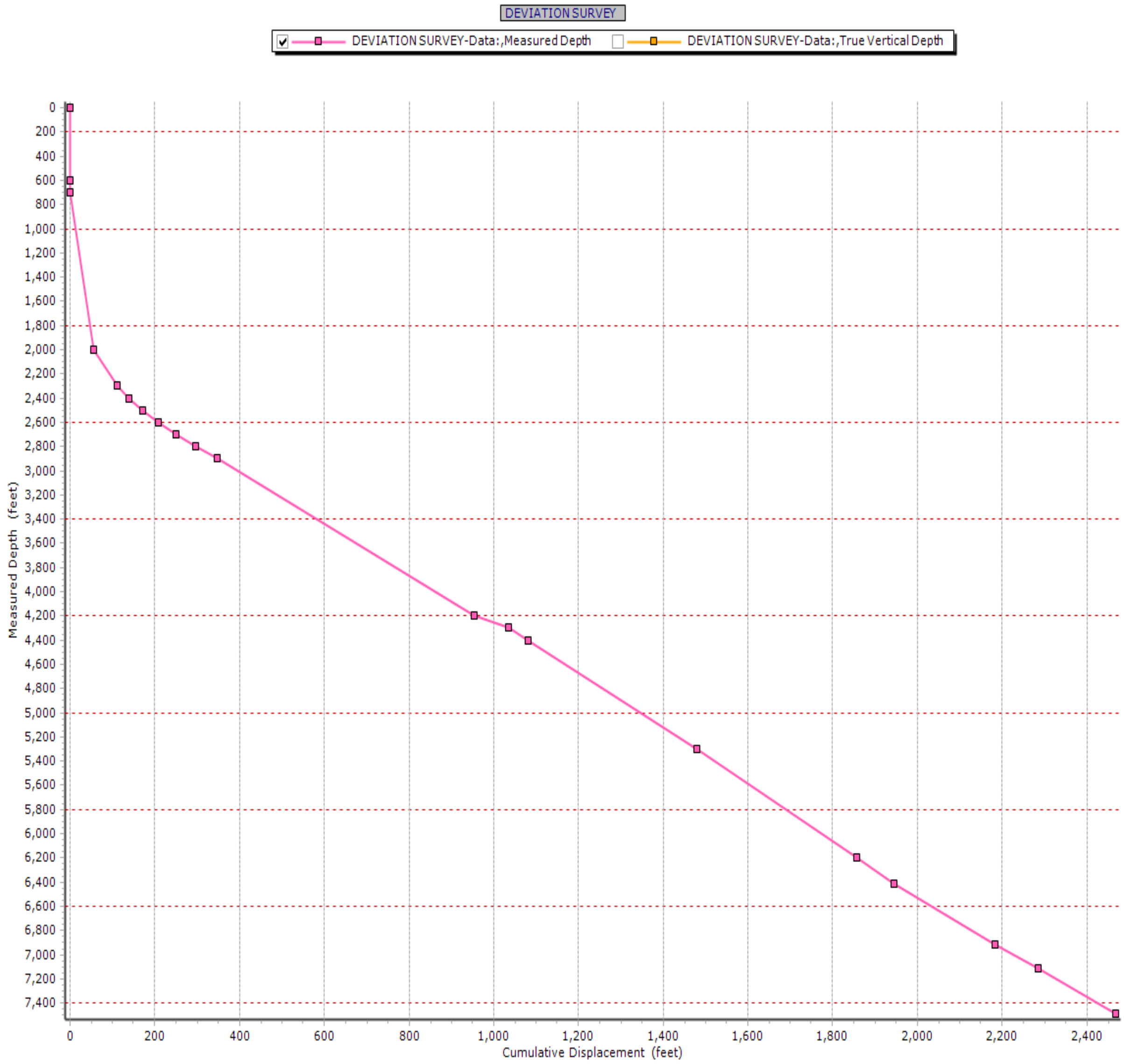

Figure 60: SS7 well inclination and depth

d) SS7 Gas liquid ratio (GLR).

Gas to liquid ratio (GLR) determination for SS7 was necessary because it has been reported that higher GLR may limit the selection of some methods. Higher GLR produced from gas well limit the application of most pumping method as it causes gas interference which can damage the pump.

Based on the historical well production provided by well operator (PAET), the produced GLR from SS7 was computed and plotted as in Figure 61. Because liquid loading analysis was predicted to have occurred in the well in 2016, then the GLR to be used in evaluation was based on the latest fluid production and its estimated value was 52,061scf/STB.

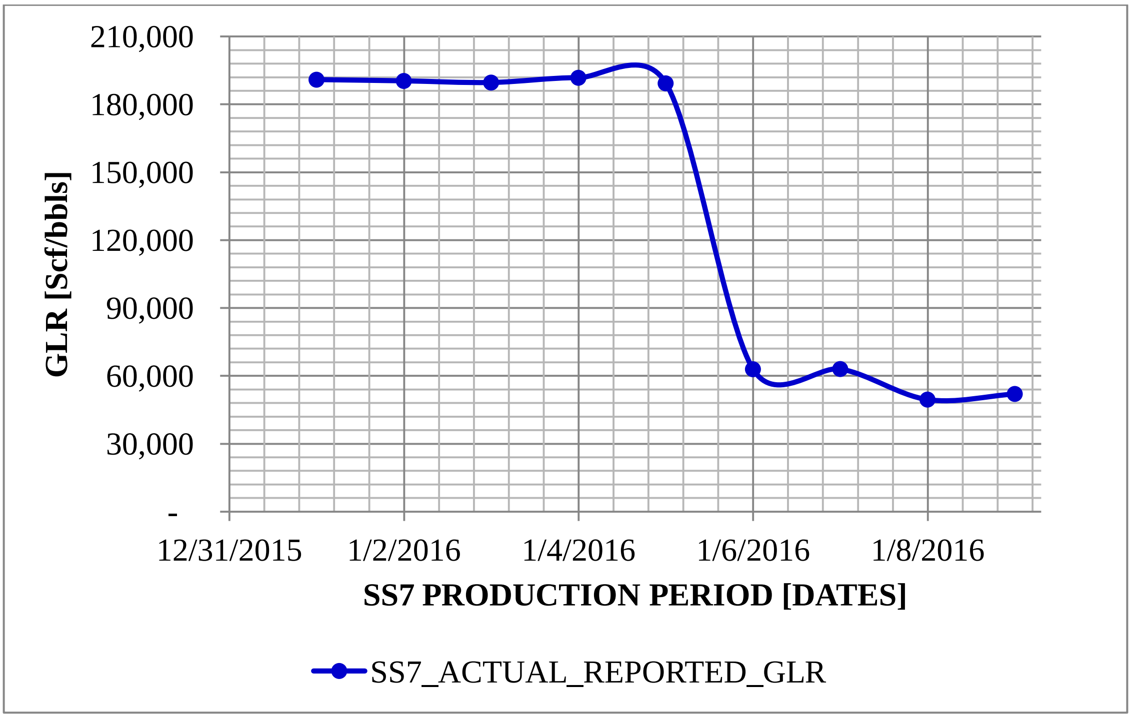

Figure 61: SS7 GLR variation

e) Condensate Gravity

The hydrocarbon liquid specific gravity for fluid produced from SS7 was reported to have average value of 45 API.

f) Average Reservoir Pressure

Based on Table 7, different deliquification techniques are suitable for a certain operating average reservoir pressures. An average reservoir pressure computed from back pressure equation at the operating period in 2016 was 2273.5 psia. This reservoir pressure was computed from the estimated flowing bottomhole pressure calculated from Cullender and Smith correlation assuming only dry gas is produced from SS7 and at fixed top node pressure of 1644psia.

g) Well Completion

The type of well completion can restrict the selection of a certain deliquification method for unloading gas well. The well completed with packer restrict the selection of the methods such as Plunger lift and rod pump as described in literature but it is suitable for selection of gas lift.

Based on the well architecture in Figure 62, the well SS7 has indicated that it was completed with packers and the selection of the most suitable method should consider the methods which are not limited by the presence of packer.

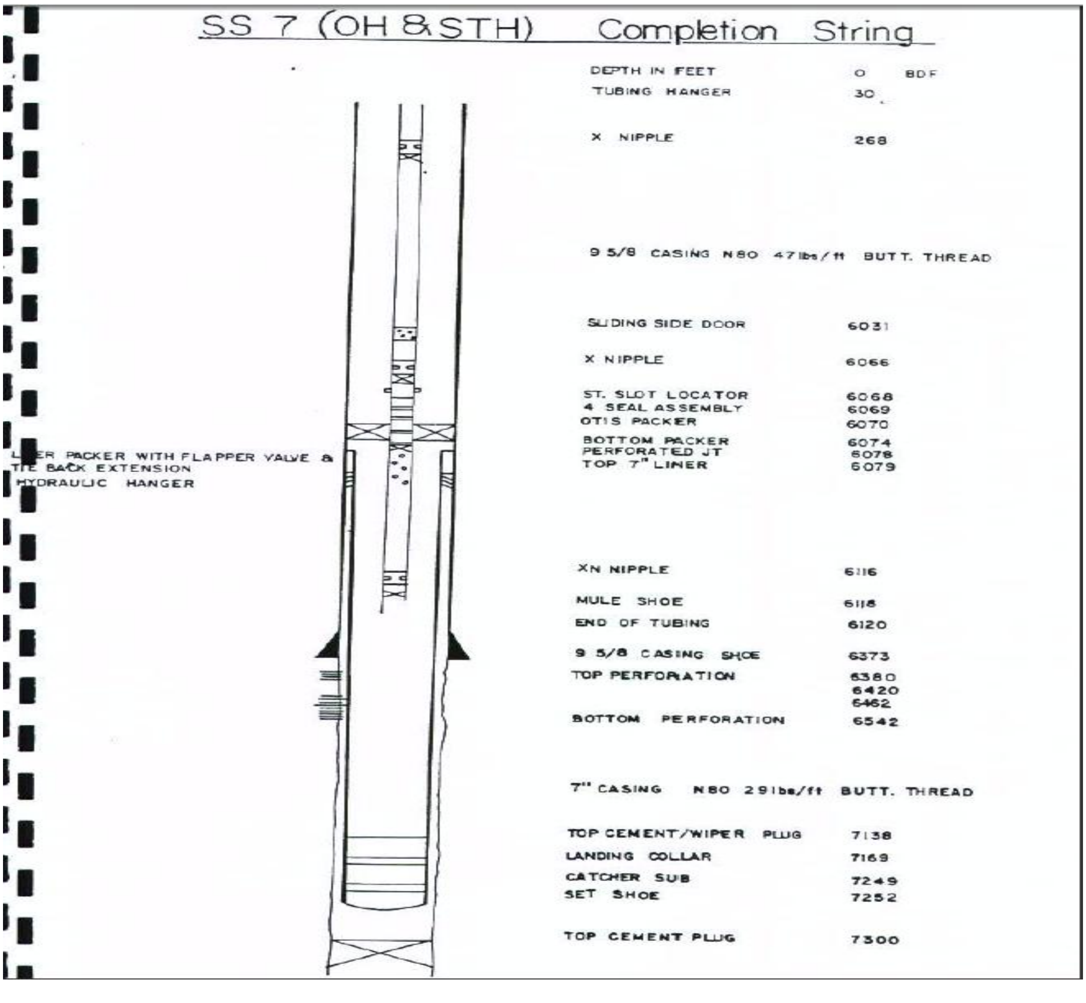

Figure 62: SS7- Gas Well Completed with Packer

6.1.2 SS7 Developed Screening Criteria.

The collected information from SS7 gas well was used as the technical evaluation criteria and Table 14 is the summary table. Different liquid unloading methods will be evaluated across each criterion to determine its suitability for SS7.

Table 14: Summary of established technical screening criteria for SS7.

No.	Attributes	Units	Value
1	SS7 Well Depth	[ft]	7300
2	SS7 well Deviation	[degree]	29
3	SS7 Liquid Volume	[bbls/d]	122
4	SS7 Condensate gravity	[API]	45
5	SS7 GLR	[Scf/bbl.]	52,061
6	SS7 Location	[-]	Offshore
7	Average Reservoir Pressure	[psia]	2273.5
8	SS7 Packer completion	[-]	Yes

6.1.3 Economical Information Gathering

The information about CAPEX, OPEX for each selected technically viable deliquification options was determined in order to estimate the option's worth before it can be installed in the well SS7. The evaluation of the deliquification method in the Songo-Songo gas field was never been conducted thus there were no information about costs estimates obtained from the company.

This made the costs estimates to be determined from different sources in the internet and some assumptions. In this study, the costs estimates presented in Table 11, Table 12 and Table 13 were employed in performing the economical evaluation for the selected technical viable method for SS7. Summaries of the selected costs estimate from Table 11, Table 12 and Table 13 to be used in performing economic analysis was given in Table 15.

Table 15: Cost Estimates for Economic Analysis of SS7 Gas Well

Method		CAPEX [$]	OPEX [$/Year]	Fuel cost [$/Year]
1.	Plunger lift (from EPA 2011)	7772	1300	0 (natural)
2.	Gas lift (Khamehchi, et al., 2016)	5,000,000	1,000,000	9,969 Depends on injected gas rate
3.	Velocity string	1,300,000	500,000	0 (natural)
4.	ESP	2,325,000	500,000	9,545 from Chevron

After determining the cost estimates for the selected liquid unloading method from technical factors in Table 15 above, the following assumption was made to assist economical evaluation.

Assumptions

i. CAPEX were invested at the beginning of 2016.
ii. Discount rate of 10%
iii. The predicted evaluation period of 22 years for each method.
iv. Gas price: The constant gas price of $3.323 /MSCF over the life of the project.
v. Additional Gas injection rate of 3 MMSCFD.
vi. Electric power price 159 TZS/Kwh (0.071$/Kwh) (Kasumuni, 2013)

Determination of Cumulative Gas Production for Revenue Calculation

Gas revenue expected during the forecasted production period was computed from the forecasted cumulative gas production assuming normal decline curve and gas price. Gas price is usually not a fixed number as it changes depending on the dynamic of the oil price in the market. For this case the gas price was assumed a constant during the evaluation period and later sensitivity analysis was performed to study the effects of its variation on the generated NPV.

The study of gas production decline over time was performed using Decline Curve Analysis (DCA) concept. DCA was a graphical procedure used for analysing declining production rates and forecasting future performance of gas wells (SS7).

The historical production recorded from the well SS7 was used in constructing the well SS7 decline curve. Fitting a line (trendline) through the performance history in Figure 63 and assuming this same trend will continue in future provided the better way to estimates the cumulative gas production.

The trendline equation generated in Figure 63 was used to compute the projected gas production rate over the production period of 2016-2038 from which cumulative gas production was calculated.

Figure 64 summarizes graphically the estimated gas production and cumulative gas production for the well SS7 determined from the trendline equation for forecasting gas production decline. The values of the computed cumulative gas production used in producing the curves in Figure 64 were presented in APPENDIX Y.

Determination of Revenue

The expected gas revenue from the well SS7 was calculated using the forecasted cumulative gas production for the assumed evaluation period of 2016-2038 and gas price. Gas revenue was calculated as the product of cumulative gas production with gas price as will be discussed in the economical evaluations part.

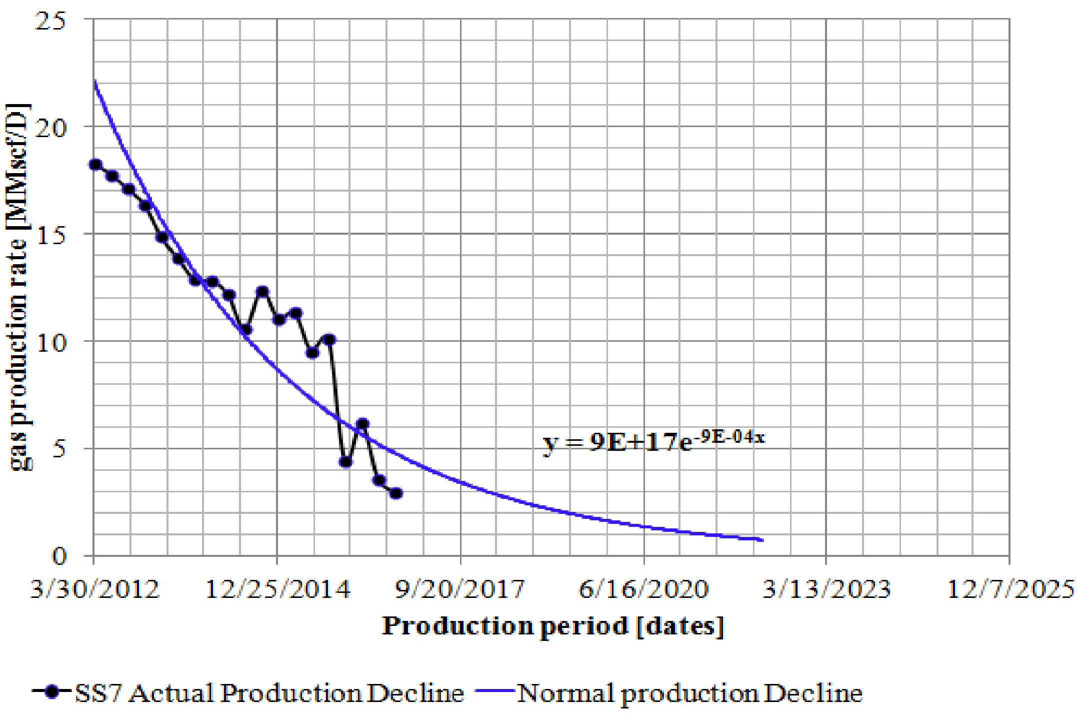

Figure 63: Production decline curve comparison for well SS7

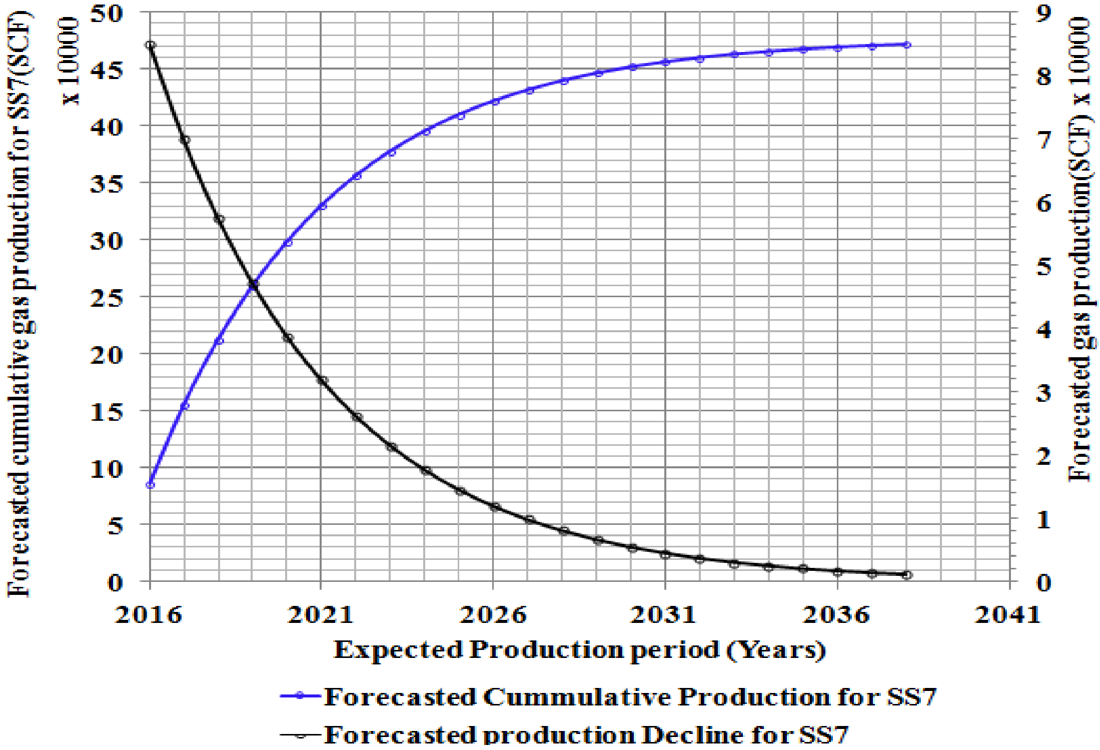

Figure 64: Expected production decline and cumulative gas production from well SS7.

6.2 Technical Evaluation for SS7

As per the identified technical evaluation procedures given in Figure 56, the technical evaluation of the deliquification method for SS7 was done in two rounds, round 1 and round 2. In round 1 different liquid unloading method were evaluated across the seven identified criteria presented in Table 14 by comparing with the literature identified limitations for each method.

In round 1, the primary screening of the unloading method across each criterion was performed to identify how much the certain method complies with the well condition in Table 14.

Round 2 involved ranking of the methods evaluated in order of their score across several evaluated technical criteria. This was done because each deliquification method will have different limitations on different well and field conditions. Thus in this round each method was ranked based on their relative closeness to ideal solution computed using TOPSIS method explained above.

6.2.1 Round 1: Preliminary Screening.

This was the first evaluation stages which involved identifying the evaluation criteria as well as the method to be evaluated across each criterion. In this master thesis study the preliminary screening of deliquification method was performed by using the developed screening criteria in Table 14. Each method was evaluated across each identified criteria by comparing the SS7 well condition with the established criteria in table 9.

The main evaluation criteria developed from SS7 depending on the well information availability used in this study were as follows;

a) Well Depth
b) Well operating volume
c) Well operating GLR
d) Well location
e) Condensate gravity
f) Operating reservoir pressure
g) Presence of packers

The decision were either to reject the alternative using criteria when the actual SS7 well condition was found to be out of the operating range or accepting the alternatives when the SS7 condition fall in the operating range proposed by Weatherford in table 9.

The results to be used for decision making was established using a logical statement written in excel with two output. The output of the logical statement were ACCEPTED or REJECTED depending on how the collected well and field condition for Songo-Songo gas (SS7) complied with the Weatherford technical screening criteria.

When the choice was REJECTED means that the given method was not appropriate at the given conditions and when the choice was ACCEPTED means that the given method was appropriate for lifting the liquid from gas well at the given conditions.

The logical statement established in excel sheet for evaluation in round 1 using IF statement as given below; IF **‘’The well SS7 conditions fall within the range established by Weatherford in table 9 for the given method then the method were ACCEPTED else REJECTED by criteria’’**

The summary results of the preliminary screening of deliquification method across the established criteria were provided in Table 16.

Table 16: The results of the preliminary screening of the deliquification method under criteria.

TECHNIQUES	Well_Depth (ft)	Well_Deviation (Degree)	Well_Operating_Volume (bbl)	GLR (scf/bbls)	Reservoir_Pressure (Psia)	Packer_Completion (-)	Condensate_Gravity (API)
Plunger	SELECTED	SELECTED	SELECTED	SELECTED	REJECTED	REJECTED	SELECTED
Gas lift	SELECTED	SELECTED	SELECTED	SELECTED	REJECTED	SELECTED	SELECTED
ESP	SELECTED	SELECTED	SELECTED	REJECTED	REJECTED	REJECTED	SELECTED
PCP	REJECTED	SELECTED	SELECTED	REJECTED	REJECTED	REJECTED	REJECTED
Rod Pump	SELECTED	REJECTED	SELECTED	REJECTED	REJECTED	REJECTED	SELECTED
Jet Lift	SELECTED	REJECTED	SELECTED	REJECTED	REJECTED	REJECTED	SELECTED
Piston Pump	SELECTED	REJECTED	SELECTED	REJECTED	REJECTED	REJECTED	SELECTED
Foam Injection	SELECTED	REJECTED	SELECTED	REJECTED	REJECTED	SELECTED	SELECTED
Velocity tubing	SELECTED	SELECTED	SELECTED	SELECTED	SELECTED	SELECTED	SELECTED

Based on the results given in Table 16, each method were evaluated across the seven established criteria in Table 14 for SS7 and it has indicated that different methods will be accepted and rejected by different criteria.

For example most deliquification methods were rejected when evaluated across the SS7 reservoir average pressure except Velocity string which was found to be appropriate at that pressure. Also the presence of packer in the well SS7 rejected most of the method selection for removing the accumulated liquid from the wellbore except Gas lift and velocity string which were found to be appropriate method.

According to the evaluation by using liquid volume, the reported liquid rate from SS7 was about 122STB/d, which was appropriate for most methods this was the reason why all methods were selected by using liquid volume criteria.

Based on the results on Table 16, the criteria which were found to have good performances in most methods were well depth, condensate gravity, liquid volume, well deviation and GLR. The worst performing criteria in the selection of the deliquification method were presence of packers in the well and the level of the operating average reservoir pressure. These criteria were considered the worst criteria because they limited the large number liquid unloading application for SS7 and rejected most and accepted only very few.

Generally in evaluating the deliquification method through round 1 by using the established technical criteria, the methods were accepted or rejected depending on the limitation of application a certain method has on the given condition.

Further technical evaluation were required to generally rank the performance of each methods across the multi criteria established and finally select the most suitable method to be proposed for implementation in the well SS7.

6.2.2 Round 2: Ranking of the Method

After preliminary screening of the liquid unloading methods by using technical criteria the next task ahead were to rank these methods for decision making. TOPSIS method were applied in round 2 of technical evaluation by combining the effects multi criteria established to rank the methods in order of their performances.

The main inputs into TOPSIS method were the technical criteria established in Table 14, identified deliquification methods and the results of preliminary screening in round 1. There were several procedures required in ranking the alternatives from multi criteria.

The first step was to establish the scores of each method across several criteria and in this work two score were used. When the preliminary screening has indicated that a certain method was applicable at a certain criterion then the method was awarded a score of 0.75 was awarded to a method.

And when the results have shown the method to be limited by certain criteria the score of 0.25 were awarded to the method at that criterion. After estimating various scores to each method across different criteria, the determination of the weighted average of each criterion was very important.

The calculation of the criteria weighted average was based on the scores of different methods on the criteria and the following expression in equation 43 was employed in the calculation.

$$\text{Weighted average} = \frac{\sum_{\text{i}}^{\text{n}} \text{Score each method across one criteria}}{\sum_{\text{i}}^{\text{n}} \text{score of each method across all criteria}}, \qquad \textbf{43}$$

$$\text{i} = \text{Plunger lift}, \ldots,,,,..,\text{velocity tubing}.$$

The summary table showing different scores and the estimated weighted average from the above expression was presented in Table 17.

Table 17: Lifting method Scores across criteria and the estimated weighted average for criteria.

CRITERIA	PLUNGER LIFT	GAS LIFT	ESP	PCP	ROD_Pumping	JET_PUMP	PISTON_PUMP	FOAM_LIFT	VELOCITY_TUBING	WEIGHTED AVERAGE
Well_Depth	0.75	0.75	0.75	0.25	0.75	0.75	0.75	0.75	0.75	0.19
Well type_Deviation	0.75	0.75	0.75	0.75	0.25	0.25	0.25	0.25	0.75	0.14
well_Operating_volume	0.75	0.75	0.75	0.75	0.75	0.75	0.75	0.75	0.75	0.20
GLR	0.75	0.75	0.25	0.25	0.25	0.25	0.25	0.25	0.75	0.11
Reservoir pressure	0.25	0.25	0.25	0.25	0.25	0.25	0.25	0.25	0.75	0.08
Completion_Packer_Avaiable	0.25	0.75	0.25	0.25	0.25	0.25	0.25	0.25	0.75	0.10
Condensate_Gravity	0.75	0.75	0.75	0.25	0.75	0.75	0.75	0.75	0.75	0.19
										1.00

Following the TOPSIS procedure identified in literature, the evaluation to determine the relative closeness to ideal solution was performed separately using equation 38, 39 and 40 for each method.

The results of the estimated relative closeness to ideal solution for various deliquification methods evaluated for SS7 conditions were presented in appendix K to Appendix S.

The summary of the calculated relative closeness from equation 40 was used in ranking the method based on the size of relative closeness as given in Table 18.

Table 18: TOPSIS Ranking Results

TECHNIQUES	Relative closeness to ideal solution C*	RANKING
	$0 < C^* < 1$	
Plunger	0.544	2
Gas lift	0.585	1
ESP	0.506	4
PCP	0.374	6
Rod Pump	0.462	5
Jet Lift	0.462	5
Piston Pump	0.462	5
Foam Injection	0.462	5
Velocity tubing	0.511	3

6.2.3 Technical Evaluation Results

The findings presented in Table 18 from round 2 has indicated that the most suitable method for implementation in SS7 in order of their preference were Gas lift, Plunger lift, Velocity string, ESP, Foam lift, piston pump, Rod pump, Jet lift and finally progressive cavity pump.

In this study the methods which were considered to be technically feasible for the well SS7 were one with relative closeness higher than 0.5. Using relative closeness of 0.5 as the cut off criteria for final selection resulted to the decision that Gas lift, Plunger lift, ESP and Velocity String were the appropriate methods for SS7.

The round 1 evaluation results in Table 16 indicated that velocity string was the most appropriate methods followed by Gas lift, Plunger lift and ESP while the rest of the methods were rejected because they were disqualified in most SS7 selected evaluation criteria. Results in Round 1 and round 2 gave good agreement because the selected four methods in round 1 were ranked the highest in round 2 though there were some twisting in their preferences as described above.

The results in round 2 was used for further analysis in round 3 to evaluate the economics of methods and select the most suitable method implementation in the well SS7 by considering technical and economic viability.

6.3 Economical Analysis for Well SS7

The selected four deliquification methods from technical evaluation were further analysed on basis of their economics aspects. In the economical evaluation each options NPV and the payback period were computed from the estimated CAPEX and OPEX in Table 15 and the assumptions above.

The revenues were estimated by assuming the constant gas price during the evaluation period and the cumulative annual gas production forecasted from the decline curve (blue curve) in Figure 64 which assumed natural production without liquid loading problem.

Annual revenue was computed as the product of the increased gas production with gas price for the evaluation period (2016-2038). The economical analysis in this study was involved cash flow analysis to determine the alternative NPV and discounted payback period. Usually the options that gave the positive NPV are considered productive and may be accepted for implementations and when several options exists with positive NPV then the magnitude of the NPV can be considered in comparing them. Sometime payback period are also used in making decision of which option should be selected among the many economical viable options.

Cash flow analysis were performed by using the determined costs in Table 15 and the basic assumptions made to estimate the generated net present value of each technically selected liquid unloading methods.

For each liquid unloading method evaluated NPV was obtained as the sum of the cumulative discounted cash flow across the evaluation period. The following are the brief description of general calculation results of the NPV and its corresponding discounted payback period for each method.

6.3.1 Gas Lifts Economical Evaluation Results.

Cash flow analysis for gas lift were carried out in excel to determine its economic worth once selected as suitable method for removing liquid from the well SS7. The analysis involves the calculation of Net Present Value (NPV) and its corresponding discounted payback period for comparison with other alternatives. The calculation results for cash flow analysis by the application of gas lift was given in APPENDIX B.

The generated NPV by the application of gas lift in SS7 was $ 8,018,788.545. The plot of the cumulative discounted cash flow for SS7 with gas lift operation during the evaluation period was presented in Figure 65.

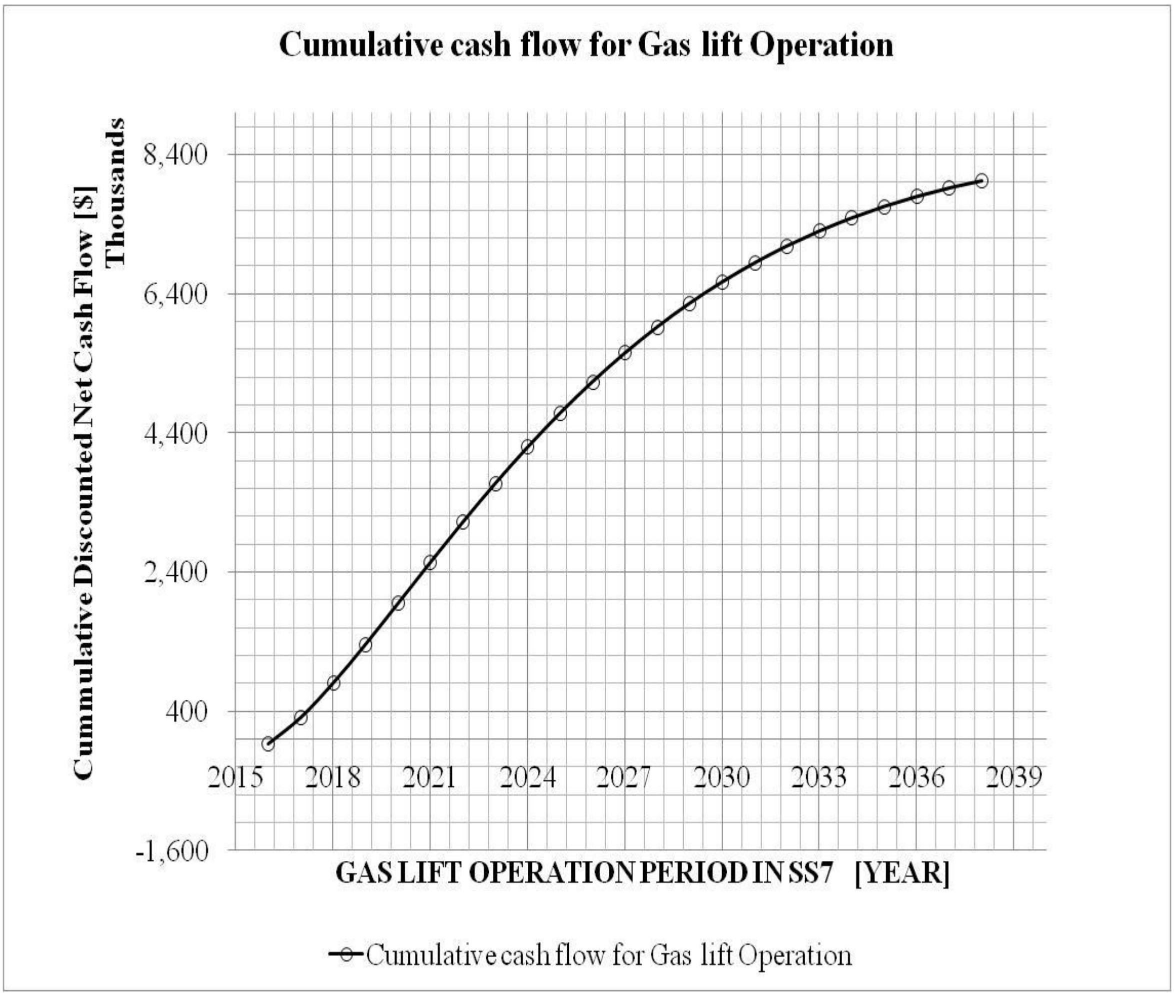

Figure 65: Cumulative discounted cash flow for gas lift

This method is economically viable for implementation in the well SS7 as it has a positive NPV. Since the estimated NPV for SS7 with gas lift has the positive value, and then the determined discounted payback period was estimated to be 0.36 years (5months).

Gas Lift Sensitivity Analysis.

Sensitivity analysis to determine the effect of various costs on the generated NPV was performed using Tornado plot. The sensitivity cases involved evaluating effect of four cost figures which were CAPEX, OPEX, and Gas injection cost and gas price variation by the application of gas lift on NPV.

In performing sensitivity analysis the NPV at base case was calculated using the cost figures given in Table 15. Sensitivity analysis for Tornado plot generation was calculated by setting the % increase above and below the base case for each cost category identified and deploying what if analysis, several NPV for each case were computed following the procedure indicated next.

Sensitivity analysis for different deliquification methods were performed by varying the given base case cost figure in the range of +-20% to study its impact on the generated NPV. For example when the base case CAPEX for gas lift was $64,420 resulted to generated NPV of $8,018,788.5. The base case CAPEX represents 100% and several (8) cases was performed to study the impact of increasing or lowering gas lift installation costs as given in Table 19.

Table 19: Calculated CAPEX for gas sensitivity analysis

Sensistivity Analysis Cases base case CAPEX	CAPEX ($)
80%	51,536
85%	54,757
90%	57,978
95%	61,199
100%	64,420
105%	67,641
110%	70,862
115%	74,083
120%	77,304

Calculation of the NPV for each cases was calculated using **what if analysis** in excel where the first row of the NPV (red) should have the base case NPV, and the NPV corresponding to new calculated CAPEX for different cases were calculated by replacing CAPEX with the base case CAPEX through the column input cell in Table 20.

Table 20: what if analysis calculation of NPV from Data Table.

Sensistivity Analysis Cases base case CAPEX	CAPEX ($)	NPV($)
		8,018,789
80%	51,536	
85%	54,757	
90%	57,978	
95%	61,199	
100%	64,420	
105%	67,641	
110%	70,862	
115%	74,083	
120%	77,304	

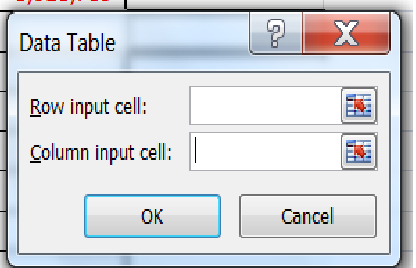

Different NPV was computed for different values of gas lift installation costs (CAPEX) while keeping the other costs such as OPEX, and revenue fixed. NPV was calculated by using ‘What if analysis’ in excel which replaced the base case CAPEX with the new estimated CAPEX for different cases.

Because the new CAPEX in Table 19 were arranged column wise, then the column input cell in data table in Table 20 was used to input the base case CAPEX. What if analysis was activated to calculate the various NPV generated when using different values of CAPEX and the results were summarized in Table 21.

Table 21: Calculated NPV using what if analysis for sensitivity analysis.

Sensistivity Analysis Cases	CAPEX	NPV($)
base case CAPEX	($)	8,018,789
80%	51,536	8,031,673
85%	54,757	8,028,452
90%	57,978	8,025,231
95%	61,199	8,022,010
100%	64,420	8,018,789
105%	67,641	8,015,568
110%	70,862	8,012,347
115%	74,083	8,009,125
120%	77,304	8,005,904

The row with green color represents the base case while the rest 8 rows are the sensitivity cases developed. The same procedure described above was employed for other costs categories selected for analysis and the summary of their results were presented in APPENDIX T.

Tornado Plot.

To generate the Tornado plot for sensitivity analysis only two cases were selected. The first case was when each cost category was reduced by 20% below the base case and the second case was when the each cost category was increased by 20% above base case.

The summary of the estimated NPV for the above two cases were presented in Table 22. The results in Table 22 were used to construct the Tornado plot for Gas lift sensitivity analysis.

Table 22: Summary of different values of Gas Lift NPV for sensitivity analysis.

Sensitivity Cases	CAPEX($)	OPEX($)	INJECT COST($/Mscf)	Gas price($/Mscf)
80%	8,031,673	8,034,945	8,058,665	6,006,825
100%	8,018,789	8,018,789	8,018,789	8,018,789
120%	8,005,904	8,002,632	7,978,913	10,030,752

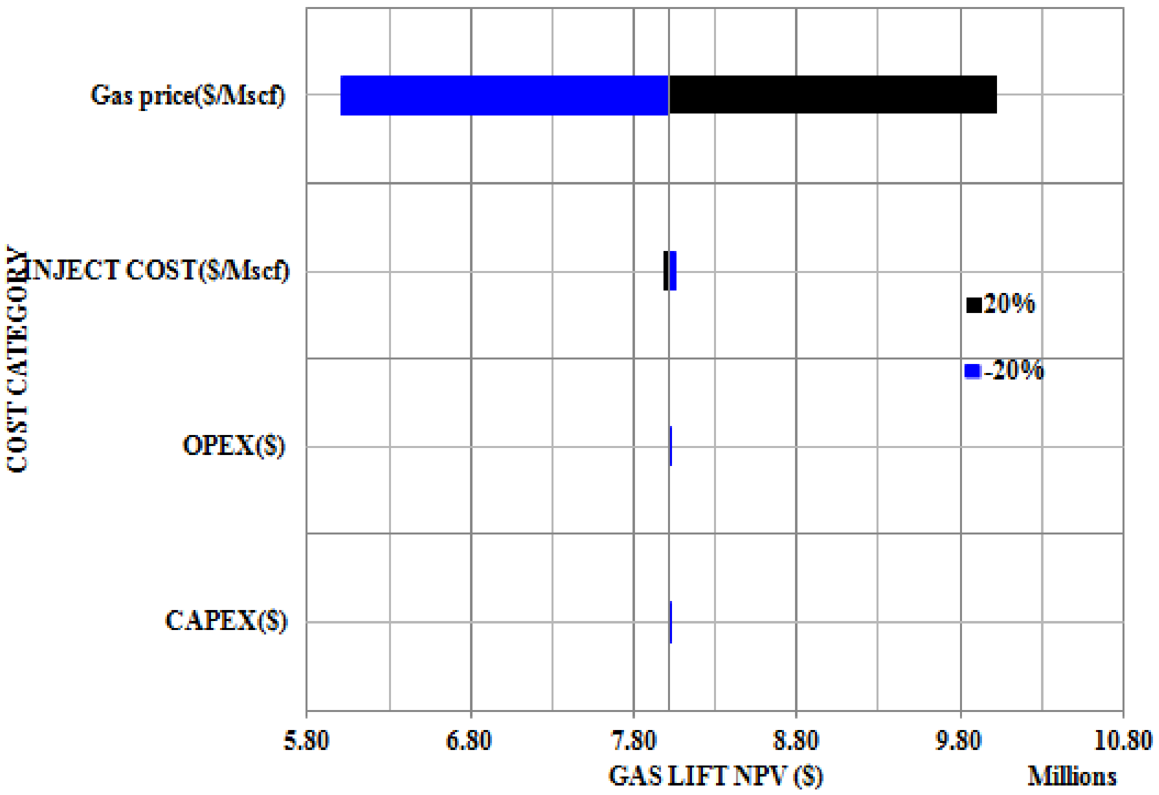

Figure 66: Tornado plot for gas lift sensitivity analysis.

The effect of various costs category on the option NPV was investigated individually by only varying the cost to be studied and keeping the other costs constant. Their relationship to NPV was presented on the Tornado plot in Figure 66. It was found that gas price has a significant impact on the generated NPV compared to other costs category analysed.

6.3.2 Plunger Lifts Economical Evaluation Results.

Plunger lift was ranked in the second position by technical criteria but it was very important to assess its economic viability before final decision to install in the well. The economics analysis for Plunger lift was performed using the gathered information in Table 15 and some basic assumptions made during information gathering.

The Plunger lift economical evaluation was associated with the cash flow analysis for determining the net present value (NPV) and also the discounted payback period when the NPV was positive.

The same procedure used in performing cash flow analysis for gas lift was applied for Plunger lift operation using Plunger lift estimated costs. It was assumed that Plunger lift operation in the well SS7 were to be from 2016-2038.

Cash flow analyses for Plunger lift was carried out in excel and the results of the calculations were presented in Appendix C. The generated NPV by using Plunger lift was estimated to be $9,993,081 and because NPV was a positive value then the calculation of the discounted payback period became necessary.

Equation 42 was deployed in the calculation of the discounted payback period taken by Plunger lift system NPV to turn positive. It was found that only 1.48 ≈ 2 years of Plunger lift operation were necessary for generating the positive NPV in the well SS7.

Figure 67 is the plot showing the cumulative discounted cash flow for Plunger lift operating from which the generated NPV was calculated. The nature of the plot has indicated that with time the discounted cash flow will keep on increasing towards the positive which is good for generating the positive NPV.

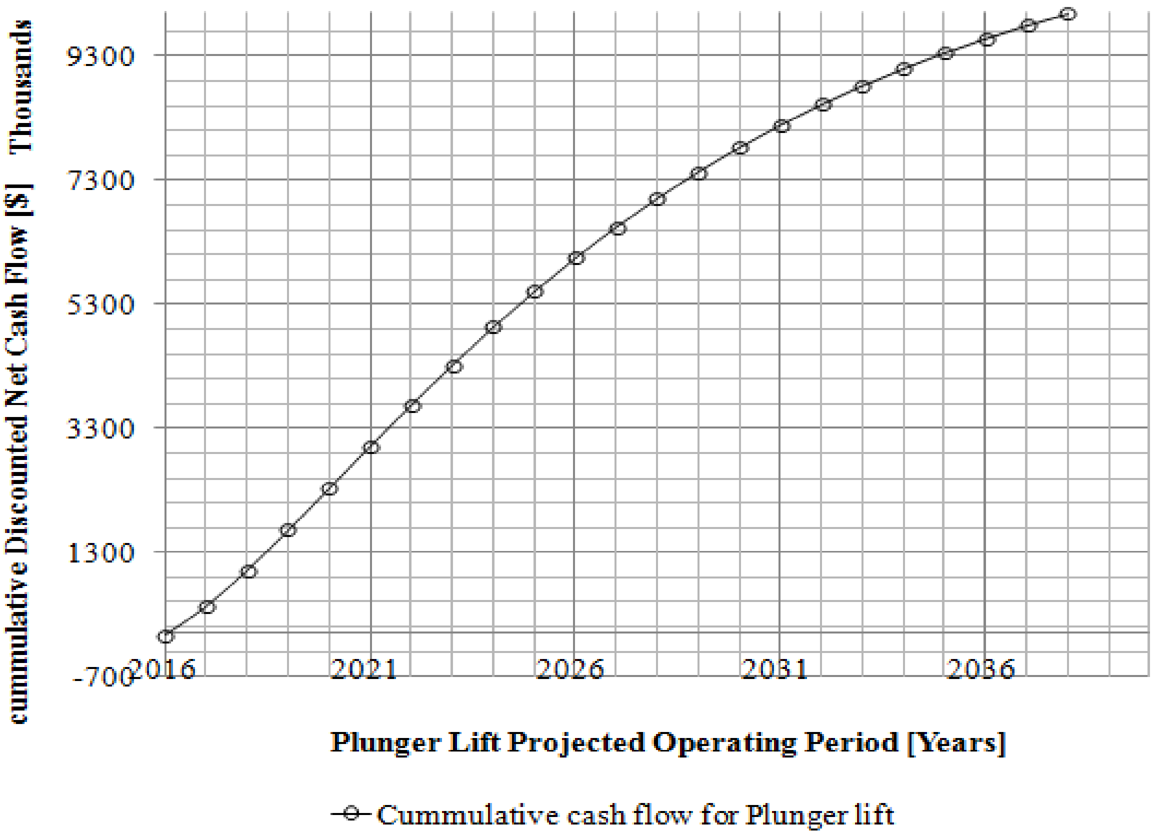

Figure 67: Cumulative discounted cash flow for Plunger lift

Plunger Lift Sensitivity Analysis

The procedures used in generating the Tornado plot for gas lift was repeated for Plunger lift operations in performing the Plunger lift sensitivity analysis. The only difference for Plunger lift operations was the costs category to be analysed at different cases developed. The three costs categories used for Plunger lift sensitivity analysis were CAPEX, Plunger lift operating costs (OPEX) and Natural Gas price.

Several sensitivity cases for the three identified cost categories were performed to estimate the generated NPV and the results were given in Appendix U.

Table 23 represents the summary of the two sensitivity cases (+-20%) selected for constructing Tornado Plot. First sensitivity case considered was to reduce the cost category by 20% below the base case and the second sensitivity case considered the increased costs categories by 20% above the base case.

Table 23: Summary table of the generated NPV ($) for various cost categories.

Cases	CAPEX	OPEX	Gas price
80%	9,995,834	10,003,675	7,981,117
100%	9,993,081	9,993,081	9,993,081
120%	9,990,327	9,982,487	12,005,044

The calculated NPV in Table 23 was used in the construction of Tornado plot in Figure 68 to evaluate the effect of each category on NPV.

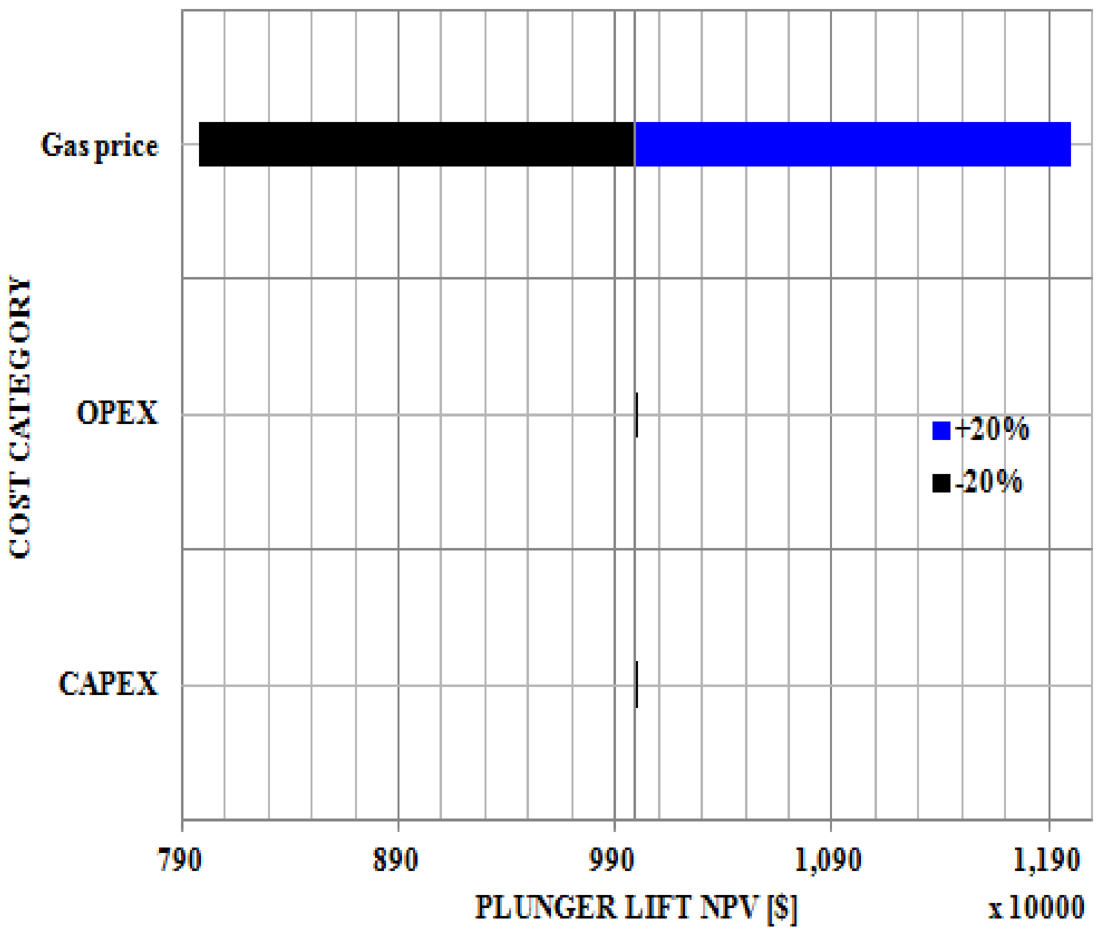

Figure 68: Tornado Plot for Plunger Lift Sensitivity Analysis

Based on the results on Figure 68, NPV was highly influenced by natural gas prices variation as compared to other cost categories analysed.

When the both OPEX and CAPEX were increased by +20% NPV goes below base case NPV and when it was decreased by -20% NPV went higher than base case NPV. But their influence on NPV was very small compared to the response of gas price.

6.3.3 Velocity String Economical Evaluation Results.

The deployment of a velocity string was ranked in the third position by technical criteria after Gas lift and Plunger lift. The economic analysis of the velocity string in determining its significance in removing the accumulated liquid from the well SS7 were performed by calculating the generated NPV.

The economical evaluation of the velocity string were performed through excel using the determined costs in Table 15 and the calculation results were given in Appendix D. The generated NPV for applying Velocity string in the well SS7 was -$2,194,726.51. The determined negative NPV for velocity string disqualify its selection for implementation in the well SS7.

Because the generated NPV was a negative value then the discounted payback would take longer than the evaluation period of 22 years for the NPV to turn positive.

Figure 69 represented the cumulative discounted cash flow for small tubing velocity analysis plotted using the results of the given in appendix D. The discounted cash flow plot has indicated that net cash flow for the velocity string increases to the negative with time during the entire evaluation period which gave no sign of generating the positive NPV or it would take long time for the curve to turn positive.

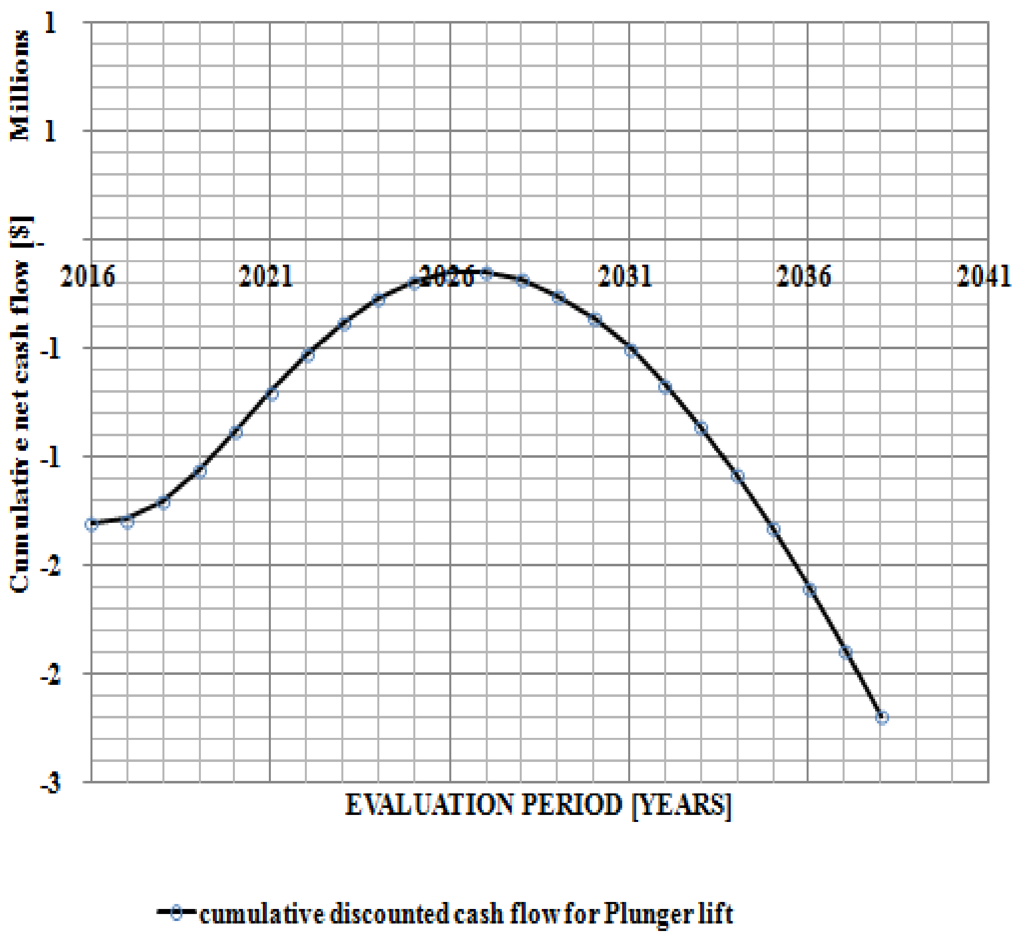

Figure 69: Cumulative discounted cash flow for velocity string

Sensitivity Analysis for Velocity String.

The same procedures used in performing the sensitivity analysis for Gas lift was applied in Velocity string to determine the effect of each costs category used in calculated NPV. The basic cost categories used in generating the Velocity string NPV were CAPEX, OPEX and Natural gas price.

Each of this costs was analysed by performing two sensitivity analysis (+-20%) which were to reduce each cost category by -20% of the base case cost and also the other sensitivity case were to increase each cost category by +20% to recalculate the new NPV.

The recalculation of new NPV for various cost categories were performed separately by applying what if analysis approach. For example performing sensitivity analysis to determine the impact of CAPEX on the velocity string generated NPV while maintaining other related costs such as gas price and OPEX same as base case value.

The summary table used to calculate NPV for various costs category for velocity string was given in Table 24.

Table 24: Velocity String estimated NPV ($) from Sensitivity Analysis for various costs category.

CASES		CAPEX	OPEX	GAS PRICE
Case 1	80%	- 1,934,727	- 3,817	- 4,206,690
Base Case	100%	- 2,194,727	- 2,194,727	- 2,194,727
Case 2	120%	- 2,454,727	- 4,385,636	- 182,763

The results in **Table 24** were used to construct the Tornado plot which shows clearly the impact of each costs estimated on NPV. Figure 70 was the generated Tornado plot for three cost categories used in the calculations of NPV.

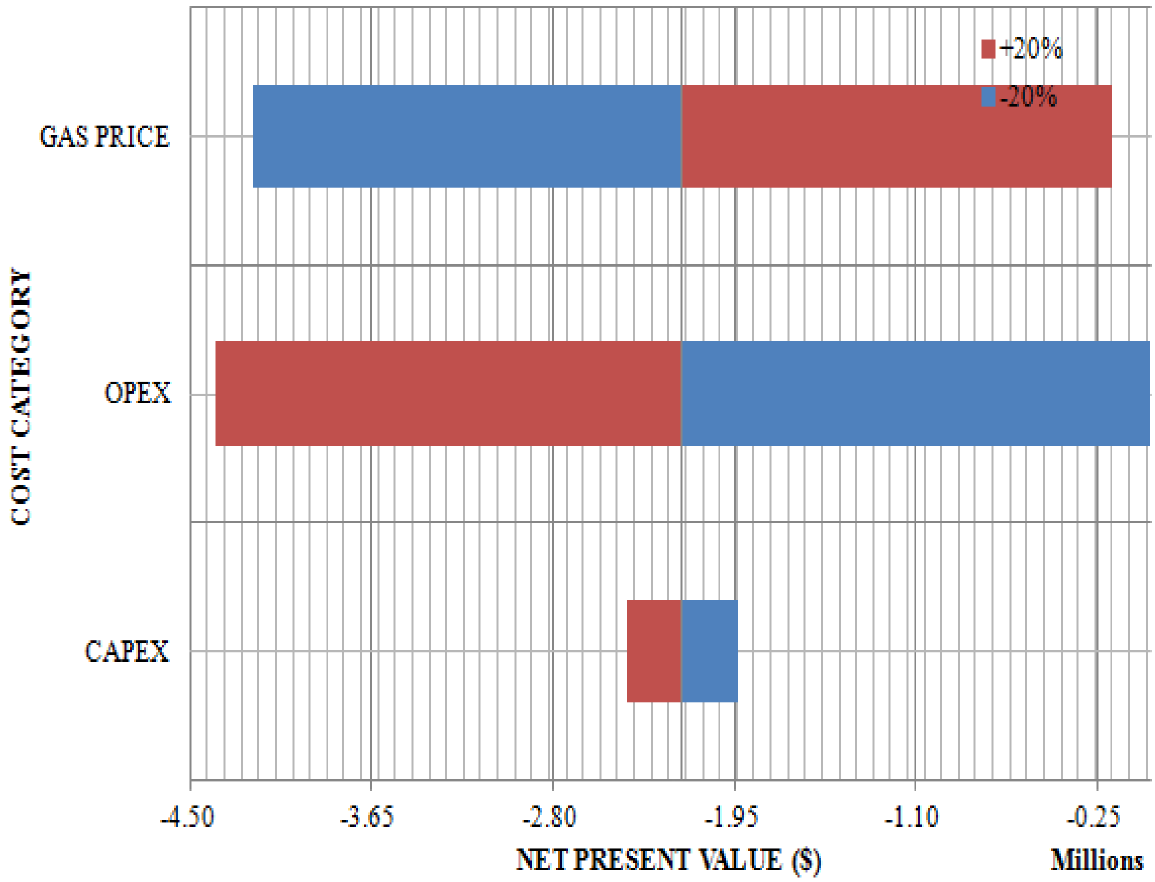

Figure 70: Tornado Plot for the Velocity String

Based on the sensitivity analysis presented on Figure 70, OPEX was found to be major influencing factor on the generated NPV. Lowering the OPEX by -20% increased the generated NPV than the impact observed on CAPEX and Gas price and it was found that CAPEX has the least influence on the generated NPV.

6.3.4 ESP Economical Evaluation Results.

ESP is the subsurface pump which is installed in the wellbore to allow liquid to be produced through the tubing and the gas produced through the casing tubing annulus. In this Master Thesis, the technical evaluation across different criteria evaluated ranked the ESP method as fourth best choice. To include the effect of economics for final decision it was necessary to perform the economic analysis for the estimated costs of an ESP.

Economical evaluation of an ESP was performed by using cash flow analysis to determine the generated NPV. The costs determined from internet in Table 15 were employed in calculating the ESP generated NPV for the well SS7.

The calculation of NPV generated by the use of an ESP was performed using excel sheet and the summary table of the calculation results was given in Appendix E, which gave NPV of $ 7,758,698.9. Figure 71 summarizes the variation of cumulative discounted cash flow with the predicted operation period in the well SS7. The final value of the cumulative discounted cash flow in Figure 71 represents the generated NPV.

Since an ESP generated a positive NPV value, the calculation of the discounted payback period was done and anticipated to be 0.71 ≈ 1years.

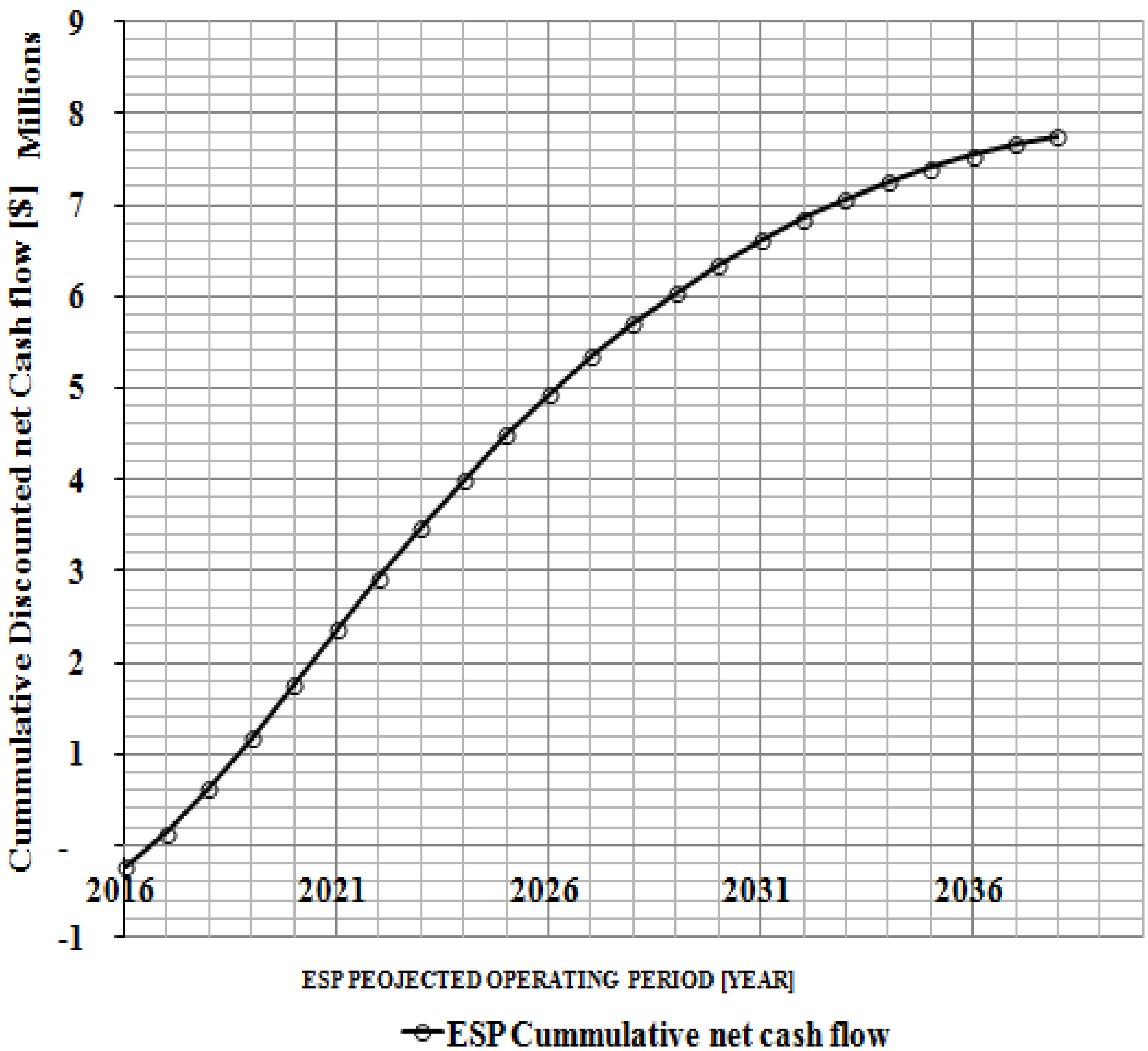

Figure 71: ESP Cumulative discounted cash flow

ESP sensitivity analysis for NPV calculation

The costs categories used in performing sensitivity analysis for NPV calculation in ESP evaluation were CAPEX, Operational costs, Electricity Costs, and natural gas price.

The influence of each costs category on the generated NPV was evaluated by performing two sensitivity analyses (+-20%) on each selected cost category. These sensitivity analyses involved reducing each cost by -20% below the base case and also increasing each cost category by +20% above the base case and the results of the estimated NPV were as given in Table 25.

Table 25: Summary table for ESP sensitivity analysis to determine NPV.

CASES	CAPEX	OPEX	Elect cost	Gas Price ($)
80%	7,805,199	8,134,243	7,796,879	5,746,735
100%	7,758,699	7,758,699	7,758,699	7,758,699
120%	7,712,199	7,383,155	7,720,519	9,770,663

The procedures of undertaking the sensitivity analysis for ESP method were the same as presented earlier in Gas lift sensitivity analysis section. The results of the generated NPV in Table 25 were used to construct the Tornado plot which a clear understanding of the influence of various cost category on NPV. The constructed Tornado plot for ESP sensitivity analysis was given in Figure 72.

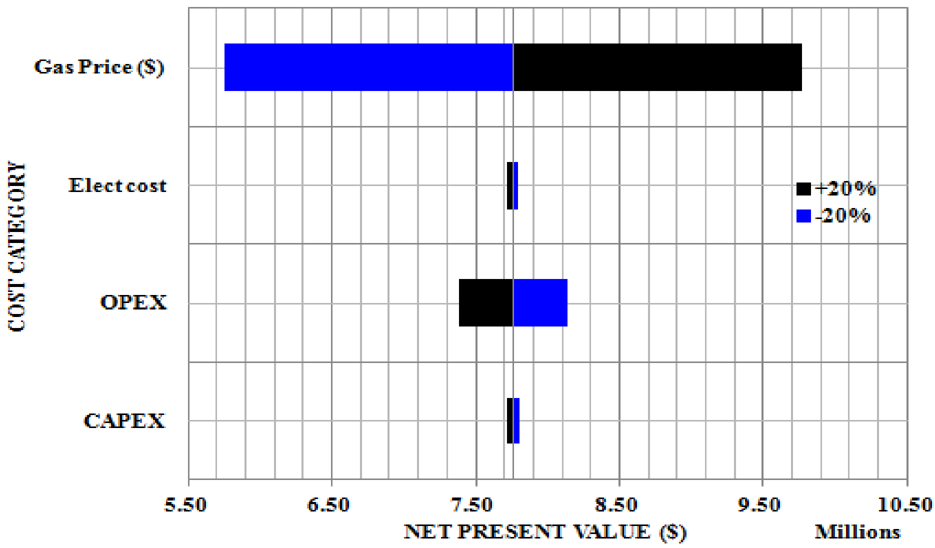

Figure 72: ESP Tornado Plot for sensitivity analysis.

The impact of various costs used in calculating NPV was investigated from sensitivity analysis represented by using Tornado plot in Figure 72. It was found that gas price had a significant effect on the generated NPV than OPEX, power costs and CAPEX.

OPEX was the second most influencing factor in the determination of NPV when using ESP as the selected liquid removal from the well. This might be because ESP operation in gas well requires intensive care to keep the gas from reaching the pump which has a direct effect on the ESP operational costs.

The influence of both CAPEX and electricity costs was found to have almost similar impact on the NPV generated from operation of ESP in the well SS7.

6.4 Final Selection of the Optimum Deliquification Method.

The selection of the optimum method for removing the accumulated liquid from the gas well (SS7) was done following the technical and economic feasibility of each option. One method can be technically feasible for implementation in a given gas well but due to limited fund availability it becomes difficult to implement. Thus both economic and technical factors need to be analysed before the final decision making.

In this study based on the technical evaluation, TOPSIS ranked different options in the order of their preferences where the most preferable with highest relative closeness(C*) to ideal solution and the first four highest ranking(C*>0.5) were considered to be the appropriate methods for SS7. Such methods selected using technical factors were Gas lift, Plunger lift, small tubing string and ESP.

To reach the final decision of the most effective method only technical viability is not enough but the technical viable options need to be analysed economically. The selected four technically feasible deliquification methods above were further analysed economically to determine the method generated NPV and Payback period using the determined costs in Table 15.

As explained in literature that the project can be rejected or accepted by using its generated NPV whereas the project are only accepted when NPV is positive and rejected when the generated NPV becomes negative regardless of the size of its absolute value.

Thus based on the economical evaluation for the four selected methods, velocity string was rejected in this evaluation because it gave a negative NPV while Plunger lift, gas lift and an ESP were selected. Their selection was based on the value of the NPV which was positive. The summary of the calculated NPV for each evaluated options were presented in Figure 73.

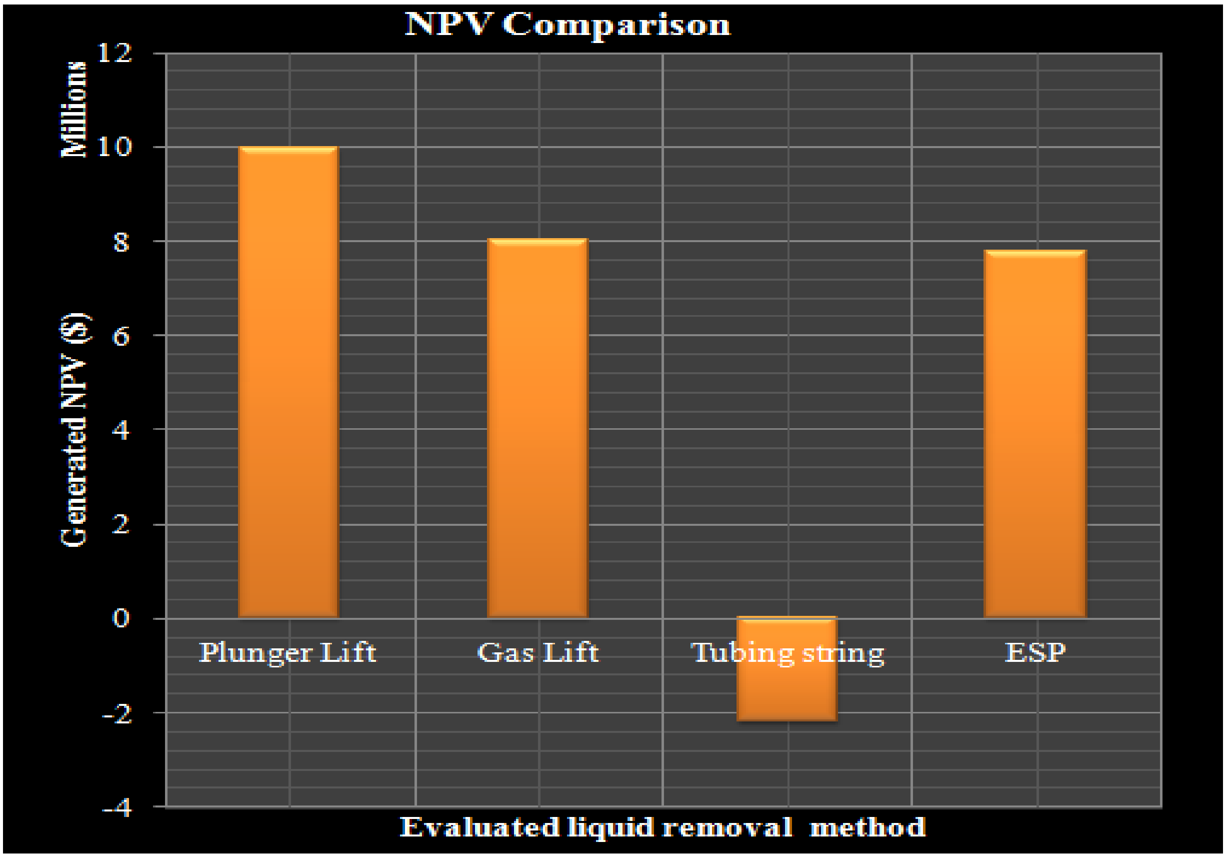

Figure 73: NPV Comparison for Different Method

Final selection was done considering the methods which gave the highest positive NPV and based on the results in Figure 73 Plunger Lift was the most suitable method compared to Gas lift and an ESP.

7.0 DESIGN OF MAIN PARAMETERS FOR PLUNGER LIFT OPERATION

The final optimum deliquification method in gas well SS7 was selected based on technical and economic factors. Technical evaluation selected four methods in order of their preferences which were Gas lift, Plunger Lift, Velocity string and ESP. The selected four methods were further evaluated economically to determine their worth before the optimum method are selected and proposed for implementation in the well SS7.

Economical evaluation selected Plunger lift as the most optimum method among the four selected from technical evaluation. The selection of the Plunger lift was based on the size of the generated NPV during its evaluation. Based on the amount of the produced liquid from the well SS7, the engineering design of the Plunger lift to determine its operating parameters becomes necessary.

Several equations for estimating Plunger lift operating parameters are available but in this study the basic equation developed by Foss and Gaul was used. It was selected for use in this master thesis study because it is simple and considers most of the necessary physics of the operation (Mower, et al., 1985).

In order to estimates the necessary parameters for Plunger operation, the direct communication between the casing-tubing annulus became important. The direct connection between the casing and tubing annulus needs to be performed by re-perforating above the packers and this will be associated with the additional costs due to perforation.

Foss and Gaul model was employed in estimating the important design parameters for efficient Plunger lift operation in the well SS7 assuming casing tubing annulus has a good communication. These parameters estimated include casing build up pressure, minimum gas required per Plunger cycle and the maximum possible cycles.

7.1 Casing Build Up Pressure

The important casing build up pressure which were estimated in this study was the minimum casing pressure for the slug arrival at the surface, maximum casing pressure required for the Plunger and the slug above it to start raising from the bumper spring to surface and an average casing pressure. The equation 27 developed by Foss and Gaul was employed in estimating the minimum casing pressure and the following were the basic assumptions made:

a) Line pressure equals to Songo-Songo separator pressure

b) Plunger set at the bottom of the tubing for SS7 gas well

c) The other assumption used in the study was based on the data presented on table 16.2 accessed from: (http://petrowiki.org/images/0/09/Vol4_Page_855_Image_0001.png). Which has the following values which will be considered in the design;

    a. Liquid gradient =0.45psi/ft

    b. Plunger weight=10lbs

    c. Plunger rising velocity = 750 ft/min

    d. Plunger falling velocity through liquid =150ft/min

    e. Plunger falling velocity through gas =1000ft/min

d) K values and Plh+Plf were 57600 and 63 respectively based on the SS7 tubing size.

e) Assumed several slug volumes required to be lifted per cycle as presented in Table 26 below.

Table 26: Liquid slug size per Plunger cycle

Slug sizes (bbl/cycle)	0.05	0.1	0.25	0.5	1	2	3	4	5

The data recorded from well SS7 was used in estimating the minimum casing pressure build up for Plunger design was presented in Table 27 below.

Table 27: SS7 well data for Plunger lift design

Tubing ID, inches	3.83
Casing ID, inches	9.625
Tubing depth , ft	6219
Tubing OD, inches	4.5
Wellbore Temperature, F	203
Surface Temperature, F	85
Tubing Average Temp, F	144
Separator Pressure, Bar	70
Liquid rate, bbl./day	122

Equation 27 was used to estimate the minimum casing pressure from the assumed liquid slug volume in Table 26 and well data in Table 27. The input data into equation 27 was required to be determined before minimum casing pressure could be estimated. Plunger weight pressure Pp was estimated based on the tubing cross section area and the Plunger weight.

Tubing cross section area was estimated using equation 29 above which depended on the tubing internal diameter. The tubing size for SS7 gas well to be used in equation 29 was presented in Table 27 above.

$$\text{Tubing area}(A_t) = \frac{\pi}{4} * \left(\frac{3.83}{12}\right)^2 = 0.08\ \text{ft}^2 = 11.52\ \text{in}^2$$

Then Plunger weight pressure Pp can be estimated from Plunger weight (10lbs) and the estimated tubing inner cross section area calculated above as follows:

$$P_p = \frac{W_p}{A_t} = \frac{10\text{lbs}}{11.52\ \text{in}^2} = 0.87\text{psia}$$

After estimating the Plunger weight pressure the calculation to determine the required minimum casing pressure for the Plunger and the liquid slug to arrive at the surface was performed at different assumed liquid slug volume given in Table 26.

At liquid slug size of 0.05 and line (separator) pressure of 1015psia the minimum casing builds up pressure (**P_{Cmin}**) was computed from equation 27 as follows.

$$P_{Cmin} = [1015 + 0.87 + 14.7 + (63) * 0.05]\left(1 + \frac{6219}{57600}\right) = 1145\text{Psia}$$

At several liquid slug volume indicated in Table 26 the minimum casing build up pressure was computed and summarised in Table 28.

Gas deviation factor ‘Z’ was estimated from Standing and Kartz chart given in Figure 8 after estimating the Pseudoreduced conditions corresponding to the average casing build up pressure using equation 5, 6, 7 and 8. The final results of gas deviation factor obtained for each casing build up pressure was presented in Table 28.

Table 28: Estimated Plunger operating ranges for different liquid slug volumes.

V_{slug} (bbl)	P_{Cmin} (psia)	P_{Cmax} (psia)	P_{Cavg} (psia)	Z	V_t (Mcf)	V_g (Mscf)	N_{Cmax} (cyc/day)	q_{Lmax} (bbl/day)	GLR_{min} (Mscf/bbl)	GLR_{min} (scf/bbl)
0.05	1,145	1,377	1,261	5.9561	0.4970	7.28	154	7.7	145.55	145548.76
0.10	1,149	1,382	1,265	5.5997	0.4967	7.76	154	15.4	77.60	77597.67
0.25	1,159	1,394	1,277	4.7477	0.4959	9.22	153	38.2	36.88	36880.10
0.50	1,177	1,415	1,296	3.7941	0.4945	11.68	151	75.7	23.36	23355.94
1.00	1,212	1,457	1,334	2.7321	0.4917	16.60	148	148.4	16.60	16603.83
2.00	1,281	1,541	1,411	1.7696	0.4861	26.80	143	285.9	13.40	13400.65
3.00	1,351	1,625	1,488	1.3119	0.4805	37.68	138	413.5	12.56	12559.92
4.00	1,421	1,709	1,565	1.0322	0.4748	49.78	133	532.3	12.44	12444.13
5.00	1,491	1,793	1,642	0.8705	0.4692	61.19	129	643.2	12.24	12238.37

7.2 Maximum and Average Casing Pressure

For each estimated $P_{C\ min}$ in Table 28, the level which the casing pressure must reach before the slug and the Plunger are allowed to begin to rise was estimated. At this level the pressure in the casing is the maximum possible and was estimated using equation 28 given above.

In estimating maximum pressure in the casing required for the Plunger and liquid slug to start raising the main input into equation 28 were:

a) The estimated minimum pressure (P_{Cmin}) in the casing estimated from equation 27 at certain slug volume.
b) Tubing inner cross section area 'A_t' and
c) Annulus inner cross section area 'A_a' from equation 30 as follows;

$$A_a = \frac{\pi}{4 * 144}[9.625^2 - 3.83^2] = 56.83\ in^2 = 0.39\ ft^2$$

Using equation 28 for a specific liquid slug volume the maximum casing pressure required was estimated as follows.

Assuming the liquid slug volume of 0.05bbl, the estimated minimum casing pressure from Table 28 was found to be 1145Psia then

$$P_{c\,max} = 1145\ \text{psia} * \frac{(56.83 + 11.52)\ \text{in}^2)}{56.83\ \text{in}^2} = 1{,}377\ \text{psia}$$

This means that 1,377 psia is the maximum pressure build in the casing to start lifting the Plunger weight of 10 lbs and liquid slug of 0.05 bbls in a single cycle. After the Plunger and the liquid begin rising to surface the average casing pressure required to transport them in the annulus was estimated using equation 31. Taking the same liquid slug assumed above and the estimated minimum casing pressure the average casing pressure was calculated as follows:

$$P_{c\,average} = 1145\ \text{psia} * \left[1 + \frac{11.52\ \text{sqr inches}}{2 * 56.83\ \text{sqr inches}}\right] = 1{,}261\ \text{psia.}$$

The calculations above was used to illustrate how casing build up pressure was calculated for various liquid slug volume and the same procedures were repeated for several liquid slug volumes in excel and the general results were presented in Table 28.

The relationship between maximum, average and minimum casing build up pressure for a given liquid slug volume in Table 28 were plotted in Figure 74 and this plot represented the performance envelope of designed Plunger to be installed in SS7.

At the current reservoir operating pressure the estimated casing build up pressure required to lift the Plunger and the liquid above it to surface from the well SS7 was not feasible because the maximum casing pressure was far less than the bottomhole pressure. Maximum casing pressure represent the pressure required to start the Plunger and the liquid raising from the well bottom (bumper spring) to the surface which sometimes are the same as the flowing bottomhole pressure. It was expected that the difference between the flowing bottomhole pressures for the well SS7 to be close to the maximum casing build up pressure but higher than the recorded wellhead pressure.

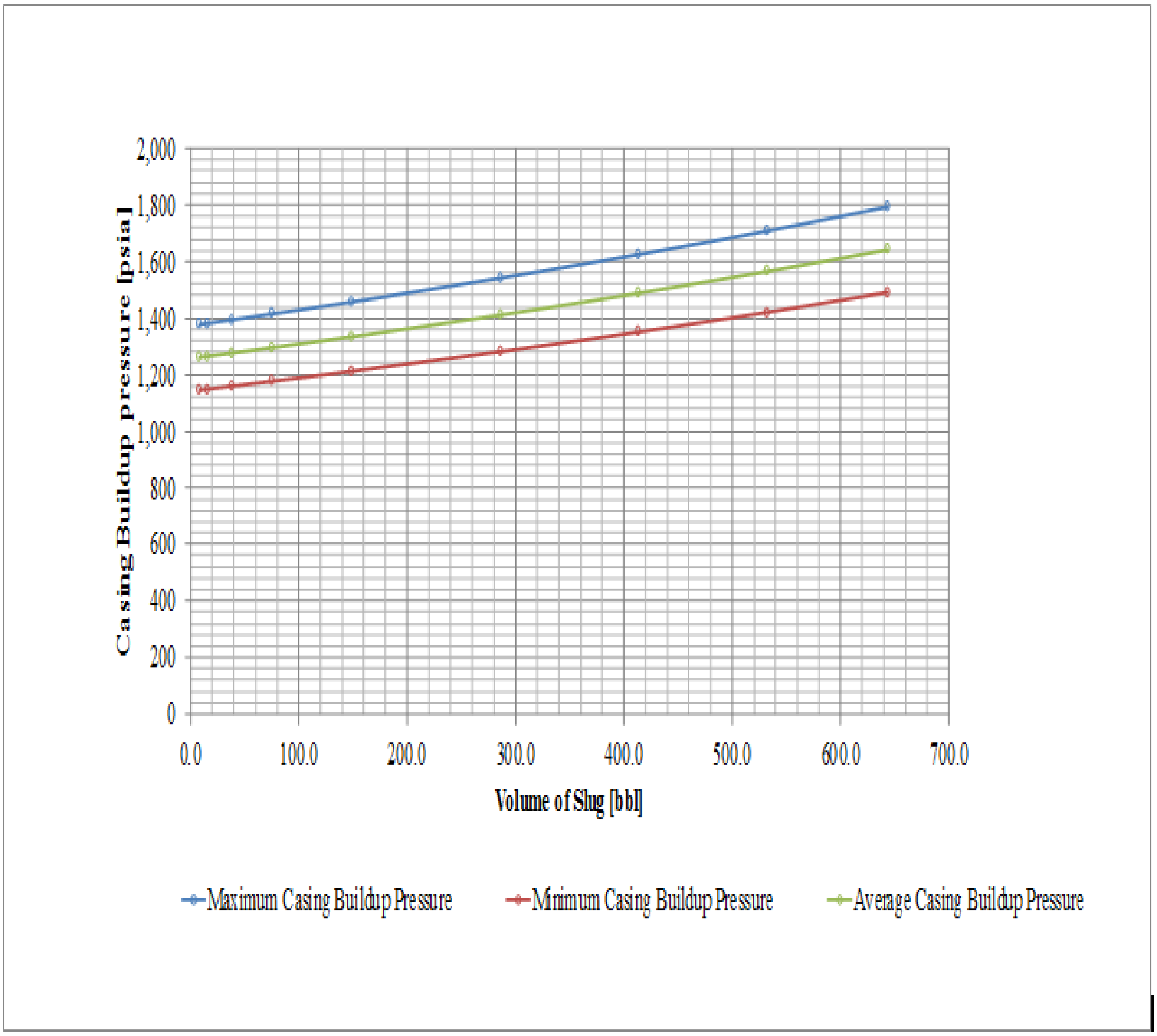

Figure 74: Operating envelope of the designed Plunger Lift for SS7

For a given liquid production from SS7 the appropriate Plunger required to lift such liquid to surface its average casing pressure should be between the average estimated casing pressure and the maximum casing pressure given in Figure 74.

The reported average water production rate from SS7 was 115.99bbl/day and average condensate produced from SS7 5.95 bbl/day, which make a total liquid production of 122 bbl. Linear interpolation method was applied in determining the necessary Plunger operating parameters for removing the reported produced liquid from the assumed liquid slug volume in Table 28. The summary of the estimated required Plunger parameter for removing liquid from the well bottom were given in Table 29.

7.3 Gas Rate Required Per Plunger Cycle.

Equation 32 was used to calculate the minimum gas lift required to lift the Plunger and the liquid above it to surface. The main input into the equation included the following

i. Average casing pressure estimated above,

ii. Slippage factor was estimated from Plunger depth, slippage factor was related to depth to Plunger using the following expression:

Actual tubing volume which was estimated at Plunger lift depth (D) of

$$F_{gs} = \text{Slippage factor} = 1 + \frac{0.02 * 6219}{1000} = 1.124$$

iii. 6219ft, assumed slug volume per cycle (S) of 0.05bbl, tubing inner capacity (L) = 70.2 ft/bbl and tubing inner cross section area A_t = 0.08 ft^2 using the following relation:

$$V_t = \text{Actual tubing volume, cuft} = A_t * \frac{(D - S * L)}{1000}$$

$$= 0.08 * \frac{\left(6219 - (0.05 * 70.2)\right)}{1000} = 0.497 \text{ ft}^3$$

iv. Average tubing temperature(T_{avg}) for SS7 of 604^{o}R

v. Gas deviation factor estimated at T_{avg} and estimated average casing pressure when liquid slug was 0.05bbl.

The gas deviation factor (Z) was estimated using Standing correlation for SS7 gas with gas specific gravity of 0.56 and at the average casing temperature of 604^{o}R and average casing pressure of 1,261psia to be 0.93.

After estimating the above inputs equation 32 was employed in computing the minimum gas required by the Plunger per cycle and the results were obtained as follows:

$$V_g = 1.124 * 1{,}261 * \left(\frac{0.497}{14.7}\right)\left(\frac{520}{604 * 0.93)}\right) = 46.6\text{Mscf/cycle.}$$

The same procedure of calculating the minimum gas require to lift the Plunger and the liquid above it were repeated for other assumed liquid slug volumes and several gas rate were obtained as presented in Table 28.

After understanding the minimum gas rate required to lift the Plunger and the assumed liquid rate in one cycle per day, then it was very important compute the maximum possible Plunger trip required per day. Estimating the maximum possible Plunger trips in the liquid loaded gas well became important because it was finally employed in calculating the maximum liquid rate expected for the given casing pressure.

7.4 Maximum Plunger Cycles

Because Plunger lift operation is the cyclic process, estimating Plunger cycles became very important in this study. The cyclic process of the Plunger lift begins with the shut-in period that allows the Plunger to fall from the surface to the bottom of the wellbore. During shut in period the well builds sufficient gas pressure to lift both the Plunger and liquid slug to the surface.

Unloading process began when the sufficient gas pressure has been reached to move the Plunger to surface and the process is repetitive. The analysis to determine the maximum number of Plunger cycles required to unload SS7 gas well per day was performed using Foss and Gaul model implemented in excel.

To determine the maximum possible Plunger lift trips in a given gas well, equation 33 was employed. The main inputs into equation 33 in estimating the maximum possible Plunger cycles per day were tubing inner capacity (L), produced liquid volume per cycle (S), depth to Plunger (D), Plunger fall velocity through liquid (v_{fl}) and gas (v_{fg}) and Plunger rising velocity (v_r).

Tubing inner capacity was a constant for a given tubing sizes and it was estimated from tubing cross section area using the following expression.

$$\mathrm{L} = \text{Tubing inner capacity} = \frac{5.615}{\mathrm{A_t}}, \frac{\mathrm{ft}}{\mathrm{bbl}} = \frac{5.615}{0.08} = 70.2\mathrm{ft/bbl}$$

The maximum possible cycles per day required during Plunger operation in SS7 were calculated for several assumed liquid lifted per cycle and for illustration slug volume of 0.05 bbl was used. The other information needed were Plunger rise velocity of 800 ft/min, Plunger fall velocity through liquid of 150ft/min and through gas of 750ft/min and depth which the Plunger needs to travel of 6219ft. The above Plunger velocities were the average velocity of the operating range of the Plunger velocity obtained from literature as defined in equation 33.

With the above information maximum possible Plunger operating cycles expected was estimated from equation 33 as follows:

$$C_{max} = \frac{1440}{\frac{6219\text{ft} - 0.05\text{bbl} * 70.2\text{ft/bbl}}{750\text{ft/min}} + \frac{6219\text{ ft}}{800} + \frac{0.05\text{bbl} * 70.2\text{ft/bbl}}{150}} = 154\text{ cycle/day}$$

After determining the maximum possible trips which the Plunger will need to perform per day then it was then possible to estimates the maximum liquid rate need to complete the estimated cycles.

$q_{L\,max} = C_{max} * S$, where S stands for volume of liquid slug (V_{slug}) per cycle

Thus with S=0.05bbl/cycle and the estimated $C_{max} = 154$ cycles/Day, the maximum liquid rate to be produced during Plunger lift operation = $154\,\frac{\text{cycles}}{\text{Day}} * \frac{0.05\text{bbl}}{\text{cycle}} = 7.7\text{bbl/day}$.

For various assumed liquid volume in Table 26 to be lifted by the Plunger to surface in single cycle the same procedure used to estimate the maximum Plunger cycles were repeated and the results of C_{max} were presented in tabular form as shown in Table 28.

The relationship between Plunger cycles and the minimum casing pressure required for the Plunger and the liquid to arrive at the surface were established graphically and found that at lower minimum casing pressure Plunger execute many cycles in lifting a certain liquid rate to surface. As the casing pressure in the casing increases the maximum number of Plunger trips per day decreases and the results were given in **Figure 75**.

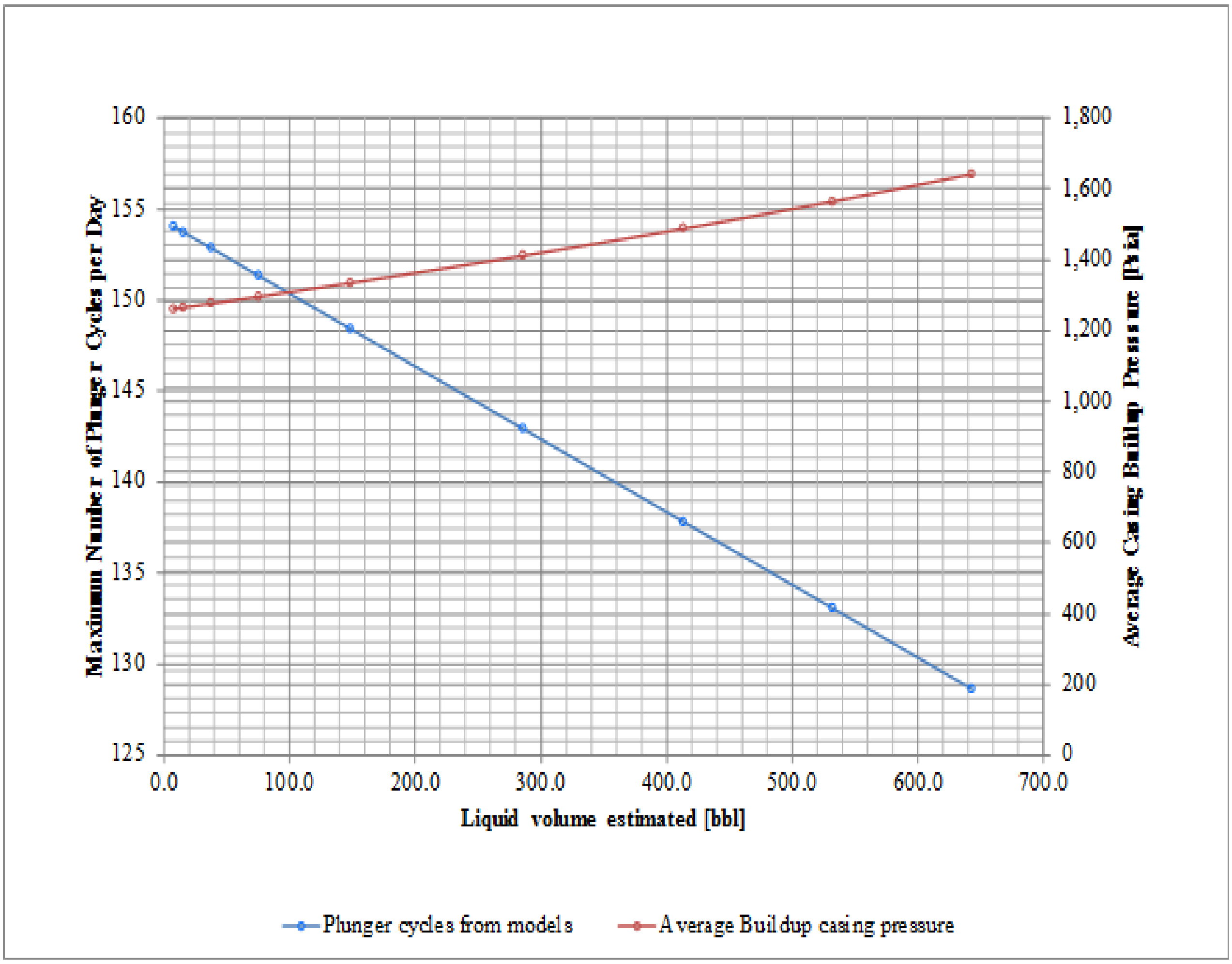

Figure 75: Relationship between maximum Plunger cycles with average casing pressure for given slug volume.

7.5 Estimating the SS7 Plunger Operating Range.

The results given in Table 28 were used to find the Plunger operating parameters suitable for lifting the produced liquid from SS7. So based on the reported average liquid production rate from SS7 the required Plunger parameters to be installed in the well was obtained by linear interpolation method.

Using the SS7 liquid rate recorded during when the well began experiencing liquid loading in Table 27, the parameters such as required gas rate to lift the Plunger and the liquid above to surface, average casing build up pressure and the number of Plunger trips necessary during Plunger operation were estimated. The general linear interpolation formula used was given in equation 44.

$$y_2 = y_1 + \frac{(y_3 - y_1)(x_2 - x_1)}{(x_3 - x_1)} \quad \textbf{44}$$

With '**x**' stands for liquid rate and '**y**' stands for the required Plunger parameters such as Plunger cycle, gas lift rate and average casing pressure build up in lifting the produced liquid slug and Plunger weight to surface.

The interpolation formula in equation 44 was implemented in the excel VBA using the function given in the snapshot below to find the required parameters for lifting the produced liquid and the Plunger to the surface.

```
Function lin(x1, y1, x3, y3, x2)
'lin =y2 whic is the plunger parameters to be estimated'
'x2 is the SS7 reported liquid rate'
'x1 and x3 is the maximum estimated liquid rate based on the assumed liquid slug size per cycle'
'y1, y3 are the plunger parameters corresponding to liquid rate x1, x3'
lin = y1 + ((y3 - y1) * (x2 - x1) / (x3 - x1))
End Function
```

The final estimated operating parameters such as gas rate, average casing build up pressure, minimum casing pressure and maximum Plunger cycles required per day for Plunger to be installed in SS7 were summarized in Table 29 given below.

Table 29: The estimated Plunger parameters for SS7.

	q_{max}	V_g	P_{Cavg}	P_{Cmin}	P_{Cmax}	N_{Cmax}
	(bbl/day)	(Mscf)	(psia)	(psia)	(psia)	(cyc/day)
x1	75.7					
x2	122	15	1320	1199	1442	149
x3	148.4					

Based on the results obtained in Table 29 the designed Plunger lift system required for SS7 will need a gas rate of 15 Mscf per cycle, 149 cycles per day, maximum casing pressure build-up of 1442 psia to starts the Plunger rising to surface and Plunger will arrive at the surface with the casing pressure of 1199 psia.

8. CONCLUSION AND RECOMMENDATIONS

This study was the continuation of my specialization project which involves the study of liquid loading in the SS7 following its declined gas production in recent years. Liquid loading study began by identifying the liquid produced sources in the well by studying condensation as well as possibility of water coning.

Water of condensation was found to have started at the reservoir operating conditions and WGR of 1.03bbl/MMscf was estimated from McKetta and Wehe correlation. Because the estimated WGR from condensation was less than the actual WGR recorded in the well SS7, It became important to investigate the other sources. A simplified coning model was employed and it seems plausible that there is water coning into the gas well from the bottom aquifer and it was suspected to be the main contribution of liquid flow into the well SS7.

The prediction of liquid loading was done by using Turner droplet model as well as the performance curve developed in Prosper software. These predictions gave the onset for liquid loading in the well SS7 and if there will be no immediate measures taken probably the well was going to cease producing in not longer time. This gave challenges to initiate another study on identifying and determining the most optimum method which can be useful in accordance to SS7 well conditions to remove the accumulated liquid to surface.

Several deliquification methods were evaluated both by considering the technical and economic factors. The technical factor selected the four most effective method based on the TOPSIS ranking method. The selected methods in orders were Gas lift, Plunger lift, and ESP and velocity string.

Further evaluation was performed by considering the economical factor to select the most appropriate methods based on the calculated NPV. The methods which generate the positive NPV were selected and the method with negative NPV was rejected as it was regarded uneconomical.

Based on the presented economic analysis in Figure 73, Plunger lift, Gas lift and ESP gave the positive NPV and they were regarded to be economically viable for well SS7. Plunger lift was regarded as the most suitable method for SS7 as it gave the highest NPV compared to Gas lift and ESP.

The engineering design of the selected Plunger lifts method was done using analytical Foss and Gaul equation to determine its operating parameters. The calculations were performed assuming that there was a good casing-tubing annulus communication which could be achieved by re-perforating above the packer. It was found that the minimum pressure build up in the casing for Plunger and the liquid above it to arrive to surface was 1199psia and the maximum casing build up required to start the Plunger rising from the bumper spring was 1442 psia.

The minimum gas rate required to lift the Plunger and the accumulated liquid to surface per cycle was 15Mscf/day and the maximum Plunger cycles required for lifting the liquid produced from the well SS7 was 149 cycles/day.

This analysis was based on the literature identified cost estimates, the study recommends the same analysis to be performed using the current costs estimates from the service company so that to get the realistic of the best alternatives.

9. APPENDICES

APPENDIX A: Z - FACTOR ESTIMATION CHART

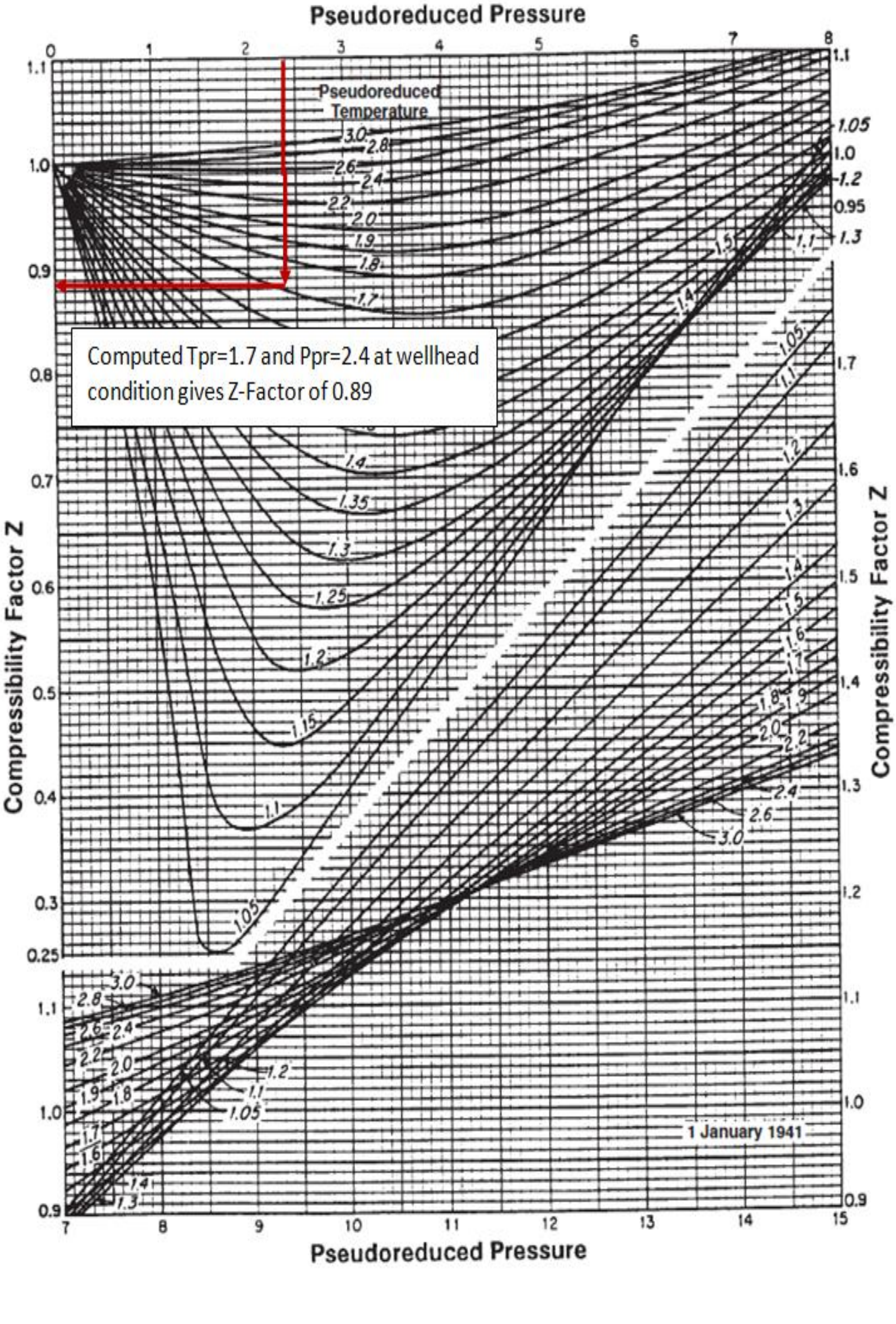

APPENDIX B: GAS LIFTS ECONOMICAL ANALYSIS.

	Forecasted production period		2016	2017	2018	2019	2020	2021	2022	2023	2024	2025	2026	2027	2028	2029	2030	2031	2032	2033	2034	2035	2036	2037	2038
	Cummulative gas produc	Mscf	85027	154889	212292	259456	298208	330049	356210	377706	395368	409880	421803	431600	439650	446264	451698	456163	459832	462846	465323	467358	469030	470404	471533
	Gas price	3.323	$/Mscf																						
Year	2016	2017	2018	2019	2020	2021	2022	2023	2024	2025	2026	2027	2028	2029	2030	2031	2032	2033	2034	2035	2036	2037	2038		
Discounting Period	0	1	2	3	4	5	6	7	8	9	10	11	12	13	14	15	16	17	18	19	20	21	22		
Discount factor	1.00	0.91	0.83	0.75	0.68	0.62	0.56	0.51	0.47	0.42	0.39	0.35	0.32	0.29	0.26	0.24	0.22	0.20	0.18	0.16	0.15	0.14	0.12		
Gas lift installation cost $	64,420																								
Gas lift operating cost $	-	88,861	97,748	107,522	118,275	130,102	143,112	157,424	173,166	190,483	209,531	230,484	253,532	278,885	306,774	337,451	371,197	408,316	449,148	494,063	543,469	597,816	657,597		
Gas lift injection cost $	-	9,969	10,966	12,062	13,269	14,596	16,055	17,661	19,427	21,369	23,506	25,857	28,443	31,287	34,416	37,857	41,643	45,807	50,388	55,427	60,969	67,066	73,773		
Revenue from increased gas production $		514698	705445	862171	990945	1096752	1183687	1255117	1313808	1362030	1401652	1434208	1460957	1482935	1500993	1515830	1528022	1538038	1546269	1553031	1558587	1563153	1566904		
Cash flow $	- 64,420	415,867	596,731	742,586	859,402	952,054	1,024,520	1,080,033	1,121,215	1,150,178	1,168,615	1,177,867	1,178,982	1,172,762	1,159,803	1,140,522	1,115,182	1,083,915	1,046,733	1,003,542	954,149	898,271	835,533		
PV $	- 64,420	378,061	493,166	557,916	586,983	591,151	578,315	554,228	523,055	487,788	450,552	412,835	375,660	339,707	305,412	273,032	242,696	214,447	188,264	164,087	141,828	121,384	102,642		
cumulative pv	- 64,420	313,641	806,807	1,364,723	1,951,706	2,542,857	3,121,171	3,675,399	4,198,454	4,686,242	5,136,794	5,549,629	5,925,289	6,264,996	6,570,409	6,843,441	7,086,137	7,300,583	7,488,848	7,652,935	7,794,763	7,916,147	8,018,789		
cumulative pv postive?	FALSE	TRUE	TRUE	TRUE	TRUE	TRUE	TRUE	TRUE	TRUE	TRUE	TRUE	TRUE	TRUE	TRUE	TRUE	TRUE	TRUE	TRUE	TRUE	TRUE	TRUE	TRUE	TRUE		
NPV $	8,018,789																								

APPENDIX C: PLUNGER LIFTS ECONOMICAL ANALYSIS

Forecasted production period		2016	2017	2018	2019	2020	2021	2022	2023	2024	2025	2026	2027	2028	2029	2030	2031	2032	2033	2034	2035	2036	2037	2038
Cummulative gas production	Mscf	85027	154889	212292	259456	298208	330049	356210	377706	395368	409880	421803	431600	439650	446264	451698	456163	459832	462846	465323	467358	469030	470404	471533
Gas price	3.323	$/Mscf																						
YEAR	2016	2017	2018	2019	2020	2021	2022	2023	2024	2025	2026	2027	2028	2029	2030	2031	2032	2033	2034	2035	2036	2037	2038	
Discounting Period	0	1	2	3	4	5	6	7	8	9	10	11	12	13	14	15	16	17	18	19	20	21	22	
Discounting factor	1.0	1.1	1.2	1.3	1.5	1.6	1.8	1.9	2.1	2.4	2.6	2.9	3.1	3.5	3.8	4.2	4.6	5.1	5.6	6.1	6.7	7.4	8.1	
Plunger Lift Equipment and Set Up Co	13769																							
Plunger Lift Maintenance Cost		2533	2787	3065	3372	3709	4080	4488	4937	5430	5973	6571	7228	7951	8746	9620	10582	11641	12805	14085	15494	17043	18747	
Gas Revenue from Increased Gas Production		514698	705445	862171	990945	1096752	1183687	1255117	1313808	1362030	1401652	1434208	1460957	1482935	1500993	1515830	1528022	1538038	1546269	1553031	1558587	1563153	1566904	
cash flow	-16072	512164	702658	859106	987573	1093043	1179607	1250629	1308871	1356600	1395679	1427637	1453729	1474984	1492247	1506210	1517439	1526398	1533464	1538946	1543094	1546110	1548156	
present value	-16072	465604	580709	645459	674526	678693	665857	641771	610598	575331	538095	500378	463203	427250	392955	360575	330239	301990	275807	251630	229371	208927	190185	
Cummulative net present value	-16072	449532	1030242	1675701	2350226	3028920	3694777	4336548	4947146	5522477	6060571	6560949	7024152	7451402	7844358	8204933	8535172	8837161	9112968	9364598	9593969	9802896	9993081	
Cumulative cash flow positive?	FALSE	TRUE	TRUE	TRUE	TRUE	TRUE	TRUE	TRUE	TRUE	TRUE	TRUE	TRUE	TRUE	TRUE	TRUE	TRUE	TRUE	TRUE	TRUE	TRUE	TRUE	TRUE	TRUE	
NPV	9.99E+06																							

APPENDIX D: VELOCITY STRING ECONOMICAL ANALYSIS.

SS7 Forecasted production period		2016	2017	2018	2019	2020	2021	2022	2023	2024	2025	2026	2027	2028	2029	2030	2031	2032	2033	2034	2035	2036	2037	2038
Cummulative gas production	Mscf	85027	154889	212292	259456	298208	330049	356210	377706	395368	409880	421803	431600	439650	446264	451698	456163	459832	462846	465323	467358	469030	470404	471533
Gas price	3.323	$/Mscf																						
Year	2016	2017	2018	2019	2020	2021	2022	2023	2024	2025	2026	2027	2028	2029	2030	2031	2032	2033	2034	2035	2036	2037	2038	
Discounting Period	0	1	2	3	4	5	6	7	8	9	10	11	12	13	14	15	16	17	18	19	20	21	22	
Discount factor	1.00	1.10	1.21	1.33	1.46	1.61	1.77	1.95	2.14	2.36	2.59	2.85	3.14	3.45	3.80	4.18	4.59	5.05	5.56	6.12	6.73	7.40	8.14	
Tubing CAPEX	1,300,000																							
Tubing OPEX	-	500,000	605,000	665,500	732,050	805,255	885,781	974,359	1,071,794	1,178,974	1,296,871	1,426,558	1,569,214	1,726,136	1,898,749	2,088,624	2,297,486	2,527,235	2,779,959	3,057,955	3,363,750	3,700,125	4,070,137	
Electrical Cost	-	-	-	-	-	-	-	-	-	-	-	-	-	-	-	-	-	-	-	-	-	-	-	
Tubing Revenue		514,697.69	705445	862171	990945	1096752	1183687	1255117	1313808	1362030	1,401,652.40	1434208	1460957	1482935	1500993	1515830	1528022	1538038	1546269	1553031	1558587	1,563,152.72	1,566,903.78	
Cash flow $	- 1,300,000	14,698	100,445	196,671	258,895	291,497	297,907	280,759	242,013	183,057	104,781	7,649	- 108,258	- 243,201	- 397,756	- 572,794	- 769,465	- 989,197	-1,233,690	-1,504,923	-1,805,163	- 2,136,972	- 2,503,234	
PV $	- 1,300,000	13,362	83,012	147,762	176,829	180,996	168,161	144,074	112,901	77,634	40,398	2,681	- 34,494	- 70,447	- 104,742	- 137,122	- 167,458	- 195,707	- 221,890	- 246,067	- 268,326	- 288,770	- 307,512	
cumulative pv	- 1,300,000	- 1,286,638	- 1,203,626	-1,055,864	- 879,035	-698,039	-529,878	-385,805	- 272,904	- 195,270	- 154,872	- 152,191	- 186,685	- 257,132	- 361,874	- 498,996	- 666,454	- 862,161	-1,084,051	-1,330,118	-1,598,444	- 1,887,214	- 2,194,727	
cumulative pv postive?	FALSE	FALSE	FALSE	FALSE	FALSE	FALSE	FALSE	FALSE	FALSE	FALSE	FALSE	FALSE	FALSE	FALSE	FALSE	FALSE	FALSE	FALSE	FALSE	FALSE	FALSE	FALSE	FALSE	
NPV $	-2,194,727																							

APPENDIX E: ESP ECONOMICAL ANALYSIS.

		2016	2017	2018	2019	2020	2021	2022	2023	2024	2025	2026	2027	2028	2029	2030	2031	2032	2033	2034	2035	2036	2037	2038
Cumulative gas prod	Mscf	85027	154889	212292	259456	298208	330049	356210	377706	395368	409880	421803	431600	439650	446264	451698	456163	459832	462846	465323	467358	469030	470404	471533
	3.323	$/Mscf																						
Year	2016	2017	2018	2019	2020	2021	2022	2023	2024	2025	2026	2027	2028	2029	2030	2031	2032	2033	2034	2035	2036	2037	2038	
Discounting Period	0	1	2	3	4	5	6	7	8	9	10	11	12	13	14	15	16	17	18	19	20	21	22	
Discount factor	1.00	0.91	0.83	0.75	0.68	0.62	0.56	0.51	0.47	0.42	0.39	0.35	0.32	0.29	0.26	0.24	0.22	0.20	0.18	0.16	0.15	0.14	0.12	
ESP CAPEX	232,500																							
ESP OPEX	-	93,886	103,275	113,602	124,962	137,458	151,204	166,325	182,957	201,253	221,378	243,516	267,868	294,654	324,120	356,532	392,185	431,404	474,544	521,998	574,198	631,618	694,780	
Electrical Cost	-	9,545	10,500	11,549	12,704	13,975	15,372	16,910	18,601	20,461	22,507	24,757	27,233	29,956	32,952	36,247	39,872	43,859	48,245	53,069	58,376	64,214	70,635	
ESP Revenue		514698	705445	862171	990945	1096752	1183687	1255117	1313808	1362030	1401652	1434208	1460957	1482935	1500993	1515830	1528022	1538038	1546269	1553031	1558587	1563153	1566904	
Cash flow $	- 232,500	411,267	591,671	737,020	853,278	945,318	1,017,110	1,071,883	1,112,250	1,140,317	1,157,768	1,165,934	1,165,856	1,158,324	1,143,921	1,123,051	1,095,965	1,062,776	1,023,480	977,963	926,013	867,321	801,489	
PV $	- 232,500	373,879	488,984	553,734	582,801	586,968	574,132	550,045	518,873	483,606	446,369	408,653	371,478	335,525	301,230	268,850	238,514	210,265	184,082	159,905	137,646	117,202	98,460	
cumulative pv	- 232,500	141,379	630,363	1,184,097	1,766,897	2,353,866	2,927,998	3,478,043	3,996,916	4,480,522	4,926,891	5,335,544	5,707,022	6,042,547	6,343,777	6,612,627	6,851,141	7,061,405	7,245,487	7,405,392	7,543,038	7,660,239	7,758,699	
cumulative pv postiv	FALSE	TRUE	TRUE	TRUE	TRUE	TRUE	TRUE	TRUE	TRUE	TRUE	TRUE	TRUE	TRUE	TRUE	TRUE	TRUE	TRUE	TRUE	TRUE	TRUE	TRUE	TRUE	TRUE	
NPV $	7,758,699																							

APPENDIX F: SUMMARY TABLE FOR TURNER CRITICAL VELOCITY CALCULATIONS AND ACTUAL FLUID PRODUCTION FOR WELL SS7 (Magige, 2016).

TIME	pwh	Tpr=Twh/Ppc	Ppr=Pwh/Ppc	Z_factor	Gas density	Critical velocity	rate at ID=2.992 Inches THEN 3.83 i	critical gas rate at ID=2.992 Inches	Actual Gas rate	Water	Condensate
[Date]	[Psia	[-]	[-]	[-]	lb/ft3	ft/s	MMscf/d	MMscf/d	MMscfd	bbls	bbls
3/30/2012	1671	1.65	2.52	0.87	5.2113	6.5142	3.2131	3.2131	18.3	0.0	0.0
6/30/2012	1665	1.65	2.51	0.87	5.1944	6.5252	3.2081	3.2081	17.8	0.0	0.0
9/30/2012	1664	1.65	2.51	0.87	5.1905	6.5277	3.2069	3.2069	17.1	0.0	0.0
12/30/2012	1685	1.65	2.54	0.87	5.2554	6.4856	3.2261	3.2261	16.4	9.6	1.6
3/30/2013	1662	1.65	2.51	0.87	5.1842	6.5319	3.2051	3.2051	14.9	11.6	6.4
6/30/2013	1687	1.65	2.55	0.87	5.2634	6.4804	3.2284	3.2284	13.9	8.7	9.4
9/30/2013	1617	1.65	2.44	0.88	4.9876	6.6646	3.1462	3.1462	12.9	8.1	9.3
12/30/2013	1595	1.65	2.41	0.88	4.9176	6.7138	3.1249	3.1249	12.8	9.0	8.8
3/30/2014	1570	1.65	2.37	0.88	4.8420	6.7681	3.1018	3.1018	12.2	15.0	9.2
6/30/2014	1649	1.65	2.49	0.87	5.1444	6.5581	3.1933	3.1933	10.6	28.5	8.0
9/30/2014	1545	1.65	2.33	0.89	4.7105	6.8656	3.0610	3.0610	12.4	43.3	9.5
12/30/2014	1568	1.65	2.36	0.88	4.8340	6.7739	3.0993	3.0993	11.1	45.9	9.9
3/30/2015	1527	1.65	2.30	0.89	4.6549	6.9079	3.0435	3.0435	11.3	50.8	9.0
6/30/2015	1545	1.65	2.33	0.89	4.7097	6.8661	3.0607	3.0607	9.5	42.8	7.8
9/30/2015	1506	1.65	2.27	0.89	4.5932	6.9559	3.0240	3.0240	10.2	45.6	7.8
12/30/2015	1669	1.65	2.52	0.92	4.9238	6.7094	5.1236	3.1268	4.4	19.8	3.2
3/30/2016	1668	1.65	2.52	0.87	5.2018	6.5203	5.2604	3.2103	6.2	27.7	5.0
6/30/2016	1753	1.65	2.64	0.91	5.2288	6.5028	5.2734	3.2183	3.5	24.7	2.5
9/30/2016	1823	1.65	2.75	0.86	5.7511	6.1873	5.5188	3.3680	2.9	57.0	2.2

APPENDIX G: SS7 LIQUID RATE ESTIMATES EXTRACTED FROM PROSPER

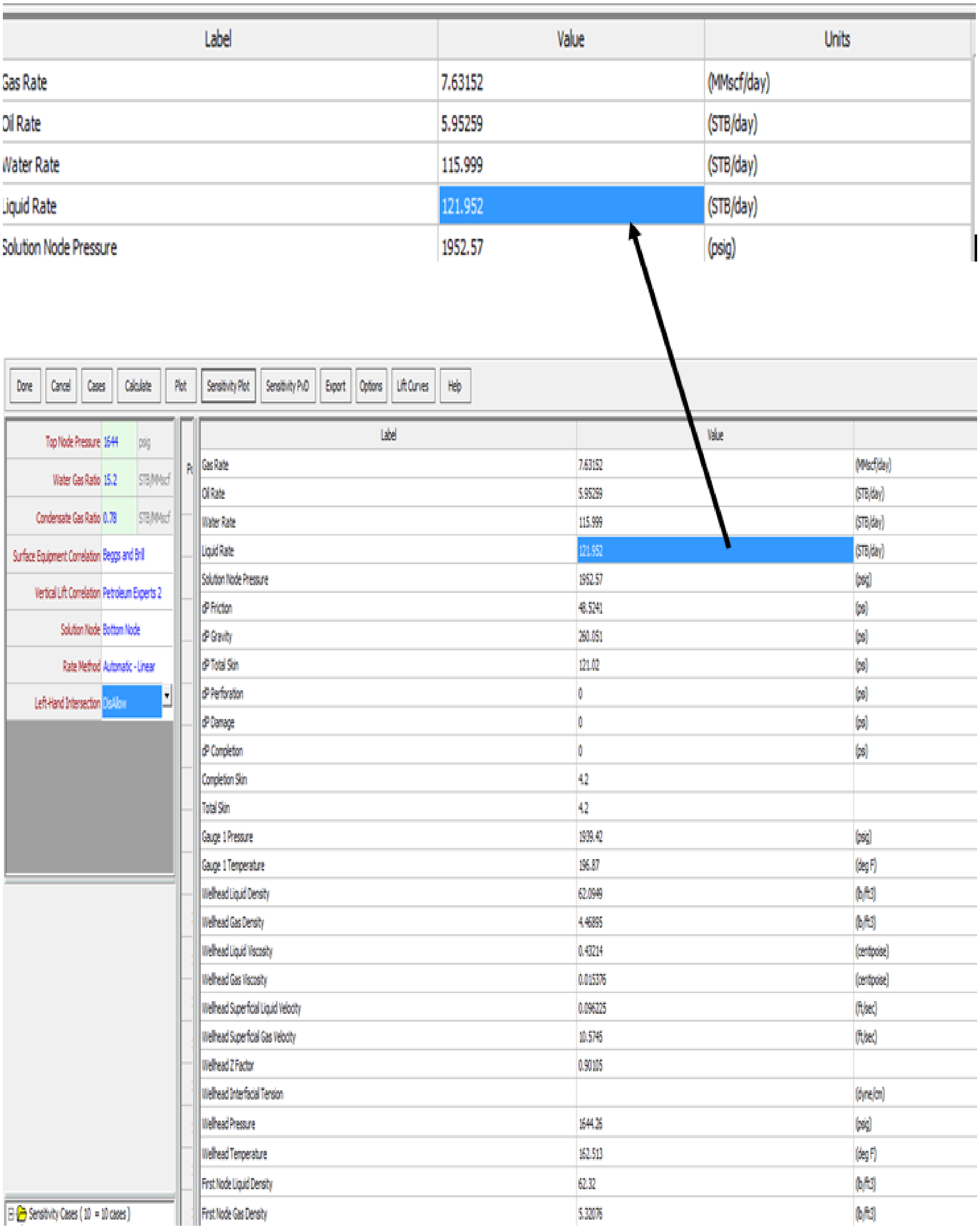

Label	Value	Units
Gas Rate	7.63152	(MMscf/day)
Oil Rate	5.95259	(STB/day)
Water Rate	115.999	(STB/day)
Liquid Rate	121.952	(STB/day)
Solution Node Pressure	1952.57	(psig)

Top Node Pressure	1644	psig
Water Gas Ratio	15.2	STB/MMscf
Condensate Gas Ratio	0.78	STB/MMscf
Surface Equipment Correlation	Beggs and Brill	
Vertical Lift Correlation	Petroleum Experts 2	
Solution Node	Bottom Node	
Rate Method	Automatic - Linear	
Left-Hand Intersection	DisAllow	

Label	Value	
Gas Rate	7.63152	(MMscf/day)
Oil Rate	5.95259	(STB/day)
Water Rate	115.999	(STB/day)
Liquid Rate	121.952	(STB/day)
Solution Node Pressure	1952.57	(psig)
dP Friction	48.5241	(psi)
dP Gravity	260.051	(psi)
dP Total Skin	121.02	(psi)
dP Perforation	0	(psi)
dP Damage	0	(psi)
dP Completion	0	(psi)
Completion Skin	4.2	
Total Skin	4.2	
Gauge 1 Pressure	1939.42	(psig)
Gauge 1 Temperature	196.87	(deg F)
Wellhead Liquid Density	62.0949	(lb/ft3)
Wellhead Gas Density	4.46895	(lb/ft3)
Wellhead Liquid Viscosity	0.43214	(centipoise)
Wellhead Gas Viscosity	0.015376	(centipoise)
Wellhead Superficial Liquid Velocity	0.096225	(ft/sec)
Wellhead Superficial Gas Velocity	10.5745	(ft/sec)
Wellhead Z Factor	0.90105	
Wellhead Interfacial Tension		(dyne/cm)
Wellhead Pressure	1644.26	(psig)
Wellhead Temperature	162.513	(deg F)
First Node Liquid Density	62.32	(lb/ft3)
First Node Gas Density	5.32076	(lb/ft3)

APPENDIX H: COST OF ARTIFICIAL LIFT FOR GAS WELLS FROM CHEVRON

Artificial Lift Type	Sucker Rod Pump		ESTSP	Hydraulic reciprocating piston pump-closed loop	Conv. PCP (<250F)	I-PCP (<250F)	Mechanical lock PCP (upto 300F)	Metal-Metal PCP (>300F)
Pump description	Sucker Rod Pump with Beam Pumping Unit		Electrical Sumbersible Twin Screw Pump	3 tbg in the well connected to piston pump through BHA, closed loop power fluid (PF)	tubing retrievable PCP	rod retrievable PCP (Insert-PCP)	Mechanical lock PCP	Metal-Metal PCP
Flow Rate (gross)	200	500	500	500	500	500	500	500
Fluid Density (90% cut, 12 degree API)	0.993	0.993	0.993	0.993	0.993	0.993	0.993	0.993
Depth (ft)	2,000	2,000	2000	2,000	2000	2000	2000	2000
Downhole Pump Cost	$26,500	$46,500	160,000	$70,300	$55,000	$53,000	$56,300	
Driver Cost (e.g., pumping unit, VFD, etc.)	$50,000	$50,000	$60,000	$38,000	$0	$0	$0	$0
Tubing/ Sucker rod/ Shaft/ CT Cost	$10,000	$10,000	$0	$0	$0	$0	$0	$0
Rig/ CTU/ Crane Costs	$5,000	$5,000	$5,000	$2,500	$5,000	$5,000	$5,000	$5,000
Surface Facilities Cost (pad, controls)	$15,000	$15,000	$7,500	$15,000	$7,500	$7,500	$7,500	$7,500
Total Installed Cost	**$106,500**	**$126,500**	**$232,500**	**$125,800**	**$67,500**	**$65,500**	**$68,800**	**$12,500**
Estimated Mean Time Between Failures	2	2	2.85	0.8	2.5	2.5	2.5	2.5
Estimated Pump Repair Cost	$10,000	$10,000	$64,000	$5,100	$13,900	$12,500	$15,400	$15,900
Estimated Hoist / Rig/ CTU Cost	$5,500	$5,500	$5,500	$2,750	$5,500	$2,750	$5,500	$5,500
Average pull costs per year	$7,750	$7,750	$24,386	$9,458	$7,760	$6,100	$8,360	$8,560
Pumping System Overall Efficiency (%)	45.0%	45.0%	40%	70%	65%	65%	65%	45%
Annual Electrical cost @ $.08 / kw-hr	$3,394	$8,485	$9,545	$5,455	$5,874	$5,874	$5,874	$8,485
Total Annual Operating Cost + Prod Loss	**$11,144**	**$16,235**	**$33,931**	**$14,912**	**$13,634**	**$11,974**	**$14,234**	**$17,045**
NPV @ 10% over 10 years	**$181,822**	**$236,232**	**$461,843**	**$226,593**	**$159,653**	**$146,433**	**$165,009**	**$127,706**

APPENDIX I: ARTIFICIAL LIFT CRITERIA USED FOR GAS WELLS FROM CHEVRON

	Rod pump	ESP	Gas Lift	PCP	Plunger lift	Hydraulic Reciprocating Piston Pump	Hydraulic Jet	Cap. String
Operating well depth, ft (TVD)	16000 *4875*	15000 *4572*	18000 *4572*	12000 *3658*	19000 *5971*	17000 *5182*	15000 *4572*	22000 *6705*
Operating volume (min.- max.), BFPD	6000	350-135,000	100-30,000	20-7,500	200	8000	20000	500
Operating temp. °F (max.)	600	410	400	250	550	550	550	400
Deviation well applicability	Generally operated upto 30-40' ; but known to have installed in 60 degree deviated wells	0-90	0-70	application dependent	Typically near vertical wells; maximum devaition of 60'	0-90	0-90	Typically < 5', max 60'
Casing/ Tubing diameter range, inch	(> 2 3/8") Plunger OD 1 1/2"-5 3/4"	Casing diameter 5.5-13 5/8" MIN	All API casing sizes available	4.5&5.62	< 3 1/2" (though any Tubing size works; it is related to efficiency)	Tubing diameter > 2 3/8"	Insert inside 2 7/8" tbg	any tubing size; but efficiency reduces for large diameters
Gas Handling	Fair to Good	Fair	Excellent	Good	Excellent	Fair	Good	Excellent
Solid handling	Fair to Good	Poor to Fair	Good to excellent	Excellent	Poor to Fair	Fair	Good	Fair to moderate
Offshore application	Limited	Excellent	Excellent	Applicable - Limited by depth	Installed in some locations below SSSV	Excellent	Excellent	Excellent
Installation costs ($000)	234	103	40	53	8	134	134	44
Monthly Operating costs ($)	2800	3987	4180	700	200	3380	3380	400

APPENDIX J: TECHNICAL EVALUATION MATRIX BY CHEVRON

Considerations			Plunger	Gas lift	ESP	PCP	Rod Pump	Jet lift	Piston Pump	Foam Injection	Velocity String	Heated Tubing
1	Well Location	Offshore	0.00	0.90	0.90	0.75	0.00	0.90	0.75	0.75	0.75	0.75
		Onshore	0.75	0.75	0.75	0.75	0.75	0.75	0.75	0.75	0.75	0.75
2	Well Type	Vertical	0.75	0.75	0.75	0.75	0.75	0.75	0.75	0.90	0.90	0.90
		0 deg - 40 deg	0.90	0.90	0.90	0.90	0.90	0.25	0.25	0.75	0.75	0.75
		40 deg - 70 deg	0.75	0.25	0.90	0.90	0.25	0.25	0.25	0.50	0.75	0.50
		70 deg - 90 deg	0.75	0.00	0.90	0.90	0.00	0.25	0.25	0.25	0.25	0.25
		Horizontal	0.00	0.00	0.90	0.90	0.00	0.25	0.25	0.00	0.00	0.00
3	Well Depth (ftTVD)	<12000ft	0.75	0.75	0.75	0.75	0.75	0.75	0.75	0.75	0.75	0.75
		12000<D<15000	0.75	0.75	0.75	0.00	0.75	0.75	0.75	0.50	0.75	0.25
		15000<D<16000	0.75	0.75	0.00	0.00	0.75	0.00	0.75	0.25	0.75	0.00
		16000<D<17000	0.75	0.75	0.00	0.00	0.00	0.00	0.75	0.00	0.75	0.00
		17000<D<18000	0.75	0.75	0.00	0.00	0.00	0.00	0.00	0.00	0.50	0.00
		18000<D<19000	0.75	0.00	0.00	0.00	0.00	0.00	0.00	0.00	0.25	0.00
		>19000	0.00	0.00	0.00	0.00	0.00	0.00	0.00	0.00	0.00	0.00
4	Operating Volume (bpd)	<200bpd	0.90	0.50	0.25	0.75	0.75	0.25	0.75	0.90	0.90	0.90
		200<V<500	0.00	0.90	0.90	0.90	0.90	0.90	0.90	0.50	0.75	0.50
		500<V<6000	0.00	0.90	0.90	0.90	0.25	0.90	0.90	0.25	0.25	0.25
		6000<V<7500	0.00	0.90	0.90	0.25	0.00	0.90	0.50	0.00	0.00	0.00
		7500<V<8000	0.00	0.75	0.75	0.00	0.00	0.50	0.25	0.00	0.00	0.00
		8000<V<20000	0.00	0.50	0.50	0.00	0.00	0.25	0.00	0.00	0.00	0.00
		20000<V<30000	0.00	0.25	0.50	0.00	0.00	0.00	0.00	0.00	0.00	0.00
		30000<V<135000	0.00	0.00	0.25	0.00	0.00	0.00	0.00	0.00	0.00	0.00
		>135000	0.00	0.00	0.00	0.00	0.00	0.00	0.00	0.00	0.00	0.00

APPENDIX K: ESTIMATION OF RELATIVE CLOSENESS FOR PLUNGER LIFT

PLUNGER LIFT							Relative closeness
		NEW _PLUNGER_LIFT_SCORE	Positive	Negative	Separation	Separation	To ideal solution
SQUARE	NORMALIZED	%WT *Normalized	Ideal Solution	Ideal Solution	From +_Ideal_SolN	From -_Ideal_SolN	C*=S-/(S+ + S-)
0.5625	0.437594974	0.08	0.09	0.01	0.00004	0.00478	0 < C* < 1
0.5625	0.437594974	0.06			0.00067	0.00247	0.544354063
0.5625	0.437594974	0.09			0.00000	0.00572	
0.5625	0.437594974	0.05			0.00151	0.00135	
0.0625	0.145864991	0.01			0.00572	0.00000	
0.0625	0.145864991	0.01			0.00540	0.00000	
0.5625	0.437594974	0.08			0.00004	0.00478	
				$\Sigma(v_j^* - v_{ij})^2$	0.01339	0.01911	
				$S_i^* = [\Sigma(v_j^* - v_{ij})^2]^{1/2}$	0.115707403	0.138234075	
					S+	S-	

APPENDIX L: ESTIMATION OF RELATIVE CLOSENESS FOR GAS LIFT

GAS LIFT			V+	V-			Relative Closeness
		NEW_GAS_LIFT_SCORE	Positive	Negative	Separation (S+)	Separation (S-)	To ideal solution
SQUARE	NORMALIZED	%WT *Normalized	Ideal Solution	Ideal Solution	From +_Ideal_SolN	From -_Ideal_SolN	C*=S-/(S+ + S-)
0.5625	0.404519917	0.074911096	0.080903983	0.010986961	0.00004	0.0041	0 < C* < 1
0.5625	0.404519917	0.056932433			0.00057	0.0021	0.585
0.5625	0.404519917	0.080903983			0.00000	0.0049	
0.5625	0.404519917	0.044946657			0.00129	0.0012	
0.0625	0.134839972	0.010986961			0.00489	0.0000	
0.5625	0.404519917	0.03895377			0.00176	0.0008	
0.5625	0.404519917	0.074911096			0.00004	0.0041	
				$\Sigma(v_j^*-v_{ij})^2$	0.00859	0.0171	
				$S_i^* = [\,\Sigma\,(v_j^*-v_{ij})^2\,]^{1/2}$	0.09267	0.1308	
					S+	S-	

APPENDIX M: ESTIMATION OF RELATIVE CLOSENESS FOR ESP

ESP							Relative closeness
		NEW_ESP_SCORE	Positive	Negative	Separation (S+)	Separation (S-)	To ideal solution
SQUARE	NORMALIZED	%WT *Normalized	Ideal Solution	Ideal Solution	From +_Ideal_SolN	From -_Ideal_SolN	C*=S-/(S+ + S-)
0.5625	0.4804	0.0890	0.0961	0.0130	0.0001	0.0058	0 < C* < 1
0.5625	0.4804	0.0676			0.0008	0.0030	0.5059
0.5625	0.4804	0.0961			0.0000	0.0069	
0.0625	0.1601	0.0178			0.0061	0.0000	
0.0625	0.1601	0.0130			0.0069	0.0000	
0.0625	0.1601	0.0154			0.0065	0.0000	
0.5625	0.4804	0.0890			0.0001	0.0058	
				$\Sigma(v_j^*-v_{ij})^2$	0.0204	0.0214	
				$S_i^* = [\,\Sigma\,(v_j^*-v_{ij})^2\,]^{1/2}$	0.1430	0.1464	
					S+	S-	

APPENDIX N: ESTIMATION OF RELATIVE CLOSENESS FOR PCP

PCP							Relative closeness
		NEW_PCP_SCORE	Positive	Negative	Separation	Separation	To ideal solution
SQUARE	NORMALIZED	%WT *Normalized	Ideal Solution	Ideal Solution	From +_Ideal_SolN	From -_Ideal_SolN	C*=S-/(S+ + S-)
0.0625	0.2085	0.0386	0.1251	0.0170	0.0075	0.0005	0 < C* < 1
0.5625	0.6255	0.0880			0.0014	0.0050	0.3745
0.5625	0.6255	0.1251			0.0000	0.0117	
0.0625	0.2085	0.0232			0.0104	0.0000	
0.0625	0.2085	0.0170			0.0117	0.0000	
0.0625	0.2085	0.0201			0.0110	0.0000	
0.0625	0.2085	0.0386			0.0075	0.0005	
				$\Sigma(v_j^*-v_{ij})^2$	0.0494	0.0177	
				$S_i^* = [\,\Sigma\,(v_j^*-v_{ij})^2\,]^{1/2}$	0.2224	0.1331	
					S+	S-	

APPENDIX O: ESTIMATION OF RELATIVE CLOSENESS FOR ROD PUMPING

ROD_PUMPING							Relative closeness
		NEW_PCP_SCORE	Positive	Negative	Separation	Separation	To ideal solution
SQUARE	NORMALIZED	%WT *Normalized	Ideal Solution	Ideal Solution	From + Ideal_SolN	From - Ideal_SolN	C*=S-/(S+ + S-)
0.5625	0.5388	0.0998	0.1078	0.0146	0.0001	0.007249878	0 < C* < 1
0.0625	0.1796	0.0253			0.0068	0.000113279	0.4625
0.5625	0.5388	0.1078			0.0000	0.00867295	
0.0625	0.1796	0.0200			0.0077	2.83198E-05	
0.0625	0.1796	0.0146			0.0087	0	
0.0625	0.1796	0.0173			0.0082	7.07996E-06	
0.5625	0.5388	0.0998			0.0001	0.0072	
					0.0315	0.0233	
					0.1775	0.1527	
					S+	S-	

APPENDIX P: ESTIMATION OF RELATIVE CLOSENESS FOR JET PUMPING

JET_PUMPING							Relative closeness
		NEW_JET_PUMPING_SCORE	Positive	Negative	Separation	Separation	To ideal solution
SQUARE	NORMALIZED	%WT *Normalized	Ideal Solution	Ideal Solution	From + Ideal_SolN	From - Ideal_SolN	C*=S-/(S+ + S-)
0.5625	0.5388	0.100	0.1078	0.0146	0.0001	0.007249878	0 < C* < 1
0.0625	0.1796	0.025			0.0068	0.000113279	0.4625
0.5625	0.5388	0.108			0.0000	0.00867295	
0.0625	0.1796	0.020			0.0077	2.83198E-05	
0.0625	0.1796	0.015			0.0087	0	
0.0625	0.1796	0.017			0.0082	7.07996E-06	
0.5625	0.5388	0.100			0.0001	0.007249878	
					0.0315	0.0233	
					0.1775	0.1527	
					S+	S-	

APPENDIX Q: ESTIMATION OF RELATIVE CLOSENESS FOR PISTON PUMPING

PISTON_PUMPING							Relative closeness
		NEW_PISTON_PUMPING_SCORE	Positive	Negative	Separation	Separation	To ideal solution
SQUARE	NORMALIZED	%WT *Normalized	Ideal Solution	Ideal Solution	From + Ideal_SolN	From - Ideal_SolN	C*=S-/(S+ + S-)
0.5625	0.5388	0.0998	0.1078	0.0146	0.0001	0.007249878	0 < C* < 1
0.0625	0.1796	0.0253			0.0068	0.000113279	0.4625
0.5625	0.5388	0.1078			0.0000	0.00867295	
0.0625	0.1796	0.0200			0.0077	2.83198E-05	
0.0625	0.1796	0.0146			0.0087	0	
0.0625	0.1796	0.0173			0.0082	7.07996E-06	
0.5625	0.5388	0.0998			0.0001	0.007249878	
					0.0315	0.0233	
					0.1775	0.1527	
					S+	S-	

APPENDIX R: ESTIMATION OF RELATIVE CLOSENESS FOR FOAM LIFT PUMPING

FOAM_LIFT_PUMPING							Relative closeness
		NEW _Foam_lift_SCORE	Positive	Negative	Separation	Separation	To ideal solution
SQUARE	NORMALIZED	%WT *Normalized	Ideal Solution	Ideal Solution	From +_Ideal_SolN	From -_Ideal_SolN	C*=S-/(S+ + S-)
0.5625	0.5388	0.0998	0.1078	0.0146	0.0001	0.007249878	0 < C* < 1
0.0625	0.1796	0.0253			0.0068	0.000113279	0.4625
0.5625	0.5388	0.1078			0.0000	0.00867295	
0.0625	0.1796	0.0200			0.0077	2.83198E-05	
0.0625	0.1796	0.0146			0.0087	0	
0.0625	0.1796	0.0173			0.0082	7.07996E-06	
0.5625	0.5388	0.0998			0.0001	0.007249878	
					0.0315	0.0233	
					0.1775	0.1527	
					S+	S-	

APPENDIX S: ESTIMATION OF RELATIVE CLOSENESS FOR VELOCITY TUBING

VELOCITY TUBING							Relative closeness
		NEW _VELOCITY_TUBING_SCORE	Positive	Negative	Separation	Separation	To ideal solution
SQUARE	NORMALIZED	%WT *Normalized	Ideal Solution	eal Soluti	From +_Ideal_SolN	From -_Ideal_SolN	C*=S-/(S+ + S-)
0.5625	0.3780	0.0700	0.0756	0.0308	0.00003	0.001536351	0 < C* < 1
0.5625	0.3780	0.0532			0.0005	0.000501666	0.5114
0.5625	0.3780	0.0756			0.0000	0.002006663	
0.5625	0.3780	0.0420			0.0011	0.000125416	
0.5625	0.3780	0.0308			0.0020	0	
0.5625	0.3780	0.0364			0.0015	3.13541E-05	
0.5625	0.3780	0.0700			0.0000	0.001536351	
					0.0052	0.0057	
					0.0724	0.0757	
					S+	S-	

APPENDIX T: GAS LIFT SENSITIVITY CASES

Sensistivity Analysis Cases	OPEX	NPV	GAS INJECTION COSTS	NPV($)	Gas Price	NPV($)	CAPEX	NPV
base case	OPEX	8018789	($)	8018789	($)	8018789	CAPEX	8018789
80%	71089	8034945	7975	8058665	2.658	6006825	51536	8031673
85%	75532	8030906	8474	8048696	2.825	6509816	54757	8028452
90%	79975	8026867	8972	8038727	2.991	7012807	57978	8025231
95%	84418	8022828	9471	8028758	3.157	7515798	61199	8022010
100%	88861	8018789	9969	8018789	3.323	8018789	64420	8018789
105%	93305	8014749	10467	8008820	3.489	8521779	67641	8015568
110%	97748	8010710	10966	7998851	3.655	9024770	70862	8012347
115%	102191	8006671	11464	7988882	3.821	9527761	74083	8009125
120%	106634	8002632	11963	7978913	3.988	10030752	77304	8005904

APPENDIX U: PLUNGER LIFT SENSITIVITY CASES

Sensitivity Analysis Cases	CAPEX($)	NPV($)	OPEX($)	NPV($)	Gas Price($)	NPV($)
base case	CAPEX	9993081	OPEX	9993081	Gas Price	9993081
80%	11015	9995834	1842	10003675	2.658	7981117
85%	11703	9995146	1958	10001026	2.825	8484108
90%	12392	9994458	2073	9998378	2.991	8987099
95%	13080	9993769	2188	9995729	3.157	9490090
100%	13769	9993081	2303	9993081	3.323	9993081
105%	14457	9992392	2418	9990432	3.489	10496072
110%	15145	9991704	2533	9987784	3.655	10999063
115%	15834	9991015	2648	9985135	3.821	11502054
120%	16522	9990327	2764	9982487	3.988	12005044

APPENDIX V: ESP SENSITIVITY CASES

Sensitivity Analysis Cases	CAPEX	NPV ($)	OPEX	NPV ($)	Electric costs	NPV ($)	Gas price	NPV ($)
base case	CAPEX	7758699	OPEX	7758699	($)	7758699	($)	7758699
80%	186000	7805199	75109	8134243	7636	7796879	2.658	5746735
85%	197625	7793574	79803	8040357	8113	7787334	2.825	6249726
90%	209250	7781949	84497	7946471	8591	7777789	2.991	6752717
95%	220875	7770324	89192	7852585	9068	7768244	3.157	7255708
100%	232500	7758699	93886	7758699	9545	7758699	3.323	7758699
105%	244125	7747074	98580	7664813	10022	7749154	3.489	8261690
110%	255750	7735449	103275	7570927	10500	7739609	3.655	8764681
115%	267375	7723824	107969	7477041	10977	7730064	3.821	9267672
120%	279000	7712199	112663	7383155	11454	7720519	3.988	9770663

APPENDIX W: VELOCITY TUBING SENSITIVITY CASES

Sensistivity Analysis Cases	Gas price	NPV($)	CAPEX	NPV	OPEX	NPV
base case	($)	-2194727	Base CAPEX	-2194727	OPEX	-2194727
80%	2.658	-4206690	1040000	-1934727	400000	-3817
85%	2.825	-3703699	1105000	-1999727	425000	-551545
90%	2.991	-3200708	1170000	-2064727	450000	-1099272
95%	3.157	-2697717	1235000	-2129727	475000	-1646999
100%	3.323	-2194727	1300000	-2194727	500000	-2194727
105%	3.489	-1691736	1365000	-2259727	525000	-2742454
110%	3.655	-1188745	1430000	-2324727	550000	-3290181
115%	3.821	-685754	1495000	-2389727	575000	-3837908
120%	3.988	-182762.73	1560000	-2454727	600000	-4385636

APPENDIX X: THE WELL SS7 COMPLETION DIAGRAM

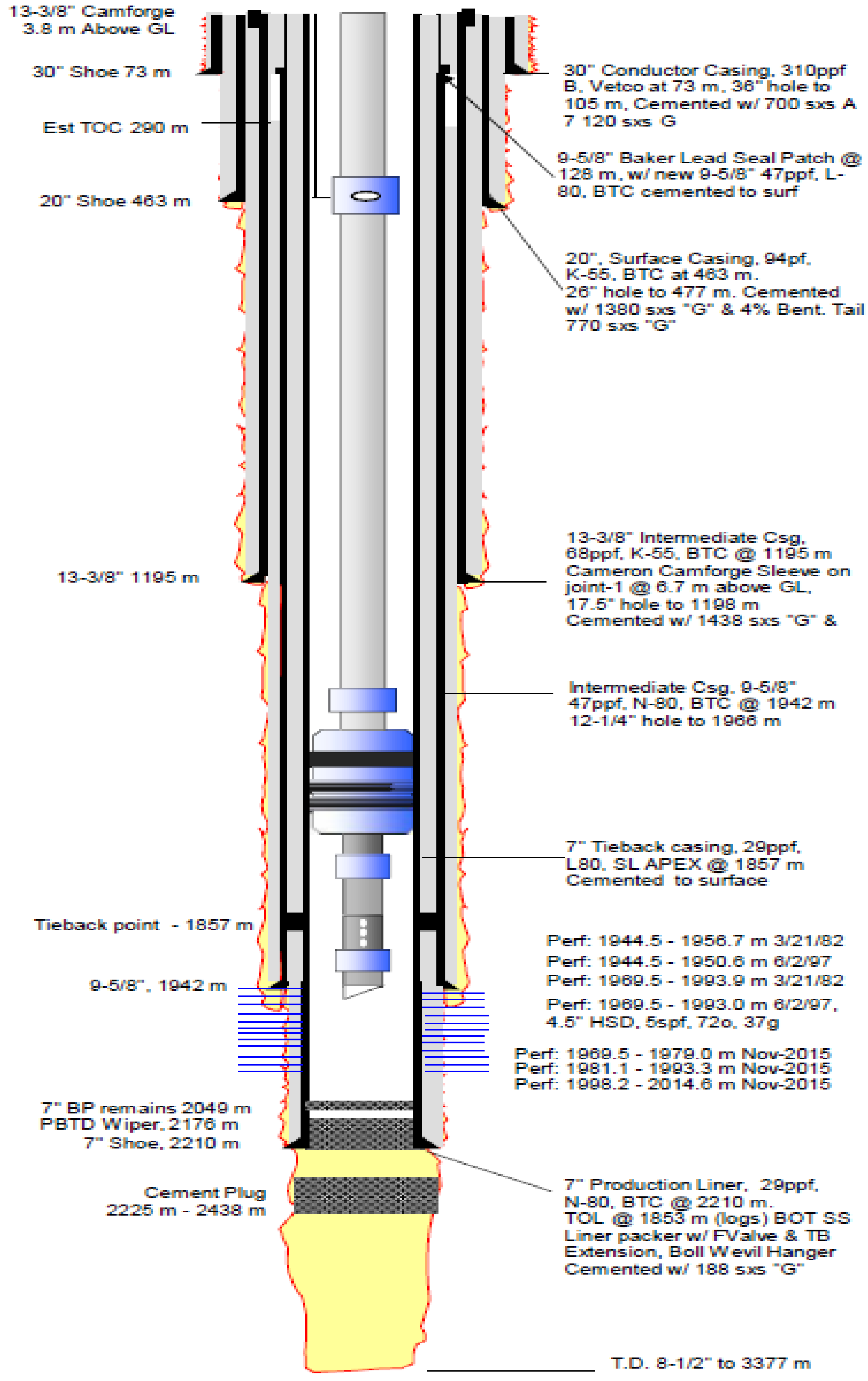

APPENDIX Y: COMPUTED CUMULATIVE GAS PRODUCTION FOR REVENUE ESTIMATION FOR WELL SS7

PERIOD [YEAR]	Anual forecasted gas production [MMSCF]	Annual GAS PRODUTION [MSCF]	Cummulative gas production [MSCF]
2016	85.0	8.50E+04	8.50E+04
2017	69.9	6.99E+04	1.55E+05
2018	57.4	5.74E+04	2.12E+05
2019	47.2	4.72E+04	2.59E+05
2020	38.8	3.88E+04	2.98E+05
2021	31.8	3.18E+04	3.30E+05
2022	26.2	2.62E+04	3.56E+05
2023	21.5	2.15E+04	3.78E+05
2024	17.7	1.77E+04	3.95E+05
2025	14.5	1.45E+04	4.10E+05
2026	11.9	1.19E+04	4.22E+05
2027	9.8	9.80E+03	4.32E+05
2028	8.0	8.05E+03	4.40E+05
2029	6.6	6.61E+03	4.46E+05
2030	5.4	5.43E+03	4.52E+05
2031	4.5	4.47E+03	4.56E+05
2032	3.7	3.67E+03	4.60E+05
2033	3.0	3.01E+03	4.63E+05
2034	2.5	2.48E+03	4.65E+05
2035	2.0	2.04E+03	4.67E+05
2036	1.7	1.67E+03	4.69E+05
2037	1.4	1.37E+03	4.70E+05
2038	1.1	1.13E+03	4.72E+05

REFERENCES

ALRDC, n.d. *Artificial Lift R&D Council (ALRDC).* [Online]
Available at: www.alrdc.com/.../gas%20well%20deliquification/.../AL%20Selection%20---%20Sect.
[Accessed 22 March 2017].

API, 2000. *Introduction to Oil and Gas Production.* 5th ed. Washington D.C: American Petroleum Institute.

Armenta, M. & Wojtanowicz, A., 2002. *Severity of Water Coning in Gas Wells..* Calgary, Alberta, Canada, Society of Petroleum Engineers..

Bondurant, A. & Hearn, B., 2008. *ALRDC.* [Online]
Available at:
http://www.alrdc.com/workshops/2010_2010EuropeanGasWell/Private/Basics%20of%20Gas%20Well%20Deliquification%20Europe%202010%20FINAL.pdf
[Accessed 22 March 2017].

Brown, K. E. et al., 1984. *The Technology of Artificial Lift Method.* Tusla, Oklahoma: PennWell Publishing Company.

Bujulu, G. N., 2013. *The Succeseful Development & Management of Songo Songo and Mnazi Bay Gas Field Against Imposing Reservoir, Market and Location Challenges.* Dar es Salaam, unpublished.

Ghiasi, M. M. & Bahadori, A., 2014. A New Correlation for Accurate Estimation of Natural Gases Water Content. *Petroleum & Coal,* 56(5), pp. 582-594.

Griffiths, A., 2010. *2010 Reservoir Engineering Review of the Songo Songo Gas Field,* Drayton, UK: Unpublished..

Hearn, W., 2010. *Gas Well Deliquification.* Abhu Dhabi, Society of Petroleum Engineers (SPE).

Heuvel, S. O., Ubbels, S. & Dijk, G. V., 2010. *Gas Well Deliquification using Foarmers: Apractical Approaches.* s.l., ALDRC.

Hutlas, E. J. & Granberry, W. R., 1972. A Practical Approach to Removing Gas Well Liquids. *Journal of Petroleum Technology*, pp. 916-922.

James, J., Huck, G. & Knobloch, T., 2002. *Identification of Effective Fluid Removal Technologies for Stripper Wells*, Marietta, Ohio 45750: James Engineering, Inc..

Jan, I., 2011 - 2013. *Accounting Explained.* [Online]
Available at: http://www.accountingexplained.com/managerial/capital-budgeting/discounted-payback-period
[Accessed 24 May 2017].

Joseph, A., Sand, C. M. & Ajienka, J., 2013. *Classification and Management of Liquid Loading in Gas Wells.* Logos, Nigeria, Society of Petroleum Engineers.

Kasheshe, R., 2017. *SS7 Gas Water Contact* [Interview] (13 March 2017).

Kasumuni, L., 2013. *The Citizen.* [Online]
Available at: http://www.thecitizen.co.tz/News/national/Electricity-tariffs-to-go-up-by-40-per-cent-on-January-1/1840392-2123688-7ehefy/index.html)
[Accessed 02 June 2017].

Kaye, L. & Shannon, C., 1982. *Songo Songo 7 Final Report,* England: Unpublished.

Khamehchi, E., Khishvand, M. & Abdolhosseini, H., 2016. A Case Study to Optimum Selection of Deliquification Method for Gas Condensate Well Design: South Pars Gas Field. *Ains Shams Engineering Journal*, Issue 7, pp. 847-853.

King, G. E., 2005. *Low Pressure Gas Well deliverability issues: Common Loading Causes, Diagnostics and Effective Deliquefication Practices.* Denver, Colorado, gekengineering.com.

Kuo, M. C. T. & DesBrisay, C. L., 1983. *A simplified Method for Water Coning Prediction.* Dallas, Texas, Society of Petroleum Engineers of AIME.

Lea, J. F. & Nickens, H. V., 2004. Solving gas-well liquid-loading problems.. *Journal of Petroleum Technology*, 56(04), pp. 30-36.

Lea, J. F., Nickens, H. V. & Wells, M. R., 2008. *Gas Well Deliquification.* 2nd ed. United State: Gulf Proffessional Publishing.

Lea, J. F. & Tighe, R. E., 1983. *Gas Well Operation with Liquid Production.* Oklahoma, Society of Petroleum Engineers of AIME.

Lea, J. F. & Tighe, R. E., 1983. *Gas Well Operation With Liquid Production.* Oklahoma, Society of Petroleum Engineers.

Lea, J., Nickens, H. & Wells, M., 2003. *Gas Well Deliquification.* 1st ed. USA: Gulf Professional Publishing- Elsevier.

Lea, J., Nickens, H. & wells, M., 2008. *Gas Well Deliquification.* 2nd ed. USA: Gulf Professional Publishing- Elsevier.

Lee, S. H. & Tung, W., 1990. *General Coning Correlations Based on Mechanistic Studies.* Richardson, Society of Petroleum Engineers Inc..

Magige, T. I., 2016. *The Study of Liquid Loading at the Songo Songo Gas Well (SS7),* Dar es Salaam: Unpublished.

Mower, L., Lea, J., Beauregard, E. & Ferguson, P., 1985. *Defining the Characteristics and Performance of Gas-Lift Plungers.* Las Vegas, Nevada, Society of Petroleum Engineers (SPE).

Mucharam, L., Permadi, A. K. & Agriawan, C., 2006. *Predicting Water CondensationAround a Dry Gas Well to Prevent Water Blocking.* Indonesia, Indonesian Petroleum Association (IPA).

Nallaparaju, Y. D., 2012. *Prediction of Liquid Loading in Gas Wells.* San Antiago, U.S.A, SPE-Society of Petroleum Engineers.

Neves, T. R. & Brimhall, R. M., 1989. *Elimination of Liquid Loading in Low Productive Gas Wells.* Oklahoma, Society of Petroleum Engineers.

Park, H. Y., Falcone, G. & Teodoriu, C., 2009. Decision Matrix for Liquid Loading in Gas Wells for Cost / Benefit Analysis of lifting Options. *Journal of Natural Gas Science and Engineering,* Issue 1, pp. 72-83.

Rowlan, O. L., McCoy, J. N. & Podio, A. L., 2006. *Acoustic Liquid Level Determination of Liquid Loading in Gas Wells.* Alaska, USA, Society of Petroleum Engineers (SPE).

Schiferli, W. et al., 2010. *Simulating Liquid Loading in Gas Wells.* Banff, Canada, BHR Group.

Schlumberger, 1999. *igs.nigc.* [Online]
Available at: http://igs.nigc.ir/STANDS/BOOK/Gas-Lift-Technology.pdf
[Accessed 18 April 2017].

Simpson, D., 2003. *Muleshoe Engineering.* [Online]
Available at: http://www.muleshoe-eng.com/id2.html
[Accessed 5 May 2017].

Simpson, D., 2006. Low-pressure gas well deliquification. *Oil and Gas Journal,* 8(104), pp. 41-50.

Soponsakulkaew, N., 2010. *Decision Matrix Screening Tool to Identify the Best Artificial Lift Method for Liquid-Loaded Gas Wells,* Texas: Master Thesis,Texas A&M University.

SPE, 2012. *Petrowiki.* [Online]
Available at: http://petrowiki.org/Plunger_lift_design_and_models?rel=1
[Accessed 12 June 2017].

SPE, 2015. *Petrowiki.* [Online]
Available at: http://petrowiki.org/Water_and_gas_coning
[Accessed 28 July 2017].

Strøm, T., 2016. *Instabart.no.* [Online]
Available at: https://ntnu.itslearning.com/File/fs_folderfile.aspx?FolderFileID=3070318
[Accessed 24 05 2017].

Sutton, R. P., Cox, S. A., Lea, J. F. & Rowlan, O. L., 2009. *Guidelines for the Proper Application of Critical Velocity Calculations.* Oklahoma, Society of Petroleum Engineers.

Triantaphyllou, E., Shu, B., Sanchez, S. N. & Ray, T., 1998. Multi-Criteria Decision Making: An. *Encyclopedia of Electrical and Electronics Engineering,* Volume 15, pp. 175-186.

US EPA, 2011. *Options for Removing Accumulated Fluid and Improving Flow in Gas Wells,* Washington DC: US EPA.

Waltrich, P. J. & Barbosa, J. R., 2011. *Performance of Vertical Transient Two-Phase Flow Models Applied to Liquid Loading in Gas Wells.* Denver, Colorado, USA, Society of Petroleum Engineers.

Wang, X., XGAS & Economides, M., 2009. *Advanced Natural Gas Engineering.* Houston, Texas: Gulf Publishing Company.

Weatherford, 2014. *uhspe.org.* [Online]
Available at: http://uhspe.org/wp-content/uploads/2014/11/Weatherford-Artificial-Lifts-Lift-Type-Selection.pdf
[Accessed 24 April 2017].

Whitson, C. H., 2016. *NTNU.* [Online]
Available at: http://www.ipt.ntnu.no/~curtis/courses/PVT-Flow/2016-TPG4145/
[Accessed 7 July 2017].

Whitson, C. H. & Brule, M. R., 2000. *Phase Behavior Monograph volume 20.* Richardson, USA(Texas): Society of Petroleum Engineers(SPE).

Whitson, C. H. et al., 2005/2006. *Understanding Gas Condensate Reservoirs.* s.l., s.n.

Williams, L., 2009. *The Songo Songo Gas Field, Tanza: Increasing Reserves and Expanding Gas Distributionnia.* London, Unpublished.

Winkler, H. W., 1987. Gas Lift. In: H. B. Bradley, et al. eds. *Petroleum Engineering Handbook.* Richardson, TX, U.S.A: Society of Petroleum Engineering, pp. 5_2 - 5_57.

Yang, J., Jovancicevic, V. & Ramachandran, S., 2006. Foam for Gas Well Deliquification. *Colloids and Surfaces A: Physicochem. Eng. Aspects,* Issue 309, p. 177–181.